AD-A133 856 STUDY OF 1/F NOISE IN SOLIDS(U) FLORIDA UNIV GAINESVILLE DEPT OF ELECTRICAL ENGINEERING C M VAN VLIET ET AL. 1983 AFOSR-TR-83-0798 1/2

UNCLASSIFIED AFOSR-82-0226 F/G 20/12 NL

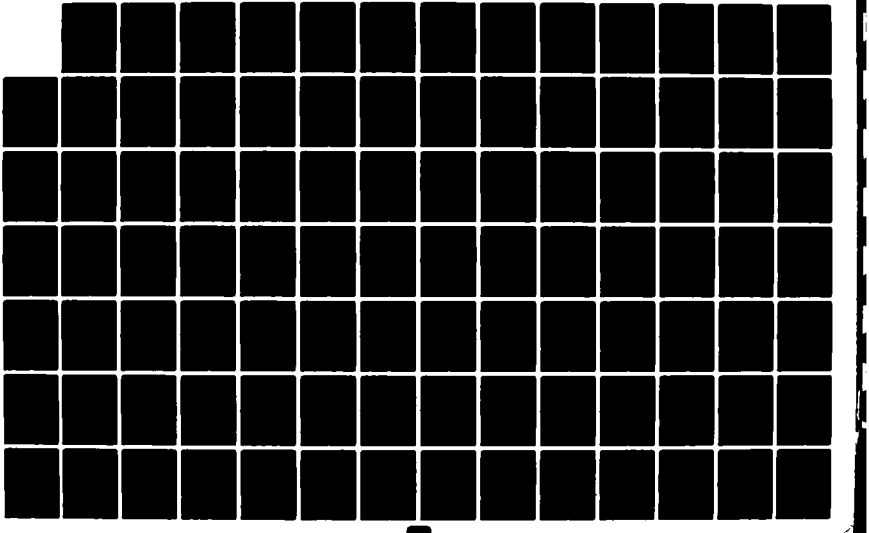

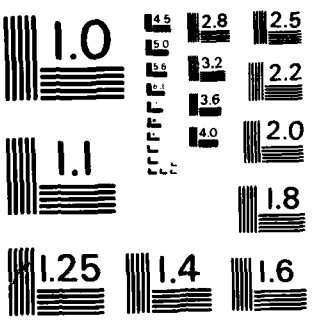

MICROCOPY RESOLUTION TEST CHART
NATIONAL BUREAU OF STANDARDS - 1963 - A

(2)

SECURITY CLASSIFICATION OF THIS PAGE (When Data Entered) Unclassified

AD-A133 856

REPORT DOCUMENTATION PAGE

READ INSTRUCTIONS BEFORE COMPLETING FORM

1. REPORT NUMBER: AFOSR-TR- 83-0798	2. GOVT ACCESSION NO.: AD-A133 856
3. RECIPIENT'S CATALOG NUMBER:	
4. TITLE (and Subtitle): STUDY OF 1/f NOISE IN SOLIDS	5. TYPE OF REPORT & PERIOD COVERED: ANNUAL REPORT 16 JUN 82 - 15 JUN 83
	6. PERFORMING ORG. REPORT NUMBER:
7. AUTHOR(s): Carolyn M. Van Vliet	8. CONTRACT OR GRANT NUMBER(s): AFOSR-82-0226
9. PERFORMING ORGANIZATION NAME AND ADDRESS: University of Florida Gainesville, FL. 32611	10. PROGRAM ELEMENT, PROJECT, TASK AREA & WORK UNIT NUMBERS: 61102F 2305/C1
11. CONTROLLING OFFICE NAME AND ADDRESS: Air Force Office of Scientific Research/NE Building #410 Bolling AFB, DC 20332	12. REPORT DATE: 1983
	13. NUMBER OF PAGES: 130
14. MONITORING AGENCY NAME & ADDRESS (if different from Controlling Office)	15. SECURITY CLASS. (of this report): Unclassified
	15a. DECLASSIFICATION/DOWNGRADING SCHEDULE:

16. DISTRIBUTION STATEMENT (of this Report)

Approved for public release; distribution unlimited.

17. DISTRIBUTION STATEMENT (of the abstract entered in Block 20, if different from Report)

18. SUPPLEMENTARY NOTES

19. KEY WORDS (Continue on reverse side if necessary and identify by block number)

20. ABSTRACT (Continue on reverse side if necessary and identify by block number)

Noise measurements were made on gold metal films . The noise above 150K is of the form $1/f^{1.2}$; below 150K the noise goes as 1/f with a maximum near 80K, then a continued decrease.
The noise in GaAs $n^+n^-n^+$ mesas of submicron dimensions is very low. The Hooge parameter is of the order of 10^{-7}, indicating that collisions are nearly absent. Intervally electron transfer is noticeable in samples with 1.1 micrometer dimensions. The $n^+p^-n^+$ structures have a great deal of noise associated with the prepunch-though current. This is attributed to

DTIC FILE COPY

DD FORM 1 JAN 73 1473 EDITION OF 1 NOV 65 IS OBSOLETE

Unclassified

SECURITY CLASSIFICATION OF THIS PAGE (When Data Entered)

recombination of injected electrons via empty acceptors, since in the unexcited specimen there are no holes due to electron spillover.
For the first time 1/f noise was observed in radioactive alpha particle decay from 241 Americium. This noise was deduced from counting statistics using the Allan variance theorem.
Calculations yielded quantitative accounts for the mobility-fluctuation noise associated with impurity scattering for silicon and gold.

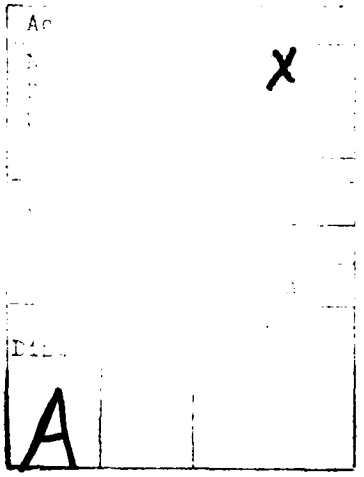

DTIC
COPY
INSPECTED
8

2305/C1

STUDY OF 1/f NOISE IN SOLIDS

Progress Report

to the

Air Force Office of Scientific Research
Bolling Air Force Base, Washington, D.C. 20332

Grant No. AFOSR 82-0226

Period Covered: June 16, 1982 - June 15, 1983

Submitted by

Carolyn M. Van Vliet
Professor and Principal Investigator

Gijs Bosman
Asst. Professor and Co-Investigator

Department of Electrical Engineering
University of Florida
Gainesville, Florida, 32611

Approved for public release;
distribution unlimited.

83 10 04 243

AIR FORCE OFFICE OF SCIENTIFIC RESEARCH (AFSC)
NOTICE OF TRANSMITTAL TO DTIC
This technical report has been reviewed and is
approved for public release IAW AFR 190-12.
Distribution is unlimited.
MATTHEW J. KERPER
Chief, Technical Information Division

Abstract

This report is divided into two main parts: Experimental Work (B) and Theoretical Work (C).

In the experimental part we first report the noise in gold metal films. The noise above 150°K (close to the Debye temperature) is of the form $1/f^{1.2}$, and requires probably a vacancy diffusion model or other specific models as in the work of Dutta and Horn. Below 150°K the noise is 1/f, with a maximum near 80K, and then a continued decrease. If the N in Hooge's formula is reinterpreted as the number of electrons within 2 kT from the Fermi surface, rather than the total number of valence electrons, then the noise can well be understood in terms of quantum 1/f noise, involving Umklapp processes.

The noise in GaAs $n^+n^-n^+$ mesas of submicron dimensions is very low. The Hooge parameter is of order 10^{-7}, indicating that collisions are nearly absent. In 1.1μ, $n^+n^-n^+$ structures intervalley electron transfer is noticeable. An attempt to measure the associated intervalley noise is being made. The $n^+p^-n^+$ have a lot of noise associated with the prepunch-through current. This is attributed to recombination of injected electrons via empty acceptors, since in the unexcited specimen there are no holes due to electron spillover. At very high currents (1 - 10 amps) requiring pulsed noise measurements, ballistic behavior with low noise takes over again, and the behavior becomes similar to that in $n^+n^-n^+$ structures.

In an entirely different experiment we observed for the first time a 1/f noise component in radioactive α-particle decay from 241 Americium. This noise was deduced from counting statistics using the Allan variance theorem.

Partition 1/f noise in pentodes was measured by eliminating the cathode 1/f noise with feedback. Van der Ziel gave an expression which modifies Handel's theory for this type of noise. The observed noise seems to be in good argument with Handel's modified theory.

In the theoretical sections some further remarks were made on the interpretation of Hooge's formula for metals. Further, we calculated quantitatively the mobility-fluctuation noise associated with impurity scattering for silicon and for gold. It is found to be extremely low, in accordance with the experimental observations that impurity scattering gives little or no noise. Computations for acoustic phonon scattering, involving both Normal and Umklapp processes, are being carried out. Further, a survey is presented of the particular features of nonequilibrium, stationary Markovian noise processes.

List of Figures

TABLE OF CONTENTS

A. INTRODUCTION

In our previous annual report (June 1982) we mentioned six types of theories, to explain 1/f noise, that have survived. Of these, we can now omit the category "transport noise theories," a specific example of which is temperature fluctuation (or heat-diffusion) noise. The measurements of J. Kilmer, performed this year under the contract, have definitively shown that the noise in electrically isolated, but thermally closely connected, metal films is uncorrelated over the entire range 300 K - 10 K. Other transport theories had already been discarded earlier due to the work of Mehta and Van Vliet (Physica Status Solidi (b) 106, 11, 1981). So far, no mathematical transport model has yielded a 1/f spectrum over many decades, and the physical evidence for the occurrence of transport noise as a basis of 1/f noise is entirely lacking.

Secondly, in the June 1982 report we mentioned the model based on phonon-distributed lifetimes, proposed by Jindal and van der Ziel. So far, however, there has not been any evidence for this model either, while the occurrence of very long phonon lifetimes remains very enigmatic. So, also ruling out this theory, four types of theory remain:

1. The universal theories;
2. The van der Ziel-Bernamont-du Pré-McWhorter theories, involving a $\tau^{-\alpha}(\alpha \approx 1)$ distribution of time constants;
3. Specific noise model theories;
4. The mobility-fluctuation bulk model, based on quantum 1/f noise (Handel, Ngai, Widom, et al.).

The "universal theories" usually seek some mathematical general model, which explains the absence of time scaling (lack of characteristic time constants) in 1/f noise. For example, Montroll and Schlesinger have explained that a log-normal distribution in leading order distributes a random variable x according to x^{-1} (Proc. Natl. Acad. Sciences USA 79, 3380-3383, 1982). Recently, Marzec

and Spiegel offered another interesting mathematical example. They showed that a distribution of tunable oscillators, having an action J on the system, and subject to the constraints

$$\int_0^\infty P_1(\omega)d\omega = 1, \quad \int_0^\infty P(J|\omega)dJ = 1,$$

maximizes the informational entropy

$$S = -\int_0^\infty\int_0^\infty P_2 \ln P_2(J,\omega)dJ\,d\omega$$

if $P_1(\omega) = N/\omega$, where N is the number of oscillators (note submitted to Nature, 1983). They proceed to give examples of the occurrence of such systems of oscillators in physical systems. We believe at present that such universal theories should not be dismissed, in particular, since the other possibilities have also their limitations.

The van der Ziel- ..... -McWhorter theories still are viable for a number of cases. In these theories there is necessarily always a lower frequency $\omega_1 = 1/\tau_1$ and an upper limit $\omega_2 = 1/\tau_2$ outside which the 1/f law does not hold. Thus, these theories are not scale-free. In some cases conclusive evidence for this mechanism has been found. Thus, Hanafi and van der Ziel found that the lower limit ω_1 could be varied by sputtering off layers of cadmium mercury telluride crystals. We note that the noise in this case stems from the surface, as in McWhorter's original experiments, and is not a bulk effect. We do not know of any physical evidence of the time-constant distribution model in cases where the noise is clearly a bulk effect.

The "specific noise models" certainly apply in certain cases. Kilmer found that the noise in gold films, above 150 K, has a $1/f^{1,2}$ spectrum; the noise rises sharply with increasing temperature up to a certain maximum, as had also been observed for other metals by the Chicago group (Dutta, Horn, and others). They suggested a model involving vacancy migration for this temperature

range. Likely, some effect of this nature is responsible for the noise. There are, of course, a host of other "specific noise model" theories, such as the recombination model by Min (Solid State Electronics, 1979) and the Island model of Pellegrini (Phys. Rev., 1981). However, there is not, in our opinion, any evidence for the validity of these models. And if examples for the occurrence of such theories are found, then still, most 1/f noise cannot be explained by these models.

The quantum theory of 1/f noise as advanced by Handel in 1975, and worked out in more detail in 1980 (Phys. Rev. A22, 745, 1980), remains the most general theory to explain 1/f noise. However, the noise calculated from Handel's theory is extremely low. Thus, indeed, this theory explains at most the "flicker floor" occurring in physical systems. For many phenomena, the observed noise exceeds Handel's theoretical results by orders of magnitude. In this report we present evidence that Handel's theory may explain 1/f noise in radioactive decay, in metal films below the Debye temperature, and it can explain partition noise in pentodes. We note, however, that Handel's work still receives much skepticism by many investigators. It has to be admitted that a number of points, in particular the coherence of various events, responsible for the 1/N dependence in Hooge's law, is not well understood in Handel's theories. This makes a quantitative comparison with observed data very difficult, as we will see in this report for the radioactive decay noise and for the 1/f partition noise in pentodes.

In summary, it appears to us that the explanation of 1/f noise is narrowed down to four types of possible theories. The time-constant distribution theory is likely only applicable to surface-generated noise. The specific models have, no doubt, validity for certain types of noise, in particular when the spectrum is not exactly 1/f, but, e.g., $1/f^{0.7} - 1/f^{1.3}$. Thus, the remaining noise theories of promise are the "universal theories" and the "quantum theories" of 1/f noise which involve infrared divergencies due to nonlinear coupling of the system with the wave field.

A point which also needs further investigation is the fact that order of magnitude variations can occur for macroscopically identical systems. This was abundantly illustrated at the Montpellier International Conference (1983) for the noise in metal films, both by Fleetwood and Giordano, and by our own findings due to Kilmer et al. Why seemingly "identical" systems can have different magnitude of noise (a factor 3 - 10) is at present an enigma.

B. EXPERIMENTAL WORK

Much experimental work was presented at the Seventh International Symposium on the Noise in Physical Systems and Third International Conference on 1/f Noise, held in Montpellier, France, May 17 - 20. Where appropriate, we reproduce the contributions of this conference.

I. 1/f NOISE IN METAL FILMS OF SUBMICRON DIMENSIONS

J. Kilmer, C.M. Van Vliet, G. Bosman and A. van der Ziel

Department of Electrical Engineering
University of Florida, Gainesville, FL 32611, USA

Photonic quantum 1/f noise has been identified in Au metal films below the Debye temperature. The low values of the Hooge parameter predicted by Handel's theory (i.e., $\alpha_{true} \simeq 10^{-6}$ to 10^{-8}) are arrived at by realizing that only the fraction $3kT/2\mathcal{E}_F$ of the total number of carriers are available for scattering at a given temperature.

In recent years considerable progress has been made in the understanding of 1/f noise. It is now well established that in many cases there is fundamental 1/f noise caused by mobility fluctuations, in particular by fluctuations in the scattering cross section of scattering of electrons by phonons.[1][2]

The only general theory of 1/f noise which can explain such fluctuations was given by Handel in 1975.[3][4]. However, until recently experimental evidence verifying the theory did not exist. Specifically, Handel's quantum 1/f noise theory was questioned as the source of 1/f noise in electronic circuits because of the low value of the Hooge parameter, α_H, calculated from his theory. Briefly, the theory states that the interference between the part of the carrier's wave function which suffers losses due to an inelastic or "bremsstrahlung" scattering under the emission of infraquanta and the part of the wave function which does not suffer losses produces very low energy beats which translate themselves ($\Delta\mathcal{E} = hf$) as 1/f noise. Handel's theory predicts that scattering involving Umklapp processes (U-processes) provides the largest source of 1/f noise in metals since the photon infraquanta coupling constant, αA, is given by[4]

$$\alpha_A = \frac{2\alpha}{3\pi}\left(\frac{\Delta p}{mc}\right)^2 \qquad (1)$$

where α is the fine structure constant $(137)^{-1}$, perhaps modified by the dielectric constant in the metal, c is the velocity of light in the metal, and $\Delta p/\hbar = \Delta k$ is the change in wave vector. Since the U-process gives the largest Δk, we expect them to be the largest contributor to 1/f noise in metals. Though the dielectric constant of metals is not well known, and may be complex, one easily sees that the corrections in α and c cancel, so that we can further take the free space values.

Gold thin-film resistors (2,000 Å thick) were prepared for us by Dr. E. Wolf and R.A. Buhrman of the National Research and Resource Facility for Submicron Structures at Cornell University. The length of the resistors is close to 800 μm, and we have measured the 1/f noise in 1 μm-width samples. These dimensions give a resistance of a few hundred ohms and the noise spectrum can be readily measured, after amplification, by an HP 3582 Spectrum Analyzer. By incorporating a calibrated noise source, the absolute magnitude of the resistor's current noise spectrum, S_I, can be directly calculated by simply comparing the relative spectra of device on, device off, and calibration source on; it can be shown that the amplifier's parameters cancel out. The gold films were mounted to the cold head of a CTI Cryogenics Model 21 liquid He closed-cycle refrigerator capable of maintaining a stable temperature (i.e., ± 0.1 K over the duration of a low-frequency noise measurement) anywhere between 300 K and 8 K.

The results of the experiment give current spectra proportional to $1/f^{\gamma}$ between 1 and 100 Hz. Below 1 Hz we have cryostat noise, and above 100 Hz we have device noise competing with the amplifier's noise and thermal noise. The slope shows $\gamma \simeq 1.2$ from 300 K to about the Debye temperature (Θ_D = 165 K for gold) in agreement with Fleetwood and Giordano.[5] Below the Debye temperature the slope evens off to $\gamma \simeq 1$, indicating a more "pure" 1/f noise present at the lower temperatures. Next, we characterize the magnitude of the 1/f noise by calculating the dimensionless Hooge parameter, α_H, according to the formula

$$\frac{S_I(f)}{I^2} = \frac{\alpha_H}{fN} \qquad (2)$$

where N is the total number of available electrons in the metal; for those spectra where $\gamma \neq 1$, we took $\gamma = 1.0$ hz. In Figure 1 we have used $N = nV$ where we set $n \approx 10^{23}$ cm^{-3} and V is the sample volume (800 μm × 1 μm × 0.2 μm). Figure 1 shows an interesting dependence of the magnitude of α_H below the Debye temperature corresponding to the occurrence of the more "pure" 1/f noise.

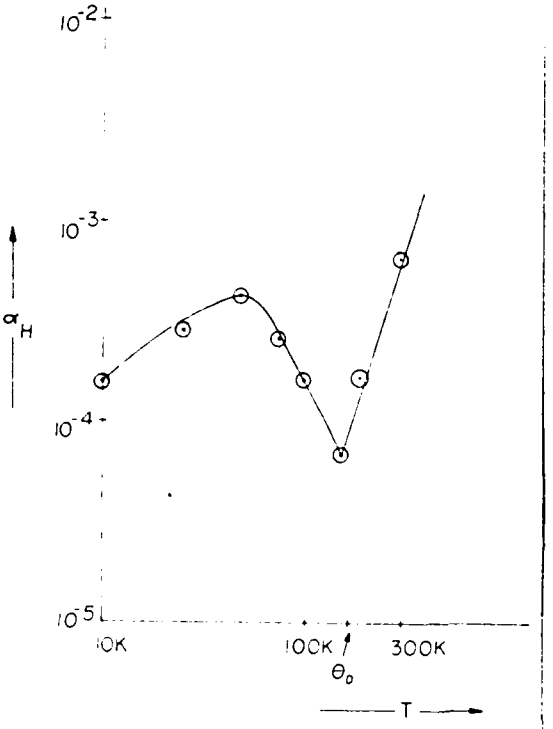

Figure 1. α_H as a function of temperature

We believe, however, that (2) is not a proper characterization of noise in metals. As was pointed out by Van Vliet and Zijlstra,[6] the basic formula for the mobility fluctuations for the scattering of a single carrier is

$$\frac{S_{\mu_i}(f)}{\mu_i^2} = \frac{\alpha_{true}}{f} \qquad (3)$$

where we subscripted the α-value as α_{true}. To obtain the fluctuations in the band mobility, or for that matter of the current I, we must sum over the scattering fluctuations of all carriers in the band.[7][8] For a nondegenerate semiconductor this provides a factor 1/N in the denominator, see (2). In metals, however, most of the carriers are "frozen" in the Fermi sea, a fact also noted by Dutta and Horn in their review paper.[9] Therefore, as we pointed out elsewhere, in connection with thermal noise from metals and the Einstein relation,[10] the result of the summation must be multiplied by $\langle \Delta N^* \rangle / \langle N \rangle$, where the subscript "*" refers to the grand canonical ensemble.[10, sec. 3] From statistical mechanics the above factor is $kT\partial(\log N)/\partial \mathcal{E}_F$ where $\mathcal{E}_F$ is the Fermi energy. Explicitly, we have

$$\frac{kT\partial(\log N)}{\partial \mathcal{E}_F} = \frac{\mathcal{F}_{\frac{1}{2}}[(\mathcal{E}_c - \mathcal{E}_F)/kT]}{\mathcal{F}_{-\frac{1}{2}}[(\mathcal{E}_c - \mathcal{E}_F)/kT]} \qquad (4)$$

where $\mathcal{E}_c$ is the bottom of the conduction band, and $\mathcal{F}_k$ is the Fermi integral of order k. For total degeneracy, $\mathcal{F}_k(\eta) = \eta^{k+1}/\Gamma(k+2)$. Thus the ratio (4) becomes $2\Delta\mathcal{E}_F/3kT$ with $\Delta\mathcal{E}_F = \mathcal{E}_F - \mathcal{E}_c$. Consequently, eq. (3) followed by the proper statistical summation leads to

$$\frac{S_I(f)}{I^2} = \frac{\alpha_{true}}{N}\,\frac{2\Delta\mathcal{E}_F}{3kT} = \frac{\alpha_{true}}{fN^*}, \qquad (5)$$

indicating that the number of carriers available for scattering is $N^* = N(3kT/2\Delta\mathcal{E}_F)$. This is also intuitively obvious: the Fermi function differs only appreciably from 1 or 0 in a slice of order kT. That such a reduction in noise must occur in metals was perhaps first pointed out in a classic paper by Brillouin[11] on the first noise observations in metals, by Bernamont.[12] Comparing now (5) with (3) we find that the "true" Hooge parameter is related to the observed Hooge parameter α_H by

$$\alpha_{true} = \frac{3kT}{2\Delta\mathcal{E}_F}\,\alpha_H. \qquad (6)$$

With $\Delta\mathcal{E}_F = 5.5$ eV,[13] the values of α_{true} were computed to yield the data of Fig. 2.

As is noted, we now obtain α-values low enough to become in the ballpark expected from the quantum theory of 1/f noise. In the latter theory, the α_{true} of eq. (3) is just twice the infrared exponent, i.e.,

$$\alpha_{true} = 2\alpha A. \qquad (7)$$

With $\Delta p/m = 2v_F \sin \vartheta/2$, where v_F is the Fermi velocity (1.39×10^8 cm/sec) and ϑ is the scattering angle ($\approx 150°$ for U-processes), we obtain from (1) $2\alpha A \approx 2.4 \times 10^{-3}$. This value is approximate since N is not exactly known and since more correctly we must take into account the detailed geometry of the Fermi surface, being a sphere with eight "necks" (see Ziman[14]). However, this value comes close to the observed value of $(\alpha_{true})_{max}$ in Fig. 2, being 4.9×10^{-3}.

Qualitatively, we believe that the observed data of Fig. 2 can be well understood. Above the Debye temperature θ_D, region C, some non-fundamental 1/f' noise occurs, similar to the "type B" noise observed by Dutta and Horn.[9] Below θ_D we have for the first time a clear indication of the occurrence of quantum 1/f

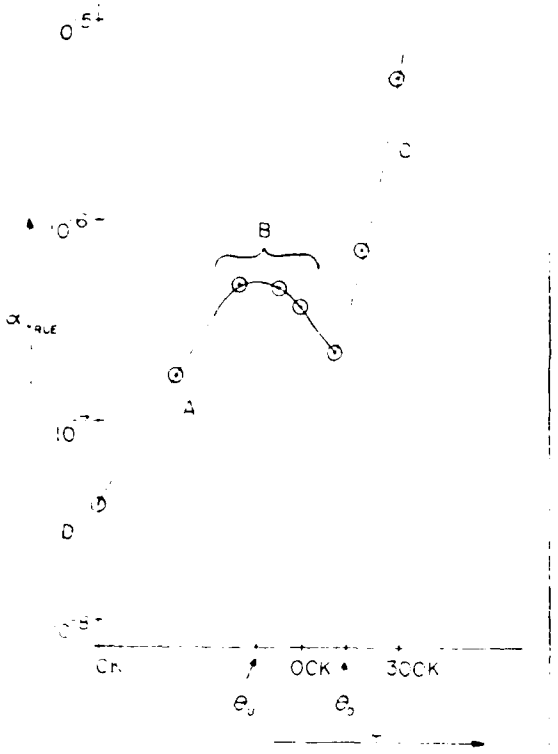

Figure 2. α_{true} as a function of temperature

noise. U-processes dominate in the region B. In the region A, U-processes freeze out and normal phonon processes (N-processes) take over. Finally, in a region D (not yet observed), ionized impurity scattering may give rise to a floor at very low temperatures.

A quantitative theory has not yet been fully developed. However, with U-processes dominating the noise, and N-processes and ionized impurity scattering dominating the resistance, one expects the temperature dependence to be of the form

$$\alpha_{true} \propto \left[\frac{T^{-} e^{\Theta_U/T}}{C + C_1 T}\right] \qquad (8)$$

where Θ_U is the Umklapp temperature, $\Theta_U = \hbar q_U v_s / k_B$, in which v_s is the transverse velocity of sound in gold, k_B is Boltzmann's constant, and q_U is a phonon vector associated with the length of the neck between adjacent Fermi surfaces in the extended zone scheme. We computed $q_U = 0.3 \times 10^{8}$ cm^{-1}, while $u_o = 1.2 \times 10^{5}$ cm/sec. This yields $\Theta_U = 57.6$ K. The observed maximum in the noise occurs at about 60 K. Though many details need fuller consideration, we believe that the observed noise can be reasonably well explained by the proposed processes. Development of a full theory and detailed 1/f noise measurements in metals may give much insight into the nature of the phonon processes undergone by the Fermi surface electrons.

We finally note that another type of confirmation of the theory of quantum 1/f noise was recently provided by α-particle decay statistics.[15]

ACKNOWLEDGEMENTS

We acknowledge support from an AFOSR contract, #82-0226, and from a user contract with NRRFSS at Cornell University.

REFERENCES

[1] Hooge, F.N., Van Damme, L.K.J. and Kleinpenning, T.G.M., Reports Progress Physics 44 (1981) 481.

[2] Hooge, F.N. and Van Damme, L.K.J., Phys. Letters 66A (1978) 315.

[3] Handel, P.H., Phys. Rev. Letters 34 (1975) 1492 and 1495.

[4] Handel, P.H., Phys. Review A22 (1980) 745.

[5] Fleetwood, D.M., Masden, J.T. and Giordano, N., "1/f Noise in Platinum Films and Ultra-thin Platinum Wires: Evidence for a Common Bulk Origin," to be published.

[6] van Vliet, K.M. and Zijlstra, R.J.J., Physica 111B (1981) 321.

[7] Hooge, F.N., Physica 114B (1982) 391.

[8] van der Ziel, A., Van Vliet, C.M., Zijlstra, R.J.J. and Jindal, R., Physica B, in press.

[9] Dutta, P. and Horn, P.M., Rev. Mod. Phys. 53 (1981) 497.

[10] van Vliet, K.M. and van der Ziel, A., Solid State Electr. 20 (1977) 931.

[11] Brillouin, L., Helv. Physica Acta 7, suppl. 2 (1934) 47.

[12] Dernamont, J., Comptes Rendues de l'Ac. Francaise 198 (1934) 1755 and 2144.

[13] Kittel, C., Introduction to Solid State Physics, 5th Ed. (McGraw-Hill, New York, 1976) 154.

[14] Ziman, J.M., Electrons and Phonons (Oxford University Press, London, 1967) 113.

[15] Gong, J., Van Vliet, C.M. and Ellis, N., Jr., "Observations of a Flicker Noise Floor in α-Particle Counting Statistics from $_{95}Am^{241}$," to be submitted to Physical Review.

Measurements on the 0.5 μm and 2 μm width gold thin film samples are presently being performed and a similar α_H vs. T plot is observed.

Also, to get a more complete picture, the same noise measurements as a function of temperature will be performed on other metal films with different Debye temperatures. Presently, masks are being prepared to evaporate aluminum on a silicon oxide substrate in a 5 μm × 1000 μm × 2000Å thin film resistor configuration here at University of Florida's microelectronics laboratory. Producing films of less than 5 μm width will be aimed for, since we desire a greater resistance from the thin film resistor samples. Aluminum is not ideal since its θ_D is 428 K and the resistor must be placed in an oven to probe the noise near the Debye temperature.

After perfection of the aluminum evaporation, palladium (θ_D = 274 K), silver (θ_D = 225 K), chromium, and indium which can be evaporated will be used to produce resistors in the same thin film configuration, and noise measurements will be performed.

Hopefully, we will be able to produce platinum films (θ_D = 240 K) in our microelectronics lab when we get the new ion-beam sputtering equipment.

Finally, provisions have been made to make noise measurements on samples in the 8 K to 2 K ambient temperature range by directly submerging the sample in a liquid helium cryostat and reducing the vapor pressure by pumping.

Solid-State Electronics Vol. 26, No. 5, pp. 437–444, 1983
Printed in Great Britain

0038-1101/83/050437-08$03.00/0
Pergamon Press Ltd

II. NOISE IN NEAR-BALLISTIC n^+nn^+ AND n^+pn^+ GALLIUM ARSENIDE SUBMICRON DIODES

R. R. SCHMIDT, G. BOSMAN and C. M. VAN VLIET
Department of Electrical Engineering, University of Florida, Gainesville, FL 32611 U.S.A.

and

L. F. EASTMAN and M. HOLLIS
School of Electrical Engineering, Cornell University, Ithaca, NY 14853, U.S.A.

(*Received* 17 *August* 1982; *in revised form* 26 *October* 1982)

Abstract Direct-current (d.c.) characteristics and noise measurements in the range 1 Hz–25 kHz are reported for n^+nn^+ and n^+pn^+ near-ballistic devices, with n regions (p regions) of 0.4 μm (0.45 μm), fabricated by molecular beam epitaxy at Cornell. The n^+nn^+ mesa structures show very low 1/f noise, indicating a Hooge parameter $\alpha_H = 6.0 \times 10^{-6}$. This very low noise is attributed to the near absence of phonon collisions. The thermal (−like) noise above 1 kHz is equal to Nyquist noise at the lowest currents, rising to slightly above Nyquist noise for high currents, indicating the presence of carrier drag effects. The n^+pn^+ noise, on the contrary, is quite high. It seems to be associated with the ambipolar effects occurring for low injection of electrons in the p region. The importance of noise measurements for confirming ballistic or near-ballistic behavior is discussed.

1. INTRODUCTION

Submicron gallium arsenide structures are of great current interest, since they permit ballistic or near-ballistic electron flow, which in turn leads to carrier velocities that far exceed the saturation velocity in collision-dominated conduction, thus enabling the design of picosecond switching devices and other novel applications. The fabrication of submicron devices has been made possible by modern MBE techniques, electron lithography, etc. For GaAs near-ballistic behavior requires that the distance to be traveled by the injected electrons is less than or of the order of 0.7 μm. Eastman *et al.* report[1] that the mean free path for phonon emission into optical polar modes at room temperature is 0.1 μm for electrons of 0.05 eV, and 0.2 μm for electrons of 0.5 eV. Phonon absorption has a longer mean free path and can be neglected for the devices reported here, having thicknesses of 0.4 μm (thickness of n layer in n^+nn^+ devices) and 0.45 μm (thickness of p layer in n^+pn^+ devices). At higher electron energy intervalley scattering becomes important, thus limiting the near-ballistic range to about 0.5 eV of electron energy. In a sample of 0.4 μm thickness about two phonon emissions may occur. These involve, however, small angle deflections only (5–10°) and have little effect on the d.c. carrier characteristics, according to Ref. [1].

The theory for "pure" ballistic behavior (no collisions suffered whatsoever) was developed by Shur and Eastman in 1979 in a basic paper on this topic[2]. They solve Poisson's equation, allowing for space charge of both fixed ionized donors (or acceptors) and injected carriers. Employing boundary conditions which neglect the initial thermal energy of the electrons injected from the n^+ into the n layer (or p layer after punch-through), they find the solid state analog of Child's law in vacuum tubes. For sufficiently small voltages there is a domain in which the current I goes as $V^{1/2}$; when the injected space charge exceeds the fixed charge due to the ionized donors or acceptors, the characteristic changes, however, to the familiar $V^{3/2}$ form. In Ref.[1] measurements are presented which fairly well support these predictions, providing the nonparabolicity of the bands and the onset of intervalley scattering at higher voltages are taken into account. In a later theory, Shur[3] and Shur and Eastman[4] extended the theory to that for "near-ballistic" devices, in which few collisions can occur. Since the Boltzmann equation would be inappropriate for that regime, the collisions are taken into account by adding momentum and energy "drag terms" to the otherwise ballistic equations of motion. In this way, the transition from Child's law ($\tau \to \infty$, where τ is the collision time) to the Mott and Gurney law, $I \propto V^2$ (finite τ) is covered by this approach.

Two modifications have been proposed by others, which may have a bearing on the present paper. First, Rosenberg *et al.*[5] discuss the effects of "spillover" of carriers at the n^+n high-low junction. This means, in essence, that the boundary conditions must be changed to account for the depletion of n^+ regions and spillover into the adjacent Debye lengths. As a result, the effective width of the n region is smaller and the current is higher than that computed in Ref. [2]. Secondly, Cook and Jeffrey[6] have indicated that the energy or velocity distribution of the electrons cannot be neglected. The velocity dispersion is accounted for by the introduction of an electron temperature gradient term in the momentum balance equation (*op. cit.* eqn (8)). Though they argue that this leads to the occurrence of a potential minimum somewhere beyond the "cathode"—rather than at the cathode—

similar to Langmuir's treatment of vacuum diodes, we have great reservations about their treatment. A more straightforward and correct approach was very recently presented by Holden and Debney [7], in a paper based on ideas from the well-known vacuum diode discussion of Fry [8]. Their results indicate that no fixed power law can be stated. For 0.5 μ samples the limiting slope is found to be 1.14. For the noise characteristics the inclusion of the velocity dispersion is essential, in particular for the high-frequency thermal-like velocity-fluctuation noise.

In this paper we describe very accurate low-frequency and high-frequency noise measurements on near-ballistic devices. Such measurements serve a threefold purpose. First, from a practical point of view noise data reveal the practical performance limitations of the novel high-speed devices. As we will indicate the noise of the n^+nn^+ devices is extremely low; the n^+pn^+ devices, however, fare much worse. Secondly, noise measurements at audio and subaudio frequencies shed much light on the $1/f$ noise problem. According to most recent theories, such noise is thought to be caused by mobility fluctuations (see, e.g. Hooge *et al.* [9] and van der Ziel [10]). If collisions in the near-ballistic regime are rare, one expects the $1/f$ noise to be very low and ultimately, in "pure" ballistic devices, to be absent. Our work on n^+nn^+ devices indicates that this could be correct. Third, and not least, we believe that the high-frequency noise (thermal, velocity-fluctuation, or diffusion noise) will shed much light on the mode of operation of near-ballistic devices. To date, no full-fledged theory for such noise exists; we only have some preliminary computations by van der Ziel and Bosman [11, 12]. However, once this noise is understood, we will have a powerful means of substantiating or amending the various theories on near-ballistic behavior.

2. EXPERIMENTAL

The near-ballistic diode (NBD) is a sandwiched mesa structure of five lightly doped p or n layers, alternating with heavily doped n^+ layers, see Fig. 1. The doping densities of the various regions are 10^{18} cm^{-3} for the n^+ regions, approx. 2×10^{15} cm^{-3} for the n regions and approx. 10^{15} cm^{-3} for the p regions. The diameter of the mesas is 100 μm. The devices were manufactured by molecular beam epitaxy at the Cornell University Submicron Research Facility. The mesas were provided with very low ohmic Au Ge contacts. A low frequency equivalent circuit of the n^+nn^+ device is given in Fig. 2. The main element (n regions) has a resistance of 0.75 Ω. To infer the correct noise of the device, the values of the parasitic resistances in Fig. 2 have been taken into account. For the n^+pn^+ devices the p layer gave a resistance of order 90 Ω at 1 mA; the parasitic resistances in this case were negligible.

The characteristics of the two types of devices are quite different. The noise measurement of the n NBD's, in particular, was a challenge. To do this we used the setup shown in Fig. 3. A Hewlett Packard

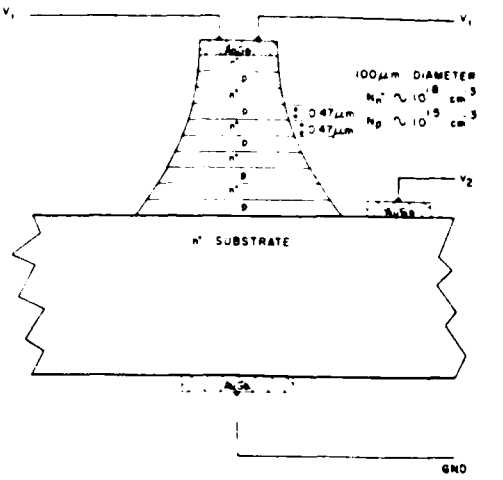

Fig. 1. P-type near-ballistic mesa structure; the n-type structure is similar.

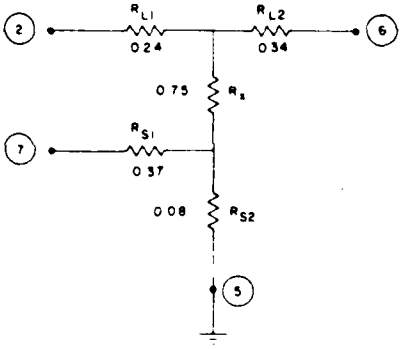

Fig. 2. Equivalent circuit of n^+nn^+ structure, showing parasitic elements. The contacts ② and ⑥ refer to the top contacts 1 in Fig. 1, contact ⑦ refers to V_2 and contact ⑤ to GND of Fig. 1.

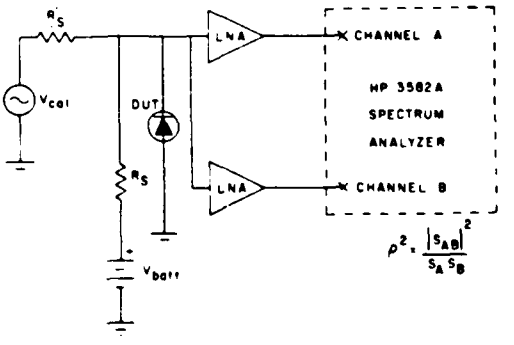

Fig. 3. Correlation measurement setup. "DUT" is device under test and LNA denotes the two linear amplifiers of the measurement channels.

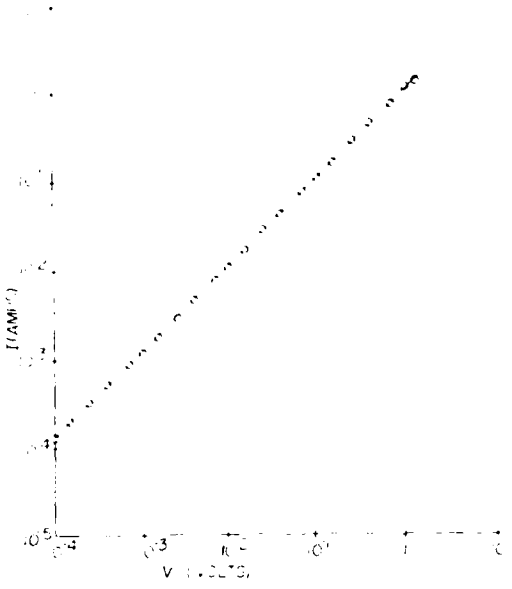

Fig. 4. I–V characteristic n^+nn^+ device.

3582 spectrum analyzer, featuring a dual-channel fast-Fourier transform method, was employed. By measuring the coherence (square of the correlation) between the two channels, noise levels significantly below the noise level of the preamplifier could be detected. For the preamplifiers we used five common emitter transistors GE82 in parallel. This resulted in a 7 Ω noise resistance for frequencies above 20 Hz. The equivalent noise resistance of the cross-correlation setup was found to be as low as 0.2 Ω, thus enabling us to accurately measure the thermal noise of the very low ohmic n^+nn^+ devices.

The d.c. I–V characteristic of an n-type device is shown in Fig. 4. For the higher voltage low duty-cycle pulsed measurements were made. The highest voltage over each layer is about 0.2 V, well below the occurrence of intervalley scattering. We notice that within the experimental errors, the characteristic is entirely linear, in agreement with the theoretical curves given in Ref. [7] (see their Fig. 2, $L = 0.5\,\mu$ sample with $V \leq 0.3$ v. In accord with their conclusions, we note that near-ballistic behavior cannot usually be deduced from just a measurement of the I–V characteristic. The resistance value deduced from Fig. 4 is 0.75 Ω.

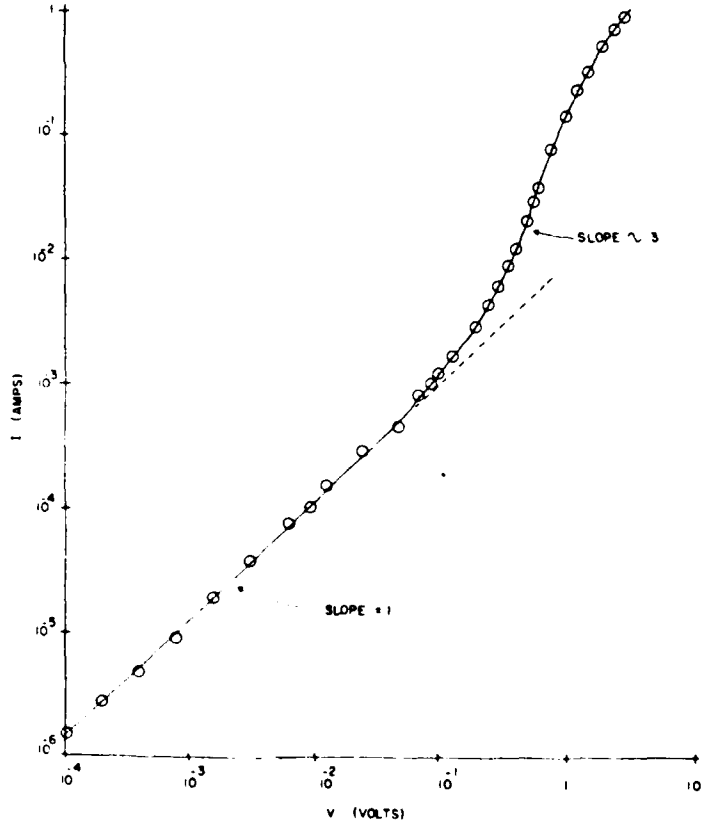

Fig. 5. I–V characteristic of n^+pn^+ device.

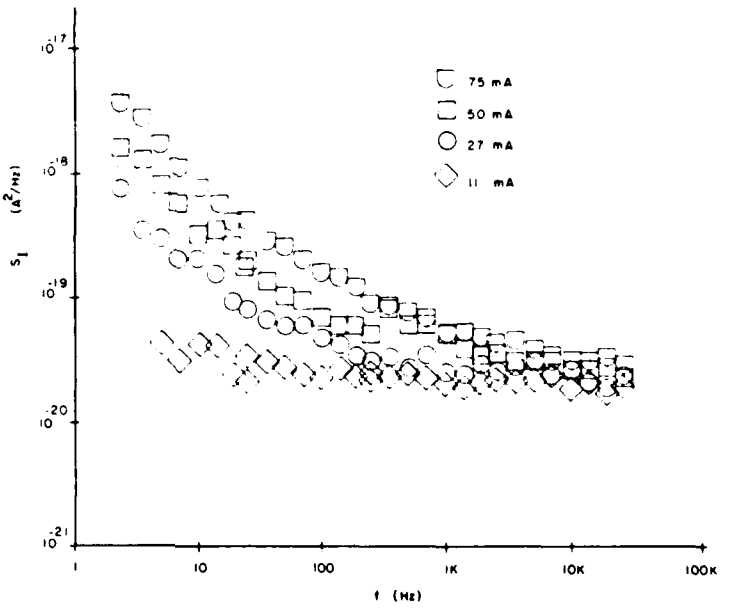

Fig. 6. Noise spectra for n^+nn^+ device.

Alternating current (a.c.) impedance measurements between 1 Hz and 1 kHz showed a flat response and confirmed this resistance value. These results are similar to the latest results reported by Hollis *et al.*[13].

The d.c. I–V characteristic of a p-type device is shown in Fig. 5. The device is linear up to a current level of 1 mA, corresponding to about $R_s = 90\,\Omega$. The slope then increases to a value of about 3 in the 10–100 mA range. Finally, at very high currents the slope becomes less, perhaps approaching three-halves as the slope falls off. The a.c. resistances are again flat for all measured frequencies (up to 100 kHz).

3. NOISE OF n^+nn^+ DEVICE

The magnitude of the noise current spectrum for four different currents, in the frequency range 1 Hz–25 kHz, is shown in Fig. 6. Thermal levels and excess $1/f$ noise are seen. To determine the thermal (-like) noise levels, the $1/f$ components are subtracted. The results are shown in Fig. 7. The levels are averaged over the frequencies for which there is a plateau (1–25 kHz; the 75 mA curve may, however, show some g–r noise from 1–7 kHz; the thermal-like noise occurs for 7 kHz and higher). The ratio of these averages to $4kT\ 0.75$ is plotted versus bias current in

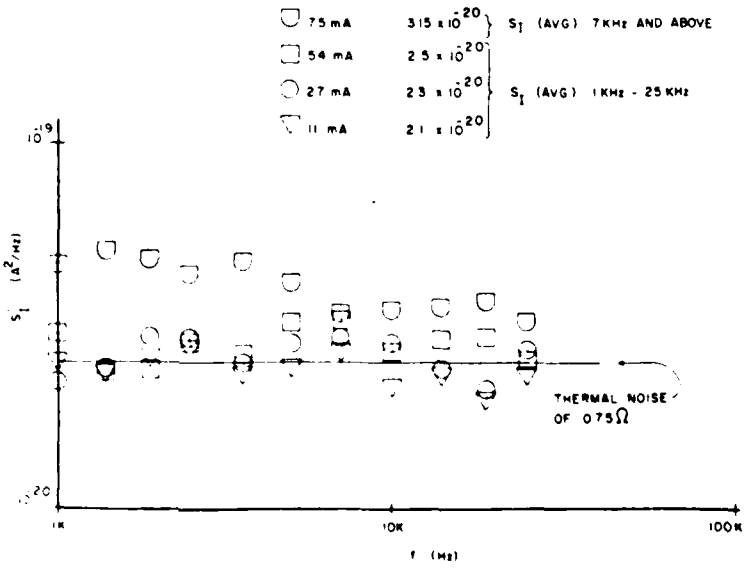

Fig. 7. Thermal (-like) noise for n^+nn^+ device.

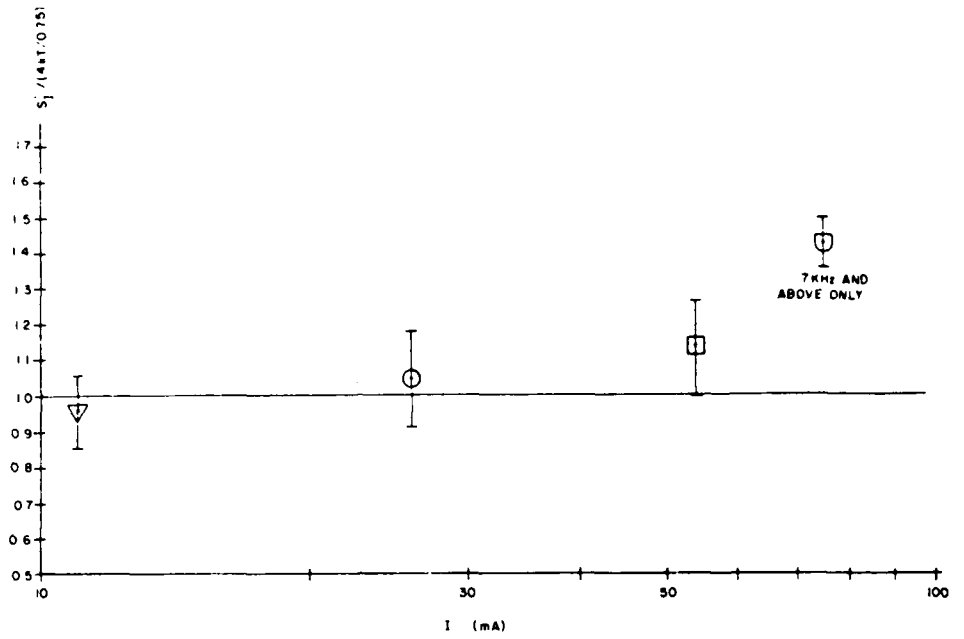

Fig. 8. Plot of thermal (-like) noise of n^+nn^+ diode vs diode current.

Fig. 8. We note that there is an indication that the noise exceeds the true thermal noise $4kTR$, at the higher bias currents.

The $1/f$ slope of the noise for the higher current levels is clearly seen, and straight-line approximations are made to the data. The values so obtained at 10 hz are plotted versus bias current in Fig. 9. We note that the expected behavior for $1/f$ noise, $S_I \propto I^2$, is well satisfied.

4. NOISE OF n^+pn^+ DEVICE

The noise current spectrum versus frequency for several bias currents of an $n^+p\ n^+$ device is shown in Fig. 10. The excess low-frequency noise of this device is orders of magnitude larger than for the n-type device. Another notable feature is the frequency dependence, which shows a slope of $f^{-0.7}$ to $f^{-0.8}$. Extrapolating to the corner frequency above which thermal noise dominates gives a value of over 100 MHz for even the lowest (100 μA) bias current.

The dependence of the noise current on bias current at 100 Hz is displayed in Fig. 11. There is an I^2 dependence up to about 1 mA. At higher currents the noise increases less fast and probably goes through a maximum.

5. DISCUSSION OF n^+nn^+ RESULTS

(a) *1/f noise*

In 1969 Hooge developed the following empirical formula for $1/f$ noise:

$$S_{VI}(f)\, I^2 = \alpha_H\, I/N, \qquad (5.1)$$

where f is the frequency, N the total number of carriers in the sample contributing to the noise, and α_H is Hooge's parameter. Initially, α_H was thought to be a constant, of order 2×10^{-3}. Later on, it was found that material variations for α_H do occur, whereas in addition α_H decreases as $(\mu\ \mu_i)^2$ if impurity scattering dominates over lattice scattering (μ_i); Bosman *et al.*[14] also found that α_H decreases due

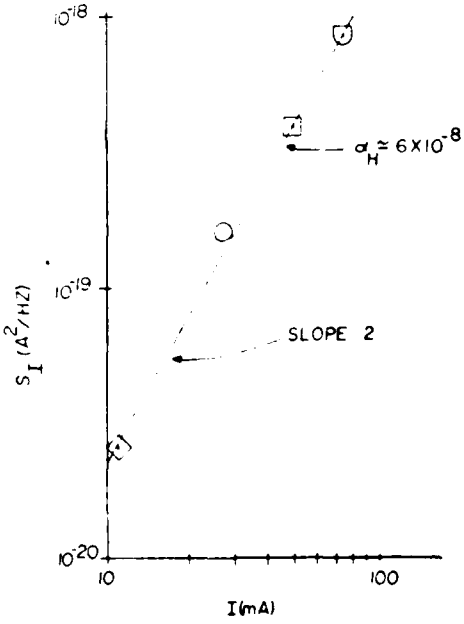

Fig. 9. $1/f$ noise of n^+nn^+ diode vs current at $f = 10$ Hz.

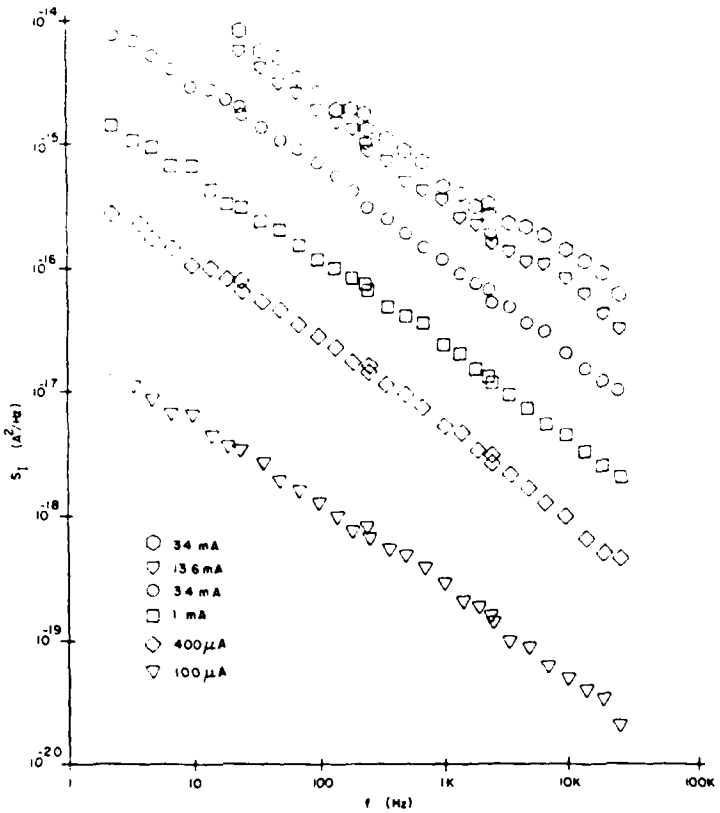

Fig. 10. Noise spectra for n^+pn^+ device.

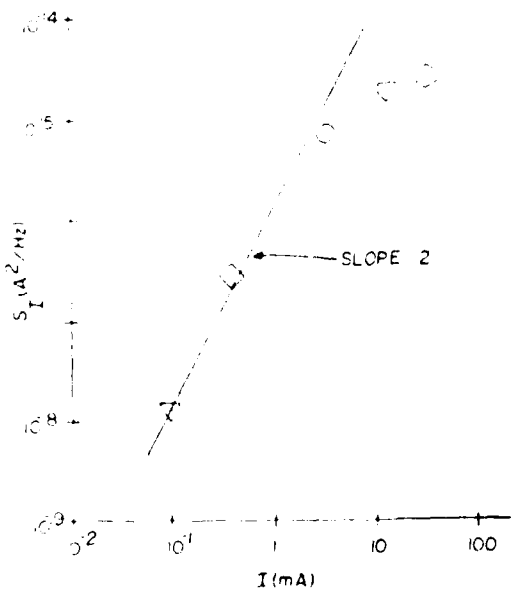

Fig. 11. Noise of n^+pn^+ device vs current at 100 Hz.

to carrier heating. In a nonhomogeneous sample in which the carrier density is a function of position, $n(x)$, such as occurs in our mesas due to spillover (Section 1) and injection, eqn (5.1) must be modified. It is easily shown (van der Ziel and van Vliet[15]) that in that case (5.1) is to be replaced by

$$S_{VI}(f)\, I^2 = (a_H / AL^2 m) \int_0^L \frac{\mathrm{d}x}{n(x)}, \qquad (5.2)$$

where m is the number of n layers in series, L the width of one n layer, and A the cross section. This formula is correct, whether or not the motion of the carriers is ballistic. Whereas the detailed profile $n(x)$ is complex due to spillover and carrier flow, we may assume that for most of the layer $n(x) \cong 1.5 n_0$, where n_0 is the doping denisty[16]. With this estimate we obtain for α_H from Fig. 19, $\alpha_H = 6 \times 10^{-3}$. This is considerably lower than the value of α_H for bulk GaAs, which Hooge *et al.*[17] list as 6×10^{-3}. Thus the measurements of this paper confirm that collisions are mainly absent in this device. Moreover, if Handel's theory of $1/f$ noise is valid[18], very low noise can be expected from those collisions which still

occur, involving polar phonon emission. As we noticed, the deflection angle θ for such processes is very small, whereas in Handel's theory of quantum 1/f noise the magnitude goes as $\sin^2\frac{1}{2}\theta$. Measurements on 0.24 μm devices are underway. Very recent data by J. Andrian *et al.* [19] indicate that for these devices α_H shows a continued decrease. So far, these results are the best confirmation yet that 1/f noise is caused by lattice phonon collisions.

(b) *Thermal noise*

The designation "thermal noise" is used here for the thermal-like noise observed at high frequencies. In a collision-limited device this noise is due to the diffusion-noise source, which by Einstein's relation transforms to a thermal-noise source for cold electrons. In the space-charge limited injection operation (Mott Gurney law), the noise becomes then $8kTR_s$ [see Ref. 12]. In a pure ballistic device, on the other hand, this noise is due to shot noise. However, the vacuum case shows that the noise is distinctly governed by the velocity distribution of the emitted particles. Thus, a treatment as the Child's law analog of Ref. 2 will not suffice to obtain the noise; the latter must be patterned after Langmuir's derivation of the d.c. characteristic; see in particular the noise treatment by D. O. North[20] and Schottky and Spenke[21]. Lacking a detailed theory, van der Ziel and Bosman[11] indicated, nevertheless, that subthermal noise, $\theta 4kTR_s$ with $\theta < 1$, can be expected. This is not corroborated by the results of Fig. 8. While it is very unlikely that the collision-limited case applies in view of the low 1/f noise reported above, it is likely that carrier drag effects, such as considered in Refs. [3, 4, 6], take place. These effects should be incorporated by considering a Langevin equation patterned after the momentum and energy balance equations of Shur and Eastman[3, 4], but with velocity dispersion as in the theory of Holden and Debney[7].

The development of a complete noise theory for ballistic and near-ballistic devices is being planned; such a theory may aid considerably in predicting the mode of operation (ballistic, near-ballistic, nonballistic) from the measured high-frequency noise.

6. DISCUSSION OF n^+pn^+ RESULTS

These devices showed large excess noise. The noise is not very close to 1/f. If, nevertheless, we apply Hooge's formula, at 10 Hz and 100 μA, we obtain $\alpha_H \simeq 3 \times 10^{-3}$.

For $V \geq 200$ mV, the I–V characteristic of Fig. 5 is in reasonable agreement with the theoretical predictions and previously reported results[1]. The current below the punch-through voltage ($\simeq 150$ mV) is not well understood. It is significant to note that the character of the noise, in particular its spectral shape, does not change when we pass the punch-through voltage, see Fig. 10, only, above the punch-through voltage the noise magnitude starts to decline, going no longer as I^2, see Fig. 11. We still remark that similar-type spectra, going slower than 1/f, were observed in 6 μm p^+np^+ punch-through diodes by van de Roer[22].

van der Ziel[23] has suggested an explanation for the n^+pn^+ d.c. characteristics, as well as the noise spectra. He interprets the low-frequency noise as a form of Hooge type 1/f noise, with a high α_H. He notes that there is a large spillover of electrons into the p region where they recombine with the holes. Though there are relatively few holes, they control the transport properties ambipolarly. Hence there are many collisions in the p region and the noise is high. At larger forward bias, the hole recombination in the p region becomes so low that it can no longer control the electron transport. Thus, the number of collisions decreases and the current becomes more ballistic; as a consequence the (I, V) characteristic curves upward and the noise decreases.

The validity of this explanation could be checked if noise measurements were made on p^+np^+ and p^+pp^+ devices. In the p^+pp^+ devices one expects a near-linear (I, V) characteristic and high noise; this noise should rise with I^2, and not go through a maximum. The p^+np^+ devices should show ambipolar transport governed by electrons. The transport should then be largely ballistic at low bias. At higher bias, the electrons would cease to act as ambipolar agents, causing the transport to become nonballistic; the (I, V) characteristic would go slower than linear and the noise would rise strongly, i.e., much faster than I^2. Noise measurements on p^+pp^+ and p^+np^+ devices are in the planning stage.

CONCLUSIONS

Near-ballistic n^+nn^+ devices exhibit extremely low 1/f noise, with a Hooge parameter of 6.0×10^{-8}. This indicates that the 1/f noise is probably caused by lattice scattering, due to polar optical phonon emission, which is rare in the near-ballistic regime. The thermal noise of these devices is slightly higher than Nyquist noise for the highest current levels observed. It indicates a near-ballistic origin, affected by carrier drag effects and by the velocity dispersion of the injected carriers.

Near-ballistic n^+pn^+ devices exhibit very large low-frequency noise. The initial current and the noise may be caused by ambipolar control of the holes in the p region. The noise rises initially as I^2, then goes through a maximum, and then decreases, due to the ballistic regime overtaking the initial current regime. Thermal noise for these devices, requiring measurements above 100 MHz, have not yet been carried out.

Similar measurements on n^+nn^+ diodes are being reported by Peczalski *et al.*[24].

Acknowledgements– We are indebted to Professor A. van der Ziel for many discussions and encouragement, and for exchange of preliminary data by the Minnesota group. This research in Florida was sponsored by AFOSR contract No 80-0050

REFERENCES

1. M. S. Shur and L. F. Eastman, *Electron. Lett.* **16**, 522 (1980); also L. F. Eastman, R. Stall, D. Woodard, N. Dandekar, C. E. C. Wood, M. S. Shur, and K. Board, *Electron. Lett.* **16**, 524 (1980).
2. M. S. Shur and L. F. Eastman, *IEEE Trans. Electron Dev.* **ED-26**, 1677 (1979).
3. M. S. Shur, *IEEE Trans. Electron Dev.* **ED-28**, 1120 (1981).
4. M. S. Shur and L. F. Eastman, *Solid-St. Electron* **24**, 11 (1981).
5. J. J. Rosenberg, E. J. Yoffa, and M. I. Nathan, *IEEE Trans. Electron Dev.* **ED-28**, 941 (1981).
6. R. K. Cook and J. Frey, *IEEE Trans. Electron Dev.* **ED-28**, 951 (1981).
7. A. J. Holden and B. T. Debney, *Electron. Lett.* **18**, 558 (1982).
8. T. C. Fry, *Phys. Rev.* **17**, 441 (1921).
9. F. N. Hooge, T. J. G. Kleinpenning and L. K. van Damme, *Reports Progress in Physics* **44**, 479 (1981).
10. A. van der Ziel, *Advances in Electronics and Electron Physics* (Edited by L. Martin), **49**, 225, Academic Press, New York (1979).
11. A van der Ziel and G. Bosman, Near thermal noise in short solid state diodes: I—ballistic regime, *Phys. Status Solidi* (a) **73**, K93 (1982).
12. A van der Ziel and G. Bosman, *ibid.* II—collision-limited regime, *Phys. Status Solidi* (a) **73**, K87 (1982).
13. M. A. Hollis, L. F. Eastman and C. E. C. Wood, *Electron. Lett.* **18**, 570 (1982)
14. G. Bosman, R. J. J. Zijlstra, and A. D. van Rheenen, *Phys. Lett.* **78A**, 385 (1980); *ibid.* **80A**, 57 (1980)
15. A. van der Ziel and C. M. van Vliet, *Physica Status Solidi* (a)**72**, K53 (1982).
16. A. van der Ziel, M. Shur, K. L. Lee, T. Chen and K. Amberiades, *IEEE Trans. Electron Dev.* (1983), in press.
17. Ref. [9], p. 496.
18. P. H. Handel, *Phys. Rev.* **A22**, 745 (1980).
19. J. Andrian, A. van der Ziel, G. Bosman, C. M. van Vliet and M. A. Hollis, to be published.
20. D. O. North, RCA Review **4**, 441 (1940); ibid. **5**, 106 (1941).
21. W. Schottky and E. Spenke, *Wissenschaftliche Veroffentlichungen aus den Siemens-Werken* **16**, 1 (1937).
22. Th. G. van de Roer, *Solid-St. Electron* **23**, 695 (1980).
23. A. van der Ziel, private communication.
24. A. Peczalski, A. van der Ziel, and M. Hollis, *IEEE Trans. Electron Dev.* (1982), in press.

Since the appearance of the above article, much more work has been done on near-ballistic devices, in particular on $n^+p^-n^+$ devices (see below) and on $n^+n^-n^+$ devices with different widths for the n^- layers (see the next section).

The $n^+p^-n^+$ device characteristic was measured at different temperatures, see Fig. 1 of Sec. E. There is still a linear I-V region at low bias, then there is a superlinear region, while at high bias the different temperature curves converge. We believe that the latter asymptote represents the true ballistic range. The results appear even clearer if we represent the data in a plot of DC conductance I/V versus the bias voltage V. This is shown in Figure 2. We now see clearly that there is an initial low conductance, which depends on the temperature (though below 77 K the data seem to coincide); then there is a transition region, followed by a final temperature-independent ballistic range. The noise spectra could initially only be measured in the low conductance region. The results for 300 K are shown in Fig. 3 and the results for 77 K are shown in Fig. 4. We note that the slopes change with temperature. The 300 K

spectra are of the form $1/f^{0.7} - 1/f^{0.8}$, while the 77 K spectra are close to the form 1/f.

The low bias current has puzzled many investigators, see the original papers by Eastman et al. (e.g., M.S. Shur and L.F. Eastman, Electronic Letters 16, 522, 1980). The expected characteristic is as in the dotted line in Fig. 1. The bias of 100 mV (20 mV per layer since the mesa contains five devices in series) is the "punch-through" voltage. The current for lower biases--which should not be there according to the pure ballistic theory--is called the pre-punch through current. Supported by the noise data, we believe that this current is recombination current, not unlike that in p-n junction depletion layers, as in the standard theory of Noyce, Shockley, and Sah. First of all, we note that for zero bias and for very low bias the p^- region is depleted of holes, due to spill-over of electrons from the n^+ regions, as was calculated quantitatively by van der Ziel and Shur. Thus the acceptor sites are all empty, the electrons being transferred to the valence band. At sufficiently forward bias, the electrons that are injected will be captured by the acceptors, and eventually by the valence band. Consequently, there is recombination current flowing, until all acceptors are filled (those before and beyond the potential minimum). This process is apparently accompanied by a very large amount of recombination noise, with distributed time constants, resulting in $1/f^{\alpha}$, $\alpha < 1$, noise. For low temperatures α increases since the shorter time constants then become less prevalent. This noise is therefore, in our opinion, not "true 1/f noise" but a form of g-r noise. This is also born out by the fact that the DC conductance in the prebreakdown region is temperature dependent. Above the "punch-through" voltage (all acceptors now occupied, $n > N_a$) the ballistic current appears. The DC conductance limit of Fig. 2 represents a conductance which is approximately a factor three lower than in the $n^+n^-n^+$ samples. This is due to the deeper space charge minimum of the former device. Note that the

space charge is $q(n - N_D)$ in the n-layer while it is $(n + N_A)$ in the p^- layer. Bosman has made quantitative computer calculations, based on the Fry-Langmuir theory, similar to those by Holden and Debney (preceding paper, Ref. 7). He found the computed DC ballistic conductance limit to be in excellent agreement with the measurements, both for the $n^+n^-n^+$ device and for the $n^+p^-n^+$ device. A paper on these data and computations is in preparation.

III. Further measurements in GaAs structures

a) 0.24μ, 0.4μ, and 1.1μ devices. Jean Andrian

1. Low-frequency measurements and I-V characteristic of $n^+n^-n^+$ diodes with different lengths

We have made systematic noise measurements on $n^+n^-n^+$ GaAs structures for various temperatures (77 K and 300 K) and various bias currents. These measurements are shown in Figs. 5, 6, 7, 8 and 9. In order to compare the magnitudes, we also plotted $(S_I/I^2) \times f$, which corresponds to α/N in Hooge's model of 1/f noise, as a function of the bias current. This is shown in Figs. 10, 11 and 12. Next we plotted this quantity as a function of the length's device. The results are shown in Fig. 13. As we note, the noise of the 0.27μ device is higher than that of the 0.4μ device. This is presently not understood, since the 0.27μ device is the nearest to collisionless, ballistic behavior.

Besides noise measurement, we have measured the I-V characteristics of these devices. These are shown in Figs. 14 and 15.

The 0.4μ device is linear, as was observed by Schmidt et al.; see preceding section. In the 1.1 μm we observed a change of conductance at higher bias ($\approx$ 0.7 volt). This phenomenon does not occur in the .4 μm device for the same applied field. We believe that the .4 μm device operates in the near-ballistic mode, while the 1.1 μm one is a bulk device. This change of conductance is probably due to intervalley transfer, i.e., the electrons go from a valley with low effective mass to a valley with a higher effective mass.

We should be able to detect the noise due to this intervalley scattering. This would be a very interesting phenomenon. In order to measure that noise we set up a noise measurement system which operates in the radio frequency range. With this system we will be able to measure the change of thermal noise with bias and the intervalley scattering noise in the transition region.

2. K-F noise measurement system

Essentially, we have to measure the thermal noise of a device with a 1Ω resistance. We set up the correlation measurement system indicated in Fig. 16. We made a preliminary test on the linearity of the mixer and the sensitivity of the system. We plotted the DC meter reading versus the power input at the power splitter. The results were excellent. The mixer has a wide range in which it operates linearly; however, we need to have a DC amplifier with a gain of 1000 (linear) in order to be able to observe the thermal noise with a bandwidth of 1 MHz. This is done by a single invertor circuit as shown in Fig. 17. Measurements with this high-frequency noise system, in an attempt to find the intervalley noise, are in progress.

b) Pulsed noise measurements on $n^+p^-n^+$ GaAs devices. Chris Whiteside

1. Pulsed bias noise measurement system

Completion of the pulsed bias noise measurement system has been accomplished. This system permits noise measurements on devices at very high bias levels. The device is pulsed at a low-duty cycle in order to avoid excessive Joule heating. Figure 18 shows the final pulsed noise measurement system.

2. Results

Initial experiments using the pulsed system were completed on a near-ballistic GaAs diode. This diode had been used in previous experiments. We wanted to extend the bias current level in order to determine the current noise in the ballistic range. According to the I-V characteristic of Fig. 1 (see previous section), it is believed that the device becomes ballistic at high

current levels. Thus a drop in the current noise must take place. Fig. 19 shows that as the current level is increased, the noise begins to fall off. This is a plot of S_I vs. f. The current through the device was increased up to one ampere. Device heating was kept low by the low-duty cycle of the measurement system. Clear plots of the noise as a function of current for 4 MHz and 8 MHz are given in Figs. 20 and 21. Though the decrease of the noise is very pronounced, we have not been able to reach the ballistic noise limit, which is estimated to be at 10^{-14} at the ordinate scale of Figs. 20 and 21. This would require current in excess of 10 amperes! Measurements as a function of temperature are in the planning stage.

c) Superlattice measurement

We have obtained a three-layer, GaAs-$Al_xGa_{1-x}As$ heterostructure device (from Dr. Morkoç) with which noise measurements can be made. Heterostructures make it possible to measure the effects of a two-dimensional electron gas.

The structure of these devices is shown in Figure 22, with the physical dimensions of the layers given in Table 1. The Al mole fraction of 20% causes a conduction band discontinuity of 0.21 eV. This bandgap difference between the GaAs and $Al_xGa_{1-x}As$ layers forms potential wells. Electrons confined in these potential wells behave like a two-dimensional electron gas.

The current-voltage characteristic of the heterostructure is shown in Figure 23. Noise measurements were also performed and are shown in Figure 24. All measurements were performed at 300 K. Problems involved with cooling the heterostructure have been solved so that noise spectra as a function of temperature will be measured in the near future.

Table 1

Device (three-period)	#337	#328
GaAs top layer (undoped)	200 Å	200 Å
$Al_xGa_{1-x}As$ (Si-doped)	250 Å $\simeq 10^{18}/cm^3$ x = 0.20	1000 Å $10^{18}/cm^3$ x = 0.20
Separation layer (undoped $Al_xGa_{1-x}As$)	150 Å	150 Å
Sheet electron concentration $n_s[cm^{-2}]$ 300 K	$2.8\ 10^{12}$	$2.67\ 10^{12}$
77 K	$2.24\ 10^{12}$	$1.02\ 10^{12}$
10 K	$2.24\ 10^{12}$	$1.88\ 10^{12}$
$\mu_{Hall}[cm^2/V\ sec]$ 300 K	$6.65\ 10^3$	$6.09\ 10^3$
77 K	$9.3\ 10^4$	$7.63\ 10^4$
10 K	$2.06\ 10^5$	$1.64\ 10^5$
Contact spacing L	400 µm	400 µm
Contact width W	40 µm	40 µm

IV. 1/f Fluctuations in Alpha Radioactive Decay from ^{241}Am*

by

J. Gong, C.M. Van Vliet, W.H. Ellis, and G. Bosman
Dept. of Electrical Engineering and Nuclear Engineering Sciences
University of Florida, Gainesville, FL, 32611

and

P.H. Handel, Department of Physics,
University of Missouri - St. Louis, St. Louis, MO, 63121

Abstract

Counting statistics of alpha particles from Americium-241 were determined over periods from 1 minute to 1,000 minutes. In particular, the two-sample variance or Allan variance was determined for many sample runs. According to a recent theorem, there is a unique relation between the particle flux spectral noise density and the Allan variance. It was found that for small counting periods the statistics were Poissonian, corresponding to shot noise of the particle flux. For long periods the counting statistics were found to be non-Poissonian, and a flicker floor of $\approx 10^{-7}$ was established. Good agreement with the quantum theory of 1/f noise was obtained. These experiments are the first quantitative confirmation of this theory.

*Submitted to Phys. Review A

1. Introduction

Whereas most of noise phenomena, like shot noise, thermal noise, and generation-recombination noise, are well understood, 1/f noise remains to some extent an enigma. This noise has been observed in a great variety of systems: semiconductor devices, music, traffic flow, hourglass flow, the frequency of sunspots, the light output of quasars, etc. Because of its universality, some investigators believe that there must be some common phenomenon operative in all of these manifestations[1]-[4].

One of the general theories of 1/f noise is the quantum theory, based on infrared divergent coupling of the system to the electromagnetic field or other elementary excitations. It was mainly developed by Handel[1][5]. This theory is fundamental in the sense that it derives the 1/f spectrum from basic quantum physics at the level of a single charged particle subject to scattering with small energetic losses due to bremsstrahlung, although the final result depends essentially on the presence of many carriers; in this respect 1/f noise is similar to electron diffraction which is a one-particle effect, but which can be seen only if many particles are diffracted. In addition, the theory is universal in the sense that any infraquanta with infrared-divergent coupling to the current carriers will give a contribution to the observed 1/f noise proportional to their coupling constant. Such infraquanta are, for example, very low-frequency photons, various types of phonons, shallow electron-hole pairs on the Fermi surface of a metal, spin waves, correlated states, etc.

Recently, this theory has been reformulated with quantum-optical terminology and compound-Poisson statistics in a paper[6] written by Van Vliet and Handel, which led to the idea of verifying the theory on a "clean" system outside the domain of currents in solids: radioactive α-decay.

In this paper we present data obtained from extensive measurements on counting techniques for α-particles radioactive decay from ^{241}Am, which have shown that the statistics are non-Poissonian for large counting times (order 1,000 minutes) in contrast with the fact that many textbooks cite α-decay as the example "par excellence" for Poisson statistics. With the help of the newly devised Allan variance transform theorem[7], we found that this excess noise does have a 1/f spectrum, and the "flicker floor" due to the presence of 1/f noise in the decay has a value of 10^{-7} which is in fair agreement with Handel's quantum 1/f noise theory. This result indicates that 1/f noise is caused by emission of long wavelength infraquanta, such as soft photons causing minute inelastic losses in the scattered wave packet.

2. Results of the Theory

2.1. Quantum approach to 1/f noise

It is known that upon scattering a beam of electrons will emit bremsstrahlung. The power spectrum W(f) of the emitted radiation is independent of frequency (W = constant) at low frequencies and decreases to zero at an upper frequency limit f_m which is approximated by E/h, where E is the kinetic energy of the electrons; h is Planck's constant. Consequently, the rate of photon emission per unit frequency interval is $N(f) = \frac{W}{hf}$, i.e., proportional to 1/f. Therefore, we conclude that the fraction of electrons scattered with energy loss ε is proportional to 1/ε, i.e., the relative squared matrix element for scattering with energy loss ε is $|b_T(\varepsilon)|^2 \propto 1/\varepsilon$.

If the incoming beam of electrons is described by a wave function $\exp[(i/\hbar)(\vec{p}\cdot\vec{r} - Et)]$, the scattered beam will contain a large nonbremsstrahlung part of amplitude a, and an incoherent mixture of waves of amplitude $ab_T(\varepsilon)$ with bremsstrahlung energy loss ε ranging from some resolution threshold ε_o to an upper limit $A \leq E$, of the order of the kinetic energy E of the electrons

$$\psi_T = \exp\left[\left(\frac{i}{\hbar}\right)(\bar{p}\cdot\bar{r} - Et)\right] a\left(1 + \int_{\varepsilon_o}^{\Lambda} b_T(\varepsilon) e^{i\varepsilon t/\hbar}\, d\varepsilon\right). \tag{2.1}$$

Here $b_T(\varepsilon) \equiv |b_T(\varepsilon)| e^{i\gamma_\varepsilon}$ has a random phase γ_ε which implies incoherence of all bremsstrahlung parts, and $|b_T(\varepsilon)|^2$ is proportional to $1/\varepsilon$, as we saw above.

In Eq. (2.1) the frequency-shifted components present in the integral interfere with the elastic term, yielding beats of frequency $\varepsilon/\hbar$. The particle density given by Eq. (2.1) is

$$|\psi_T|^2 = |a^2|\left(1 + 2\int_{\varepsilon_o}^{\Lambda} |b_T(\varepsilon)| \cos\left(\frac{\varepsilon t}{\hbar} + \gamma_\varepsilon\right) d\varepsilon + \int_{\varepsilon_o}^{\Lambda}\int_{\varepsilon_o}^{\Lambda} b_T^*(\varepsilon) b_T(\varepsilon') e^{i(\varepsilon'-\varepsilon)t/\hbar}\, d\varepsilon d\varepsilon'\right); \tag{2.2}$$

the second term in large parentheses describes the particle density beats.

If the particle fluctuation is defined by $\delta|\psi|^2 = |\psi|^2 - \langle|\psi|^2\rangle$, its autocorrelation function will be

$$\langle \delta|\psi|_t^2\, \delta|\psi|_{t+\tau}^2\rangle = \langle |\psi|_t^2\, |\psi|_{t+\tau}^2\rangle - \langle|\psi|^2\rangle^2$$

$$\approx 2|a|^4 \int_{\varepsilon_o}^{\Lambda} |b(\varepsilon)|^2 \cos\left(\frac{\varepsilon\tau}{\hbar}\right) d\varepsilon = 2|a|^4 \int_{f_o}^{\Lambda/h} h|b(\varepsilon)|^2 \cos 2\pi f\tau\, df \tag{2.3}$$

which is proportional to $|b(\varepsilon)|^2$ and hence proportional to $1/f$. Therefore, the spectral density of the particle concentration fluctuation (the Fourier transform of Eq. (2.3)) is proportional to $1/f$.

The relative bremsstrahlung rate $|b(\varepsilon)|^2$ can be derived as follows. The constant spectral energy density can be written as $w(f) = 4e^2|\Delta\vec{v}|^2/3c^3\kappa$, where e is electronic charge, κ the dielectric constant of the medium,

c is the velocity of light, and $\Delta\vec{v}$ is the velocity change in the scattering process. The relative scattering rate density with energy loss ε, $|b(\varepsilon)|^2$, is obtained by dividing W(f) by the energy of a photon $\varepsilon = hf$.

$$|b(f)|^2 = \frac{4e^2(\Delta\vec{v})^2}{3c^3\kappa 2\pi\hbar f} = \frac{e^2}{\hbar c}\,\frac{2(\Delta\vec{\beta})^2}{3\pi\kappa f} = \frac{\alpha A}{\kappa f} \tag{2.4}$$

$$|b(\varepsilon)|^2 = \frac{4e^2(\Delta\vec{v})^2}{3c^3\kappa h\varepsilon} = \frac{\alpha A}{\kappa\varepsilon} \tag{2.5}$$

where

$$A = \frac{2(\Delta\vec{\beta})^2}{3\pi}\ , \quad \Delta\vec{\beta} = \frac{\Delta\vec{v}}{c}\ , \tag{2.6}$$

and $\alpha = \frac{e^2}{\hbar c}$ is the fine structure constant. In the M.K.S. system $\alpha = \frac{e^2}{\hbar c\kappa_o}$ where κ_o is the dielectric constant of vacuum. The spectral density of the relative fluctuations is from (2.3), (2.5), and the Wiener-Khintchine theorem,

$$S_{|b|^2}(f)/\langle|b|^2\rangle^2 = 2[1+\alpha A\ln(A/\varepsilon_o)]^{-2}\alpha A/\kappa f \approx 2\alpha A/\kappa f\ . \tag{2.7}$$

2.2. The Allan variance transform theorem

The main link between counting statistics and particle current noise is provided by MacDonald's theorem[8],

$$\frac{d}{dT}\langle\Delta M_T^2\rangle = \frac{1}{\pi}\int_o^\infty S_m(\omega)\omega^{-1}\sin\omega T\, d\omega \tag{2.8}$$

with inversion

$$S_m(\omega) = 2\omega\int_o^\infty \sin\omega T\left(\frac{d}{dT}\langle\Delta M_T^2\rangle\right)dT\ ; \tag{2.9}$$

here $\langle\Delta M_T^2\rangle$ is the variance of the total number of particles detected in a time interval (t, t + T) and $S_m(\ )$ the noise spectral density of the flux fluctuations $\Delta m(t)$. This theorem is useful for Poissonian statistics.

Unfortunately, for 1/f noise Eq. (2.8) is not applicable, since the integral diverges. However, a useful concept in this case is the "two sample variance" or "Allan variance"[9]. Let $m_T^{(1)}$ be the average counting rate in $(t, t+T)$ and $m_T^{(2)}$ the counting rate in $(t+T, t+2T)$. Likewise, let $M_T^{(1)} = m_T^{(1)}T$ be the total number counted in $(t, t+T)$ and let $M_T^{(2)} = m_T^{(2)}T$ be the total number counted in $(t+T, t+2T)$. Then the Allan variance is defined by

$$\sigma^{A2}_{m_T} = \frac{1}{2} < \left(m_T^{(1)} - m_T^{(2)} \right)^2 > \tag{2.10}$$

and

$$\sigma^{A2}_{M_T} = \frac{1}{2} < \left(M_T^{(1)} - M_T^{(2)} \right)^2 > = T^2 \sigma^{A2}_{m_T} . \tag{2.11}$$

The variance σ^{A2} (which means $(\sigma^A)^2$) turns out to be finite for 1/f noise.

The transform theorem reads[7]

$$\sigma^{A2}_{M_T}(T) = \frac{4}{\pi} \int_0^\infty \frac{S_m(\omega)}{\omega^2} \sin^4 \left(\frac{\omega T}{2} \right) d\omega \tag{2.12}$$

with inversion

$$S_m(\omega) = -\frac{1}{2\pi i} \int_{-i\infty+\beta}^{i\infty+\beta} \frac{dp}{\omega^{p-2}} \frac{\cos \frac{1}{2} p\pi}{1 - 2^{p-3}} \Gamma(p) \int_0^\infty \frac{dT}{T^p} \sigma^{A2}_{M_T}(T) \tag{2.13}$$

(Slightly more complicated inversion forms using partial Mellin transforms are found in [7].) For Poissonian shot noise $S_m(\omega) = 2m_o$, where m_o is the average counting rate. Substituting $S_m(\omega)$ into Eq. (2.12), one has $\sigma^{A2}_{M_T}(T) = m_o T$. For 1/f noise, with a spectrum of $S_m(\omega) = \frac{2-C}{|\omega|}$, where C is a constant, the Allan variance $\sigma^{A2}_{M_T} = 2CT^2 \ln 2$. Now suppose that the noise is composed of shot noise and 1/f noise, i.e.,

$$\sigma^{A2}_{M_T}(T) = m_o T + 2CT^2 \ln 2 \; ; \tag{2.14}$$

We recall that $\langle M_T \rangle = m_o T$, so that a measurement of the relative Allan variance $R(T) = \sigma^{A2}_{M_T}(T) / \langle M_T \rangle^2$ yields,

$$R(T) = \frac{1}{m_o T} + 2C' \ell n 2 \quad , \tag{2.15}$$

where $C' = \frac{C}{m_o^2}$ is the characteristic strength of the 1/f noise $S_m(f)/m_o^2$. For short-time intervals the term $\frac{1}{m_o T}$ is dominant, hence R(T) is proportional to 1/T. When T is long enough, the term $2C'\ell n 2$ becomes dominant. For large T one cannot further reduce the relative accuracy by longer counting; $R(T_\infty) = 2C'\ell n 2$ is therefore called the "flicker floor".

We conclude from the above that the presence of 1/f noise in counting statistics can be determined from a measurement of the Allan variance as a function of T.

3. Experimental Method

3.1. Procedure

The block diagram of the counting system being used to investigate 1/f fluctuation in the α-particle emission rate is shown in Fig. 25. The source is ^{241}Am, which decays with a half-life of $T_{1/2}$ = 458 years with the emission of 5.48 (86%), 5.44 (12.7%), and 5.34 (1.3%) MeV α-particles into ^{237}Np. The detector, a silicon surface-barrier detector, is reverse biased at 80 volts, and the dead times of the ND575 Analog to Digital Convertor (ADC) and ND66 Multi-Channel Analyzer (MCA) are 60 nsecs and 6 usecs respectively. Therefore, no dead-time correction is necessary, as long as the counting rate is kept below 1,000 counts per second[10] (or the averaged time elapse between two counts is higher than 1,000 usecs).

A typical full energy spectrum measured in these experiments is given in Fig. 26, in semi-logarithmic scale. The spectrum is shown on a display screen while accumulating counts and the final result, after a chosen time T,

is stored in the histogram memory units of the ND66 MCA. The full width half maximum (fwhm) of the spectrum can be found by moving the CRT display cursor across the alpha-peak channel regions, with the cursor display indicating the number of counts within each energy interval (channel). The systematic range used in these experiments with respect to the 5.48 Mev peak channel was from six fwhm's below the peak channel to two fwhm's above the peak, in this manner spanning the three prince peak radiation types. Therefore, with the range being a function of the detector resolution, the total number of counts M_T, which will be analyzed later, is always a fixed portion of the full spectrum.

The counts M_T of adjacent time intervals can be read directly from the memory units of the ND66 MCA; thus the Allan variance can be calculated by

$$\sigma^{A2}_{M_T} = \frac{1}{2}\left(\frac{1}{N-1}\right)\sum_{i=1}^{N-1}\left(M_T^{(i)} - M_T^{(i+1)}\right)^2 \quad ; \tag{3.1}$$

since

$$\langle M_T \rangle = \frac{1}{N}\sum_{i=1}^{N} M_T^{(i)} \quad , \tag{3.2}$$

the relative Allan variance, R(T), defined by Eq. (2.15), can be found by using Eqs. (3.1) and (3.2).

Part of the data, mostly the total number of counts for T longer than 1000 minutes, were not read directly from the ND66 Multichannel Analyzer. An "add-up" method was adopted; namely, $M_{1000}^{(1)}$ was obtained by adding up $M_{500}^{(1)}$ and $M_{500}^{(2)}$, and $M_{1000}^{(2)}$ equals the sum of $M_{500}^{(3)}$ and $M_{500}^{(4)}$, etc. Physically, since M_{500}s were measured in adjacent time intervals, of course the first two can be added up as the total number of counts for the first 1000-minute interval, and the third and fourth can be summed up as $M_{1000}^{(2)}$. However, in order to check the validity of this method, the following experiment has been done.

By making use of a T-connector, the output signal of the Ortec 410 amplifier was fed simultaneously into two ND575 ADCs (see Fig. 25). The first one (ADC #1) counted 100-minute measurements for 310 times, and the second one (ADC #2) accumulated 500-minute counts for 62 times; hence, both ADCs covered exactly the same time span. The "add-up" method was applied to M_{100}s, obtained from ADC #1, to find out the calculated M_{500}s.

Table 1 lists the results calculated from both ADCs for 500-minute measurements. The difference between them, in each category, is $\leq 1\%$. This shows the validity of the "add-up" method.

	ADC #1	ADC #2
$\langle M_{500} \rangle$	9062464.36	9067009.84
$\sigma^{A2}_{M_{500}}$	7862171.3	7943285.5
R(500)	$9.573 \ 10^{-8}$	$9.662 \ 10^{-8}$

Table 1. Comparison of the results obtained from the "add-up" method (ADC #1) and the real-time measurements (ADC #2).

Because of the existence of "variance of variance" (or "variance noise"), the relative Allan variance itself is a fluctuating parameter. In order to obtain an accurate value of R(T), a sufficient number of measurements must be made, especially when T is short. Figure 27 shows R(T) versus the number of measurements, N, for T = 1 min. When N is small, R(T) is spread over a wide range. When N is increased, R(T) shows less spread and finally converges to a stable value. The minimum value for N is about 70. Figure 28 gives a similar plot for T = 3 min. For a reliable value of R(T), N has to be larger than 50.

Due to the presence of variance noise, the experimental results of R(T) contain a fluctuation term ΔR, i.e.,

$$R_{exp}(T) = \frac{1}{m_o T} + 2C'\ell n2 + \Delta R \ , \tag{3.3}$$

where the average value $<\Delta R>$ should be zero. The experiment was then repeated several times, and the average of $R_{exp}(T)$,

$$<R_{exp}(T)> = \frac{1}{m_o T} + 2C'\ell n2 + <\Delta R> \ , \tag{3.4}$$

is obtained. Although the value of $<\Delta R>$ in Eq. (3.4) can hardly be exactly zero for a finite number of measurements, it should be reduced a great deal compared with the value of ΔR for single measurement. The value of $<R_{exp}(T)>$ gives the best estimation to the true value of R(T).

The distance between radioactive source and detector was adjusted such that very close counting rates were obtained while repeating measurements. However, it is difficult to obtain identical counting rates. Therefore, the shot noise term in relative Allan variance, R(T), is slightly different betweeen each series of measurement.

Before the average of $R_{exp}(T)$ is taken, the shot noise term, $\frac{1}{m_o T}$, should be normalized to the same counting rate. Here a rate of 18,000 counts per minute was chosen. The normalized relative Allan variance $R_n(T)$ is then

$$R_n(T) = R_{exp}(T) - \frac{1}{m_o T} + \frac{1}{18{,}000\ T} = \frac{1}{18{,}000\ T} + 2C'\ell n2. \tag{3.5}$$

The value $<R_n(T)>$ is now used to estimate the true value of R(T). This value is calculated as follows:

$$<R_n(T)> = \frac{\Sigma R_{ni}(T) \times DF_i}{\Sigma DF_i} \tag{3.6}$$

where $R_{ni}(T)$ is the value of $R_n(T)$ obtained from the i^{th} series and DF_i stands for the degrees of freedom of that particular value, which equals the number of measured time intervals minus one.

3.2. Results

Fig. 29 shows the experimental data for $\langle R_n(T) \rangle$. The theoretical curve (solid line) is based on $R(T) = (1/18{,}000 \times T) + 1 \times 10^{-7}$ versus $1/T$, which suggests that the value of $2C'\tau n2$ is about 1×10^{-7}.

Fig. 30 shows the average value of the normalized Allan variance, $\langle \sigma^{A2}_{M_T n} \rangle$, which is obtained by

$$\langle \sigma^{A2}_{M_T n} \rangle = \langle R_n(T) \rangle \times (18{,}000 \times T)^2 \ . \qquad (3.7)$$

The theoretical curve (solid line) is based on $\sigma^{A2}_{M_T} = 18{,}000\ T + 1 \times 10^{-7} \times (18{,}000 \times T)^2$. Very good agreement is obtained as shown in these figures.

The value of $\langle R_n(T) \rangle$ and $1/18{,}000 \times T$ (shot noise level) are listed in Table 2. It shows clearly that at this counting rate, 18,000 counts per minute, for T longer than 100 minutes, 1/f noise becomes noticeable. For T longer than 1000 minutes, 1/f noise totally dominates the noise spectrum.

T(min.)	1	2	5	10	20	50
$\langle R_n(T) \rangle$	537.4	261.0	123.3	55.66	27.86	11.56
$\frac{1}{18{,}000\ T}$	555.6	277.8	111.1	55.56	27.78	11.11

T (min.)	100	200	500	1000	2000	3000
$\langle R_n(T) \rangle$	7.156	3.823	1.799	1.648	1.159	1.816
$\frac{1}{18{,}000\ T}$	5.556	2.778	1.111	0.5556	0.2773	0.1852

Table 2. The values of $\langle R_n(T) \rangle$ and $1/18{,}000 \times T$; all values $\times 10^{-7}$.

4. Discussion and Conclusions

4.1. Possible systematic sources of error

Besides the fluctuation of emission cross section described in Handel's theory, two other possibilities may contribute to the fluctuation in the total number of counts. First, the pulse height, which is produced when an α-particle is absorbed by the detector, can be a strong function of the bias voltage applied to the detector[11]. If the bias voltage were unstable, changes in the bias voltage could result in changes in the depletion depth, varying the sensitive path length experienced by the α-particle, and the depletion layer capacitance. Thus, α-particles with the same energy would have been registered under different energy channels, and would introduce unwanted fluctuations. To minimize such fluctuations, the detector control unit selected for use in these experiments, Ortec Model 210, has quite good stability: bias voltage variation with the line voltage is $\leq \pm 0.005\%$ for 105 - 125 V AC input, and the stability is $\pm 0.01\%$[12]. Also, the use of a charge-sensitive preamplifier (Ortec Model 109) diminished the system's sensitivity to changes on detector capacitance. Secondly, since a fixed portion of the full spectrum is counted, whether particles with energies near boundaries fall within or without the region they bounded contributes fluctuations to the total number of counts. However, basing the range of spectrum integration on multiples of the fwhm reduces variation due to peak spreading and gain shift.

Therefore, a wider energy range should have less fluctuations in the total number of counts in a certain time period. This is indeed the case, see Table 3. However, for T = 100 minutes, the difference between R(T)s for wider range and narrower range is negligible. For T = 500 minutes, the difference is 4%, but the value of $\langle R_n(500) \rangle$ is 62% higher than the shot noise level (see Table 2). For T = 3000 minutes, the difference is 11%, and the

value of $<R_n(3000)>$ is ten times the value for the shot noise level. Hence the energy range chosen in these experiments affected very little the final results.

T		Ch. 127-147 (Peak Channel: 142, FWHM: 2.5 channels)	Ch. 112-157
100 min.	$<M_{100}>$	1812492.94	1828630.89
	$\sigma^{A2}_{M_{100}}$	2430286.7	2472416.52
	R(100)	7.398×10^{-7}	7.394×10^{-7}
500 min.	$<M_{500}>$	9067009.8	9147489.02
	$\sigma^{A2}_{M_{500}}$	7943285.5	7762255.74
	R(500)	9.662×10^{-8}	9.277×10^{-8}
3000 min.	$<M_{300}>$	54398712.1	54881014.1
	$\sigma^{A2}_{M_{3000}}$	698293362	634854514
	R(3000)	2.360×10^{-7}	2.108×10^{-7}

Table 3. Comparison of experimental results for narrower energy range (peak channel - FWHM × 6 to peak channel + FWHM × 2) and wider energy range (peak channel - FWHM × 12 to peak channel + FWHM × 6.

4.2. Comparison with the theory of quantum 1/f noise

According to Handel's theory, the constant C' in the 1/f noise term in the relative Allan variance is, cf Eq. (2.7),

$$C' = 8\,\alpha\lambda/\kappa \tag{4.1}$$

where λ is a coherence factor; for α-particles it is expected to be close

to one; α is the fine structure constant 1/137, and $A = 2(\Delta\vec{v})^2/3\pi c^2$ where $\Delta\vec{v}$ is the velocity change of the particles in the emission process[5], c is the velocity of light. For α-particles one finds

$$\frac{\alpha A}{\kappa} = 33.28 \times 10^{-7} \times \frac{E}{\kappa} \tag{4.2}$$

where E is energy in MeV and κ is the dielectric constant of the radioactive material.

In these experiments E = 5.48 MeV, so that the value of $2C'\ell n2$ (the value of the flicker floor, F) is

$$F = 4\zeta \frac{33.28 \times 10^{-7} \times 5.48}{\kappa} \times \ell n2 = 505.6 \times 10^{-7} \times \frac{\zeta}{\kappa} . \tag{4.3}$$

To the authors' knowledge, nobody has every measured the dielectric constant of AmO_2, the α-particle source used in these experiments; thus the value of κ in Eq. (4.3) is unknown. However, since the atomic structure of AmO_2 is similar to that for UO_2, the dielectric constant of UO_2 (20.4 ±1.5[13], 21.7 ±0.5[14], and 21.0 ±1[15] can then be used as a reference.

If one considers the following factors that 1) the resulting αA in Eq. (4.2) is the sum of contributions for all types of infraquanta participating in the energy transfer, and maybe only part of them were detected, i.e., the actual value for αA in these experiments may be smaller than that given in Eq. (4.2); 2) the coherence factor, ζ, is always less than unity; 3) the dielectric constant of AmO_2 may be larger than 21; then the measured value of $F = 1 \times 10^{-7}$ is in the right ballpark to verify Handel's theory. In particular, for $\zeta = 0.05$, $\kappa = 25$, one obtains $F = 1.01 \times 10^{-7}$, in accord with the observed value of Figs. 29 and 30. We believe, therefore, that these experiments constitute the first experimental verification of Handel's quantum 1/f noise theory.

In conclusion, α-particle decay has statistics which for large counting intervals ($\simeq 10^3$ min) are non-Poissonian. We established the presence of a flicker floor $R(T_\infty) = 1.0 \times 10^{-7}$. In the frequency domain, this indicates the presence of 1/f noise in the particle flux for frequencies of the order of 10^{-4} hz or less. The magnitude of the flicker floor can well be explained as electromagnetic quantum 1/f noise, providing $\zeta = 0.05$ can be explained.

(Later note: We presently think the factor K = 25 does not belong in the formula. Thus, in reality, the theoretical noise is a factor 500 too high. See our NB at the end of Section V of this report (page 51).)

References

[1] P.H. Handel, Physical Review Letters 34, 1492 (1975).

[2] P.H. Handel, Physical Review Letters 34, 1495 (1975).

[3] K.L. Ngai, Proceedings of Second International Symposium on 1/f Noise, Orlando (U. of Florida), p. 445 (1980).

[4] S. Machlup and T. Hoshiko, Proceedings of Second International Symposium on 1/f Noise, Orlando (U. of Florida), p. 556 (1980).

[5] P.H. Handel, Physical Review 22A, 745 (1980).

[6] K.M. van Vliet, P.H. Handel, and A. van der Ziel, Physica 108A, 511 (1981).

[7] C.M. van Vliet and P.H. Handel, Physica 113A, 261 (1982).

[8] D.K.C. MacDonald, Reports Progress in Physics 12, 56 (1948).

[9] D.W. Allan, Proceedings IEEE 54, 221 (1966).

[10] G.F. Knoll, Radiation Detection and Measurement (Wiley and Sons, 1979), p. 95.

[11] W.J. Price, Nuclear Radiation Detection (McGraw-Hill, 1958), p. 237.

[12] Ortec Technical Data, 210 Detector Control (1971).

[13] A.D.B. Woods, G. Dolling, and R.A. Cowley, Proceedings 4th Inelastic Scattering Neutrons Symposium, Bombay, p. 373 (1964).

[14] D.J. Huntley, Can. J. Phys. 44(11), 2952 (1966).

[15] K. Gesi and J. Tateno, Jap. J. Appl. Phys. 8(11), 1358 (1969).

V. Partition 1/f noise in pentodes. C.J. Hsieh and A. van der Ziel

It is well known that pentodes show partition noise, in addition to space-charge suppressed shot noise. It is less known that a pentode also shows partition 1/f noise. The effect was first observed by Schwantes and van der Ziel, Physica 26, 1143 and 1157 (1960). This partition noise can be isolated by a feedback procedure that reduces the regular flicker noise with a large resistor R_c in the cathode. The then remaining noise is partition 1/f noise. This noise was remeasured in an attempt to compare it with Handel's theory.

a) Quantum picture of flicker noise

According to Handel's theory[10], there is a quantum approach 1/f noise. There should be a quantum 1/f noise part ($\sim I^2$) present in partition noise involving charged current carriers. The carriers also have infrared divergent coupling to infraquanta. The spectral density of the relative fluctuations is

$$\frac{\langle (\Delta n)^2 \rangle f}{\langle n \rangle^2} = 2 \frac{\alpha A}{f} . \tag{1}$$

The infraquanta we are going to consider here are photons, with

$$\alpha A = \frac{2\alpha}{3\pi} \left[\frac{\vec{v}_{final} - \vec{v}_{initial}}{c} \right]^2 \tag{2}$$

where $\alpha = 1/137$ is the fine structure constant and $\vec{v}_{final}$ is the velocity of a carrier at the end of the process; $\vec{v}_{initial}$ is the velocity before the process.

In the case of a pentode, three grids are present, but the screen grid is the only one carrying a positive potential. Then, the three independent noise sources present in a pentode include the partition noise $S_p(f)$, the anode noise $S_a(f)$, and grid noise S_g. The spectral density are given by

$$S_a = \Gamma^2 2eI_a + 2\frac{\alpha A_{ca}}{f}(\Gamma^2 I_a)^2 \tag{3}$$

$$S_g = \Gamma^2 2eI_g + 2\frac{\alpha A_{cg}}{f}(\Gamma^2 I_g)^2 \tag{3a}$$

$$S_p = (1-\Gamma^2)2eI_g + 2\frac{\alpha A_g}{f}[(1-\Gamma^2)I_g]^2 \ . \tag{3b}$$

Here we have denoted by Γ^2 the space charge noise suppression factor and

$$A_{ca} = 1.224 \times 10^{-5}\,(u_a - u_c) \tag{4}$$

$$A_{cg} = 1.224 \times 10^{-5}\,(u_g - u_c) \tag{4a}$$

$$A_g = 1.224 \times 10^{-5}\,u \tag{4b}$$

where u_a, u_c, u_g are the potentials of the anode, the cathode, and the screen grid, while u gives the velocity of the smoothed electrons (fraction $1-\Gamma^2$), when they arrive at the screen grid. Note that in order to take into account incoherence effects properly we have to replace f by Nf in all previous equations in the denominator. There N is the average number of electrons involved simultaneously in the process considered (e.g., transition from the cathode to the grid in the nonsmoothed way for $\alpha A_{cg}/Nf$). From the current generator defined above, we can easily obtain the spectral density of noises.

$$S_{I_a}(f) = S_a(f) + S_p(f) \tag{5}$$

$$S_{I_g}(f) = S_g(f) = S_g(f) + S_p(f) \tag{5a}$$

$$S_{I_c}(f) = S_a(f) + S_g(f) \ . \tag{5b}$$

For the partition noise Handel presents the expression

$$S_p(f) = \frac{2\alpha A_g}{f}(1-\Gamma_c^2)\,I_g^2 \tag{6}$$

where $A_g = 1.224 \times 10^{-5}$ u and u is the velocity of the smoothed electrons (fraction $1 - \Gamma_c^2$). For this expression Dr. van der Ziel expects instead

$$S_p(f) = \frac{2\alpha A_g}{f} I_a I_g \ . \tag{7}$$

The argument is as follows. Consider two pentodes, one with a screen grid transparency λ and one with a screen grid transparency $(1 - \lambda)$. Then $I_a' = I_2$ and $I_2' = I_a$. The partition noises and the partition flicker noise should be the same, so $S_{I_p}(f)$ should not change if I_a and I_g are interchanged, and Equation (7) accomplishes this. Moreover, all electrons arriving at the screen grid should distribute and not only the fraction $(1 - \Gamma_c^2)$. One might also question the factor A_g; A_{ca} is proportional to the anode potential u_a, that is to the energy with which the electrons arrive at the anode; A_{cg} is proportional to the screen grid potential u_g. So van der Ziel thinks it would be better to write

$$S_p(f) = \frac{2\alpha\sqrt{A_{ca}A_{cg}}}{f} I_a I_g \ . \tag{8}$$

In that case,

$$S_{I_a,I_g}(f) = \frac{2\alpha\sqrt{A_{ca}A_{cg}}}{f} (\Gamma_c^4 - 1)\ I_a I_g \ , \tag{9}$$

so that the fluctuations in I_a and I_g are fully uncorrelated if the cathode is saturated ($\Gamma_c^2 = 1$). This looks intuitively right.

b) Feedback effect of the cathode resistor

We apply feedback in the cathode lead by inserting R_c, as shown in Figure 31. Then,

$$v_g = -(i_c + g_{mt} v_g) R_c \ . \tag{10}$$

Simplifying the above equation, one obtains

$$v_g = \frac{-i_c R_c}{1 + g_{mt} R_c} \tag{11}$$

so that the noise current of the cathode with feedback is

$$i_c' = i_c + g_{mt} v_g = i_c \left[1 - \frac{g_{mt} R_c}{1 + g_{mt} R_c} \right] = \frac{i_c}{1 + g_{mt} R_c} . \tag{12}$$

Now we assume that the ac signals distribute between screen grid and anode in the same way as i_c. In this case

$$g_{ma} = g_{mt} \lambda \; ; \quad g_{m2} = g_{mt} (1 - \lambda) . \tag{13}$$

With feedback resistor R_c, then,

$$i_a' = i_a + g_{ma} v_g = \lambda i_c + i_p - g_{ma} \frac{i_c R_c}{1 + g_{mt} R_c} = \lambda i_c' + i_p . \tag{14}$$

So the spectrum of the anode with feedback is

$$\overline{i_a'^2} = \overline{i_c'^2} \lambda^2 + \overline{i_p^2} \; ; \; i_c' = \frac{i_c}{1 + g_{mt} R_c} \tag{15}$$

or

$$S_{I_a}(f) = \frac{S_{I_c} \lambda^2}{(1 + g_{mt} R_c)^2} + S_{I_p}(f) \tag{15a}$$

and we can also write Equation (15) and (15a) in terms of equivalent current,

$$\overline{i_a'^2} = 2q\Delta f \left[\frac{\lambda^2 I_{eq_c}}{(1 + g_{mt} R_c)^2} + I_{eq_p} \right] \tag{15b}$$

so

$$I_{eq_a} = \frac{A}{(1 + g_{mt} R_c)^2} + B \tag{15c}$$

where A and B are constants. We now define the new pentode transconductance with feedback

$$g'_{mt} = \frac{g_{mt}}{1 + g_{mt}R_c} \tag{16}$$

$$g'_{ma} = \frac{g_{mt}\lambda}{1 + g_{mt}R_c} \; ; \tag{16a}$$

i_p does not change since it flows from screen grid to anode. From Equations (12), (14), and (15) we can get

$$4KTR'_{na}df\ g_{ma}^2 = 4KTR_{nc}df \frac{g_{mt}^2\lambda^2}{(1 + g_{mt}R_c)^2} + 4KTR_{np}df\ g_{ma}^2 \tag{17}$$

since

$$g'^2_{ma} = \frac{g_{mt}^2\lambda^2}{(1 + g_{mt}R_c)^2} \; .$$

Dividing Equation (17) by $(g'_{ma})^2$, we find

$$R'_{na} = R_{nt} + R_{np}(1 + g_{mt}R_c)^2 . \tag{18}$$

According to Schwantes' results, the values of R_{np}/R_{nt} were always of the order of 0.1 and g_x/g_{mp} was always less than 0.1, so that it is negligible for most practical puposes.

c) Feedback effect with correlation between i_c and i_p

Next we consider correlation between i_c and i_p, but no feedback. Since $i_a = i_c\lambda + i_p$, the spectrum of the anode current is

$$\overline{i_a^2} = \overline{i_c^2}\lambda^2 + 2\overline{i_c i_p}\lambda + \overline{i_p^2} \tag{19}$$

and $\overline{i_c i_p} = 2qI_{eq\ cor.}f$; so one obtains

$$\overline{i_a^2} = 2q(I_{eq_c}\lambda^2 + 2I_{eq\ cor.}\lambda + I_{eq_p})\Delta f \; . \tag{19a}$$

This is without feedback. If we consider feedback and correlation, we have

$$\overline{i'^2_a} = \overline{i'^2_c}\lambda^2 + 2\overline{i'_c i_p} + \overline{i_p^2}; \quad i'_c = \frac{i_c}{1 + g_{mt}R_c} \tag{20}$$

and we can get the final formula

$$\overline{i_a'^2} = 2q\Delta f \left[\frac{I_{eq_c} \lambda^2}{(1+g_{mt}R_c)^2} + \frac{2I_{eq\ cor.}\lambda}{(1+g_{mt}R_c)} + I_{eq_p} \right]. \qquad (20a)$$

d) Transformer feedback from screen grid to control grid

As mentioned before, partition 1/f noise flows from screen grid to anode. The partition 1/f noise can be eliminated by connecting a transformer with proper turn ratio n between screen grid and control grid. The details are given in C.J. Hsieh's Engineer's thesis. The transformer feedback measurement is shown in Figure 31.

e) Experimental setup and device description

The circuit of the measurement system is shown in Figure 32. The noise devices are three pentodes, 6AUGWC (RCA), 6AG5 (RCA), and 6CE6 (GE). Since the pentode is a high-gain amplifier, we have to be careful with the input terminal. Figure 32 shows the biasing circuit of the device under test. Since the control grid is very sensitive to 60 Hz induced at the input, a low-pass filter is used, so as to reduce the 60 Hz noise as much as possible. The biasing circuit with low-pass filter consists of a 45 V DC battery, a 100 K potentiometer, and a high-quality paper capacitor (2 μF) to give the correct bias voltage needed. Similarly, we choose a wire-wound resistor Rc in the cathode lead, in order to reduce the termal noise as much as possible. Two 70 V batteries give the correct screen grid voltage. Six 70 V batteries are used as a plate power supply. The anode current I_a is monitored by an HP solid-state digital voltmeter. A 0.1 μF, 250 VW.V coupling capacitor is set in between the load resistor Rp and the Hewlett Packard 3582A spectrum analyzer to prevent the spectrum analyzer from damaging by the high-load voltage. The HP 3582A spectrum analyzer featuring a dual-channel Fast-Fourier Transform is employed essentially as a narrow-band, tunable filter.

Two I-V measurements were done on each pentode. The DC current-voltage characteristics of the pentode 6AU6WC (RCA) have the conventional form.

The whole system is first operated without cathode feedback resistor. The variable potentiometer (see Figure 32) is set to produce different biasing voltage and get different anode current. The room temperature noise current spectrum (less than 25 KHz) for three anode currents is shown in Figure 33 [for 6AU6WC (RCA)].

We next consider the measurement with cathode feedback by inserting several wire-wound resistors R_c as shown in Figure 32. The low-frequency noise spectra were measured for several resistors (R_c = 300 Ω, 500 Ω, 700 Ω, 1 KΩ, 1.5 KΩ, 2 KΩ, and 3 KΩ) up to 3 KΩ as shown in Figure 34 for 6AU6WC (RCA). The magnitude decreases with increasing resistance up to about 3 KΩ; further increasing of the cathode feedback resistor does not affect the magnitude very much, but the slope becomes less than 1/f beyond 100 Hz. Figure 35 represents the same results for the pentode 6CE6 (GE) which has a g_{mt} about 2.6 milimho and feedback resistor increasing from 500 Ω up to 10 KΩ. Table 1 lists the data obtained for several different cathode feedback resistors. The noise spectral density is obtained from the result

$$S_I \doteq \frac{S_{I_o}}{(1 + g_{mt}R_c)^2} . \tag{21}$$

Experimental results are compared with theoretical values for the pentode 6AU6WC (RCA) at 100 Hz and 1,000 Hz, and the comparison is given in Table 1 and Table 2, respectively. The comparison of the curve of S_I/S_0 versus R_c with the theoretical plots at 100 Hz and 1,000 Hz is shown in Figures 36 and 37, respectively. We note that the two curves almost coincide. Similarly, the procedure is repeated for another pentode 6CE6 (GE). Experimental results

Table 1. Comparison of experimental values with theoretical values for 6AU6WC (RCA) at various values of R_c and f = 100 Hz

R_c	No Feedback	100 Ω	300 Ω	500 Ω	700 Ω	1 KΩ	1.5 KΩ	2 KΩ
Result (S_{I_a})	-103.1 dB	-106 dB	-110.2 dB	-112.2 dB	-114 dB	-116.7 dB	-118.7 dB	-119.3 dB
Feedback Attenuation	0 dB	2.9 dB	7.1 dB	9.1 dB	10.9 dB	13.6 dB	15.6 dB	16.2 dB
Experimental Values	1	0.513	0.195	0.123	0.08	0.043	0.027	0.023
Theoretical Values	1	0.517	0.212	0.115	0.078	0.041	0.0021	0.013

Table 2. Comparison of experimental values with theoretical values for 6AU6WC (RCA) at various values of R_c and f = 1 KHz

R_c	No Feedback	100 Ω	300 Ω	500 Ω	700 Ω	1 KΩ	1.5 KΩ	2 KΩ
Results (S_{I_a})	-114.2 dB	-117 dB	-120.7 dB	-122.8 dB	-124.1 dB	-126 dB	-126.7 dB	-126.7 dB
Feedback Attenuation	0 dB	2.8 dB	6.5 dB	8.6 dB	9.9 dB	11.8 dB	12.5 dB	12.5 dB
Experimental Vlaues	1	0.524	0.223	0.318	0.102	0.06	0.056	0.056
Theoretical Values	1	0.517	0.212	0.115	0.078	0.041	0.021	0.013

are plotted and compared with the theoretical values given in Table 3 and Table 4 and are shown in Figures 38 and 39. As mentioned previously, we have

$$S_{I_a}(f) = \frac{S_{I_c}(f)}{(1+g_{mt}R_c)^2} + S_{I_p}(f) = 2q\Delta f\left[\frac{A}{(1+g_{mt}R_c)^2} + B\right] \tag{22}$$

where A and B are constants. Equation (22) can be rewritten in terms of equivalent saturated diode current.

$$Ieqa = \frac{A}{(1+g_{mt}R_c)^2} + B \ . \tag{22a}$$

Thus, suppose we plot theoretically $\log S_{I_a}$ versus $\log (1+g_{mt}R_c)$, the curve is identical to a plot of log (Ieqa) versus $\log (1+g_{mt}R_c)$. Therefore, by comparing the experimental curve of $\log (\overline{i_a^2})$ versus $\log (1+g_{mt}R_c)^2$ and $\log (\overline{i_a^2}/\overline{i_{ao}^2})$ versus $\log (1+g_{mt}R_c)^2$ with the theoretical curves for the pentode 6AU6wC (RCA), we get a result shown in Figures 40 and 41, respectively. According to the experimental data, we can calculate the A and B values as follows. From Equation (22a) and assuming $g_{mt}R_c \gg 1$, we have $(1+g_{mt}R_c)^2 \gg 1$, so that B = Ieqp and

$$2qIeqp = 2 \times 1.6 \times 10^{-19} \times Ieqp = 3 \times 10^{-21} \ ,$$

hence

$$B = Ieqp = 3 \times 10^{-21}/3.2 \times 10^{-19} = 9.6 \text{ mA} \ .$$

As mentioned before,

$$\lambda^2 = (I_a/I_c)^2 = (3.4/3.9)^2 = 0.76 \ (I_a = 3.4 \text{ mA}, \ I_c = 3.9 \text{ mA}).$$

From the experimental curve, we can find that B is less than A. So it is negligible for most practical calculation. So

$$A = Ieqc\lambda^2 = Ieqc \times 0.76$$

and

$$2qIeqc \times 0.76 = S_{I_o} = 1.224 \times 10^{-19}$$

Table 3. Comparison of experimental values with theoretical values for 6CE6 (GE) at various values of R_c and f = 100 Hz

R_c	No Feedback	500 Ω	1000 Ω	2.5 KΩ	3 KΩ	5 KΩ	7.5 KΩ	10 KΩ
Result (S_{I_a})	-92.5 dB	-98.9 dB	-101.5 dB	-105.1 dB	-105.7 dB	-107.5 dB	-108.8 dB	-109 dB
Feedback Attenuation	0 dB	6.4 dB	9 dB	12.6 dB	13.2 dB	15 dB	16.3 dB	16.5 dB
Experiment Values	1	0.022	0.125	0.05	0.045	0.031	0.023	0.022
Theoretical Values	1	0.190	0.078	0.02	0.013	0.005	0.0024	0.0013

Table 4. Comparison of experimental values with theoretical values for 6CE6 (GE) at various values of R_c and f = 1 KHz

R_c	No Feedback	500 Ω	1000 Ω	2.5 KΩ	3 KΩ	5 KΩ	7.5 KΩ	10 KΩ
Result (S_{I_a})	-103.7 dB	-110.5 dB	-112.8 dB	-116.5 dB	-117.2 dB	-119.2 dB	-119.7 dB	-120.1 dB
Feedback Attenuation	0 dB	6.8 dB	9.1 dB	12.8 dB	13.5 dB	15.5 dB	16 dB	16.4 dB
Experimental Values	1	0.20	0.128	0.05	0.04	0.028	0.025	0.022
Theoretical Values	1	0.190	0.078	0.02	0.013	0.005	0.0024	0.0013

$$I_{eq_c} = (1.224 \times 10^{-19}) / (0.76 \times 3.2 \times 10^{-19}) = 503 \text{ mA}$$

and

$$A = I_{eq_c} \lambda^2 = 503 \text{ mA} \times 0.76 = 381 \text{ mA} .$$

If Equations (22) and (22a) do not fit too well, then we have to consider the possibility of correlation between i_c and i_p. Results for the occurrence of this are found in Hsieh's thesis. See also Figure 42.

Results including transformer feedback are shown in Figure 43.

f) Effect of anode voltage on partition 1/f noise

Now we observe Figure 44; it has feedback but no transformer. We measure $\overline{i_a^2}$ at the higher R_c at $V_a = 133.74$ V and $V_a = 453.6$ V. In each case we do ten times and then calculate the average in order to improve the accuracy. The measurement of S_{I_a} may be done with a precision of 1.2% or better.

Here we measure at $V_g = 133.26$ V, $V_a = 133.74$ V, and at $V_g' = 133.43$ V, $V_a' = 453.6$ V. This hardly changed I_c (from 5.78 mA to 5.81 mA), but changed I_a (from 3.97 mA to 4.25 mA) and hence I_g changed from 1.81 mA to 1.554 mA.

As discussed in section a) for the partition noise, Handel presents the expression

$$S(f) = \frac{2\alpha A_g}{f} (1 - r^2) I_g^2 . \tag{23}$$

But van der Ziel suggested that the partition noise may be given as

$$S(f) = \frac{2\alpha \sqrt{A_{cg} A_{ca}}}{f} I_a I_g \tag{23a}$$

so that

$$\frac{[S_p'(f)]V_a'}{[S_p(f)]V_a} = \sqrt{\frac{A_{ca}'}{A_{ca}}} \frac{I_a' I_g'}{I_a I_g} = \sqrt{\frac{V_p'}{V_p}} \frac{I_a' I_g'}{I_a I_g} . \tag{24}$$

Now V_p = 133.74 − V_R = 116.36; since V_R = [illegible], [illegible] ;
V_R = 17.25 V. Hence

$$\frac{[S'_p(f)]V'_a}{[S_p(f)]V_a} = \sqrt{\frac{V'_p}{V_p}\,\frac{I'_a I'_g}{I_a I_g}} = \sqrt{\frac{436.35}{116.36}}\;\frac{(1.534 + 4.258)}{(1.81 + 3.97}$$

$$= 1.934 \times 6.613$$

$$= 1.934 \times 0.92 = 1.78 .$$

Experimentally, the noise at V'_a = 435.6 V was about 1.7 times as large as at V_a = 133.74. If we compare theoretical values with our experimental data, we find very reasonable agreement.

Handel's partition noise theory, as modified, yields

$$S_{I_1}(f) = \frac{A(V_a)}{Nf} . \tag{25}$$

The high frequencies partition noise theory gives

$$S_{I_2} = 2q\left[\frac{I_a I_g}{I_a + I_g}\right] = B(V_a) \tag{25a}$$

$$S_I = S_{I_1}(f) + S_{I_2}(f) = \frac{A(V_a)}{Nf} + B(V_a) \tag{26}$$

where $A(V_a)$ increases with increasing V_a, and $B(V_a)$ decreases. Hence

$$\frac{[S_I(f)]V_{a2}}{[S_I(f)]V_{a1}} = \frac{A(V_{a2})/Nf + B(V_{a2})}{A(V_{a1})/Nf + B(V_{a1})} . \tag{26a}$$

At low frequencies the ratio is $A(V_{a2}) / A(V_{a1})$, which is about 1.70, and at high frequencies it is about $B(V_{a2}) / V(B_{a1})$, which is about 0.90. In between there is a point where the ratio is exactly unity (crossover). So we conclude that the quantum partition noise is well verified at low frequencies by the data, but we cannot verify it well at sufficiently high frequencies.

As to the absolute magnitude of the 1/f partition noise, we have noticed already that a factor N is necessary in the denominator of Equation (7), see

Equation (25). Van der Ziel indicated that Equation (7), without the factor N, is off by a factor 10^9. For let

$$S_{I_p}(f) = \frac{2\alpha}{f}\sqrt{A_{c1}A_{c2}}\, I_a I_2 \quad A^2/Hz \tag{27}$$

where $A_{ca} = 1.224 \times 10^{-5} V_a$, $A_{c2} = 1.224 \times 10^{-5} V_2$, $\alpha = 1/137$ and I_a and I_2 are in amperes. Now if $V_a = V_2 = 133.6$ volts, $I_a = 5$ mA, $I_2 = 2$ mA, Equation (27) yields

$$S_{I_p}(f) = (2.4 \times 10^{-10}/f)A^2/H2 \ .$$

Experimentally, Hsieh observed

$$S_{I_p}(f) = (4 \times 10^{-19}/f)A^2/H2 \ .$$

This yields a ratio of 6×10^8! Thus it is certain that a factor N of order 0.6×10^9, as in Equation (25), must occur. This N must be the number of electrons in the system. If $I_c = 7 \times 10^{-3}$A, then $I_c/e = 4.4 \times 10^{16}$ electrons/sec. The transit time is

$$\tau_d = 2d/6 \times 10^7\sqrt{V_{av}} \simeq 0.48 \times 10^{-8} \text{ sec. } (V_{av} = 50\,V,\ d = 1\ cm).$$

Thus

$$N = (I_c/e)\tau_d = 4.4 \times 10^{16} \times 0.48 \times 10^{-8} = 2 \times 10^8 \ .$$

This comes very close to the experimental value involving the factor 6×10^8. Thus (25) is the correct result and not (27).

Note: It should be noted that the missing of large factors N, as indicated here, is one of the profound problems of Handel's theory. The same applies, in our opinion, to Handel's theory for emission noise involving radioactive decay (see Section IV). There a factor of $N \approx 500$ would be required in order to give a more satisfactory agreement with experiment. The apparent coherence properties of scattering particles in Handel's theory is a fact that has not yet adequately been solved. This remains one of the main obstacles of Handel's theory.

C. THEORETICAL WORK

I. Remarks on quantum 1/f noise in metal films. C.M. Van Vliet

Hooge's formula reads

$$S_I(f)/I^2 = \alpha/fN \ . \qquad (1)$$

In nondegenerate semiconductors N is the number of carriers contributing to the noise in the entire device. For metal films, N has been interpreted as the number of atoms in the film, multiplied by the valency. On the contrary, we believe that N is to be the number of electrons near the Fermi surface (a slice $\approx$ 2kT around the Fermi level), since the other carriers cannot contribute to mobility-fluctuation noise. An intuitive reasoning was presented in Section B-I. A more complete theory based on the Boltzmann transport equation is being developed. A preliminary letter to the Editor, submitted to Physica, is included herewith.

Letter to the Editor

1/f Noise in Mobility Fluctuations and the Boltzmann Equation

A. van der Ziel[1], C.M. Van Vliet[2],
Dept. of Electrical Eng., U. of Florida, Gainesville, FL, 32611, USA

and

R.J.J. Zijlstra
Natuurkundig Laboratorium Ryksuniversiteit, Utrecht, The Netherlands

and

R. Jindal[3]
Dept. of Electrical Eng., U. of Minnesota, Minneapolis, MN, 55455, USA

received 13 december 1982

Summary

The 1/f noise in mobility and diffusivity are discussed. The two noise densities are related due to an instantaneous Einstein relation, valid for times larger than the collision time. The Boltzmann equation treatment shows that Hooge's relation for the collective band mobility noise, $S_\mu/(\bar{\mu})^2 = \alpha/fN$, can be justified for a nondegenerate and spatially noncorrelated electron or ion gas.

---

1) Permanent address: Dept. of Elec. Eng., U. of Minnesota, Minneapolis, MN 55455, USA.

2) Permanent address: Centre de Recherches de Mathématiques Appliquées, Université de Montreal, Montréal, Quebec H3C3J7, Canada.

3) Present address: Bell Laboratories, Murray Hill, N.J. 07479, USA.

1. Introduction

Several recent papers have discussed the result of 1/f noise for the relative mobility-fluctuation spectrum $S_\mu(f)/(\bar{\mu})^2$ of carriers in semiconductors[1-5]. Some papers equate it to α/f and others to α/fN; here α is the Hooge parameter, f the frequency, and N the number of carriers in the sample. The discrepancy is easily resolved by distinguishing between the relative 1/f mobility-fluctuation spectrum $S_{\mu_i}(f)/(\bar{\mu}_i)^2$ of a single carrier and the 1/f mobility-fluctuation spectrum $S_\mu(f)/(\bar{\mu})^2$ for an ensemble of carriers. This was shown recently by Hooge[6]. The pertinent relations are found to be

$$S_{\mu_i}(f)/(\bar{\mu}_i)^2 = \alpha/f \tag{1.1}$$

and

$$S_\mu(f)/(\bar{\mu})^2 = \alpha/fN \ . \tag{1.2}$$

In this note we point out once more that (1.1) is the basic relation and that (1.2) follows for nondegenerate semiconductors; it may not hold for metals, degenerate semiconductors, and in ionic solutions in which carriers within a certain distance are correlated[7,8]. Our proof for the validity of (1.2) in nondegenerate semiconductors is based on the Boltzmann equation. We also derive an Einstein relation for the fluctuations and find the corresponding expression for the relative diffusivity noise $S_D(f)/(\bar{D})^2$.

2. Boltzmann equation approach

In the $\underset{\sim}{k}$-space approach we start from

$$\underset{\sim}{J}_n(\underset{\sim}{r},t) = -q \int d^3k Z(\underset{\sim}{k}) f(\underset{\sim}{r},\underset{\sim}{k},t) \underset{\sim}{v}_{\underset{\sim}{k}} \tag{2.1}$$

where $J_n(\underset{\sim}{r},t)$ is the electron current density $Z(\underset{\sim}{k}) = 1/4\,\pi^3$ is the density of states, and $\underset{\sim}{v}_{\underset{\sim}{k}}$ is the velocity in a one-particle state $|\underset{\sim}{k})$; $f(\underset{\sim}{r},\underset{\sim}{k},t)$ is the occupancy of a state $\underset{\sim}{k}$ in the vicinity of $\underset{\sim}{r}$, averaged over many collisions,

but still fluctuating due to 1/f noise. It can be computed from the mode occupancy operator average $<c_{\underset{\sim}{k}}^{\dagger} c_{\underset{\sim}{k}'}>_t$ of the quantum field, compare van Vliet et al[9].

More simply, we obtain f from the Boltzmann equation, assuming that the cross section for scattering, and thus the relaxation time τ fluctuates, either due to the fluctuating phonon population[1,2], or due to quantum 1/f noise[10]. Thus, putting $f(\underset{\sim}{r},\underset{\sim}{k},t) = f^0(\underset{\sim}{r},\underset{\sim}{k}) + f^1(\underset{\sim}{r},\underset{\sim}{k},t)$ where $f^0(\underset{\sim}{r},\underset{\sim}{k})$ is the local equilibrium distribution, we find in the usual way in the relaxation time approximation, keeping f^0 in the streaming terms and f^1 in the collision integral,

$$\underset{\sim}{J}_n(\underset{\sim}{r},t) = q\int d^3kZ(\underset{\sim}{k})\tau(\underset{\sim}{r},\underset{\sim}{k},t)$$

$$[(\underset{\sim}{v}_{\underset{\sim}{k}}\underset{\sim}{v}_{\underset{\sim}{k}})\cdot\underset{\sim}{\nabla}f^0(\underset{\sim}{r},\underset{\sim}{k}) - (q^2/\hbar)\underset{\sim}{v}_{\underset{\sim}{k}}\underset{\sim}{E}\cdot\underset{\sim}{\nabla}_{\underset{\sim}{k}}f^0(\underset{\sim}{r},\underset{\sim}{k})] \ . \qquad (2.2)$$

Writing still $\underset{\sim}{\nabla}_{\underset{\sim}{k}}f^0 = h\underset{\sim}{v}_{\underset{\sim}{k}}\partial f^0/\partial \mathcal{E}_{\underset{\sim}{k}}$, this yields the diffusion part $\underset{\sim}{J}_{n,diff} = q\underset{\sim}{\nabla}\cdot(\underline{\underline{D}}_n n)$ [for nondegenerate semiconductors, $\underset{\sim}{\nabla}\cdot(\underline{\underline{D}}_n n) = \underline{\underline{D}}_n\cdot\underset{\sim}{\nabla}n$, since $\underline{\underline{D}}_n$ does not depend on the chemical potential[11]] and the drift part $\underset{\sim}{J}_{n,drift} = q\underline{\underline{\mu}}_n\cdot E$ with

$$\underline{\underline{D}}_n(\underset{\sim}{r},t) = <<\tau(\underset{\sim}{r},\underset{\sim}{k},t)\underset{\sim}{v}_{\underset{\sim}{k}}\underset{\sim}{v}_{\underset{\sim}{k}}>> \qquad (2.3)$$

$$\underline{\underline{\mu}}_n(\underset{\sim}{r},t) = -q<<\tau(\underset{\sim}{r},\underset{\sim}{k},t)\frac{\partial \log f^0}{\partial \mathcal{E}_{\underset{\sim}{k}}}\underset{\sim}{v}_{\underset{\sim}{k}}\underset{\sim}{v}_{\underset{\sim}{k}}>> \qquad (2.4)$$

where $<< >>$ denotes a $\underset{\sim}{k}$-space average; the local, *time-fluctuating* average in $\underset{\sim}{k}$-space is defined by

$$<<\zeta(\underset{\sim}{r},t)>> = \frac{1}{\bar{n}(\underset{\sim}{r})}\int d^3kZ(\underset{\sim}{k})\zeta(\underset{\sim}{r},\underset{\sim}{k},t)f^0(\underset{\sim}{r},\underset{\sim}{k}) \qquad (2.5)$$

where we notice the occurrence of the factor $\bar{n}(r)$ in the denominator,

since distribution in k-space is normalized to n:

$$\int d^3k Z(\underset{\sim}{k})\bar{f}^0 = \bar{n}(\underset{\sim}{r}) \ , \tag{2.6}$$

(the bar denoting a time average). Restricting ourselves further to scalar D and μ and nondegenerate homogeneous semiconductors, for which $\partial \log f^0/\partial \mathcal{E}_{\underset{\sim}{k}} = -1/kT$, eqs. (2.3) to (2.5) yield

$$D_n(t) = \frac{1}{\bar{N}} \iint d^3r \ d^3k Z(\underset{\sim}{k})(v_{\underset{\sim}{k}}^2/3)\, \tau(\underset{\sim}{r},\underset{\sim}{k},t) f^0(\underset{\sim}{r},\underset{\sim}{k}) \ , \tag{2.7}$$

$$\mu_n(t) = \frac{1}{\bar{N}} \iint d^3r \ d^3k Z(\underset{\sim}{k})(q/kT)(v_{\underset{\sim}{k}}^2/3)\, \tau(\underset{\sim}{r},\underset{\sim}{k},t) f^0(r,k) \ . \tag{2.8}$$

These results show that:

(a) The fluctuating mobility, as found by the Boltzmann equation, is of the form $(1/N)\sum_{\underset{\sim}{k}} \mu_n(\underset{\sim}{k},t)$ where $\mu_n(\underset{\sim}{k},t)$ refers to the mobility of the state $|\underset{\sim}{k})$; thus, if the spectrum for $\mu_n(\underset{\sim}{k},t)$ has the form (1.1), then the spectrum of the mobility for the entire conduction band has the form (1.2) if the carrier 1/f fluctuations are independent, as in nondegenerate semiconductors. For clearly, with $S_{\mu_n(\underset{\sim}{k})}$ given by (1.1)

$$S_{\mu_{n,\text{band}}} = \frac{1}{\bar{N}^2} \sum_k S_{\mu_n(\underset{\sim}{k})} = \frac{1}{\bar{N}} S_{\mu_n(\underset{\sim}{k})} \ . \tag{2.9}$$

A more accurate computation of the band integrals involved shows that (2.9) must be modified by a factor of $3\pi/8$, cf. Kleinpenning and Bell[12]. However, in view of the experimental uncertainty of the Hooge parameter, this correction is hardly significant.

(b) There is an instantaneous Einstein relation for the fluctuating quantities $D_n(t)$ and $\mu_n(t)$:

$$D_n(t) = (kT/q)\mu_n(t) \ ; \tag{2.10}$$

Note that $t \gg \tau$ due to our assumptions of a vanishing collision integral for $f^0(\underset{\sim}{r},\underset{\sim}{k},t) \equiv f^0(\underset{\sim}{r},\underset{\sim}{k})$. We thus have the spectral relation

$$S_{D_n}(f) = (kT/q)^2 S_{\mu_n}(f) \tag{2.11}$$

or

$$S_{D_n}/(\bar{D}_n)^2 = S_{\mu_n}/(\bar{\mu}_n)^2 \ . \tag{2.12}$$

This equation was conjectured before[13,14] but never proven.

For metals and for ionic solutions above certain concentrations a coherence volume, in $\underset{\sim}{k}$-space or in position space[7], comes into play. Then $\overline{\Delta\tau(\underset{\sim}{r},\underset{\sim}{k},t)\Delta\tau(\underset{\sim}{r}',\underset{\sim}{k}',t)} \neq F(\underset{\sim}{r},\underset{\sim}{k})\delta(\underset{\sim}{r}-\underset{\sim}{r}')\delta(\underset{\sim}{k}-\underset{\sim}{k}')$. Clearly then, though (1.1) might be valid for the individual state mobilities, the band mobility fluctuations do not obey (1.2). A computation for degenerate semiconductors and metals will be published elsewhere.

Acknowledgements

This research was sponsored by AFOSR contract #82-0226. We would like to thank the reviewers for stimulating criticism.

References

1. R.P. Jindal and A. van der Ziel, Appl. Phys. Lett. 38, 290 (1981).
2. R.P. Jindal and A. van der Ziel, J. Appl. Phys. 52, 2884 (1981).
3. K.M. van Vliet and R.J.J. Zijlstra, Physica 111 B, 321 (1981).
4. A. van der Ziel and K.M. van Vliet, Physica 113 B, 15 (1982).
5. F.N. Hooge, Phys. Lett. 29 A, 139 (1969).
6. F.N. Hooge, Physica 114 B, 391 (1982).
7. T. Musha, J. Phys. Soc. Japan (Dec. 1982), in press.
8. T.G.M. Kleinpenning, Physica 103 B, 345 (1981).

9. M. Charbonneau, K.M. van Vliet, and P. Vasilopoulos, J. Math. Phys. 23, 318 (1982).

10. K.M. van Vliet, P.H. Handel, and A. van der Ziel, Physica 108 A, 511 (1981).

11. K.M. van Vliet and A.H. Marshak, Physica Status Solidi (b) 78, 501 (1976).

12. T.G.M. Kleinpenning and D.A. Bell, Physica 81 B, 301 (1976).

13. T.G.M. Kleinpenning, Physica 98 B, 289 (1980).

14. A. van der Ziel, Solid St. Electr. 25, 141 (1982).

II. 1/f noise due to impurity scattering. Ganesh Kousik

A calculation is made of the mobility (impurity scattering limited) fluctuations, assuming that the fluctuations in the scattering ion section are given by Handel's theory of fundamental 1/f noise.

We start with

$$\mu_n(t) = \frac{4e}{3m^*\sqrt{\pi}} \int_0^\infty e^{-w_w{}^{3/2}} \tau(w,t)\,dw \tag{1}$$

and

$$\frac{1}{\tau(t,w)} = N_o v_w \int (1 - \cos\theta)\sigma_\Omega(t,w)\,d\Omega \tag{2}$$

(within the relaxation time approximation).

$$\Delta\left[\frac{1}{\tau(t,w)}\right] = N_o v_w \int (1 - \cos\theta)\Delta\sigma_\Omega(t,w)\,d\Omega$$

$$\frac{<\Delta\tau^2>}{\tau^4} = N_o^2 v_w^2 \int (1 - \cos\theta)(1 - \cos\theta') <\Delta\sigma_\Omega(t,w)\Delta\sigma_{\Omega'}(t,w)> d\Omega d\Omega' \tag{3}$$

Assuming that scattering in different directions are not correlated and finding the frequency spectrum on both sides of (3), we get

$$\frac{S_\tau(w)}{\tau^4} = N_o^2 v_w^2 \int (1 - \cos\theta)(1 - \cos\theta')\ S_\sigma(\Omega,\Omega',w)\,d\Omega d\Omega' \tag{4}$$

and

$$S_\sigma(\Omega,\Omega',w) = <\sigma(\Omega,w)>^2 \frac{2\alpha A}{f}\,\delta(\Omega - \Omega')$$

$$\frac{S_\tau}{\tau^4} = N_o^2 v_w^2 \int (1 - \cos\theta)^2 <\sigma(\Omega,w)>^2 \frac{2\alpha A}{f}\,d\Omega\ . \tag{5}$$

Similarly, assuming that scattering of electrons with different energies are not correlated, we get

$$S_\mu = \left(\frac{4e}{3m^*\sqrt{\pi}}\right)^2 \int_0^\infty e^{-2w_w{}^3} S_\tau(w)\,dw\ . \tag{6}$$

According to Handel's theory

$$2\alpha A = \frac{16\alpha}{3\pi m^{*2} c^2} (p_o + mk_B T/p_o)^2 \sin^2 \theta/2 \tag{7}$$

{$mk_B T/p_o$ term is neglected}, θ is the scattering angle, and p_o is the electron momentum. Further,

$$\langle \sigma(\Omega,w) \rangle^2 = \left[\frac{2m^* z e^2}{4\pi\varepsilon\hbar^2 (4k^2 \sin^2 \theta/2 + \kappa^2)} \right]^4 \tag{8}$$

for a screened coulomb potential, κ^2 is the screening parameter which for nondegenerate semiconductors is the Debye screening and for metals is given by the Thomas-Fermi screening. Impurity scattering is assumed elastic (needed for the relaxation time approximation) and therefore $|k - k'| = 2|k| \sin \theta/2$.

Using (5), (6), (7) and (8), we get

$$S_{\mu_n} = \frac{A'}{f} \int_o^\infty e^{-2w} \frac{w^7}{\left[\ell n \left(1 + \frac{4k^2}{\kappa^2} \right) \right]^4} \left[\int_o^{\beta'} \frac{\tan^7 \beta}{\sec^5 \beta} \, d\beta \right] dw \tag{9}$$

where $\beta' = \tan^{-1} 2k/\kappa$, and $k^2 = 2m\varepsilon/\hbar^2$ for spherical energy surfaces.

$$A' = \frac{2 \cdot (16)^4 \cdot \alpha \varepsilon^4 k_B^4 T^4}{27\pi m^{*2} c^2 N_o^2 z^4 e^6} .$$

Equations (1), (2), and (8) give

$$\mu_n = B \int_o^\infty \frac{e^{-w} w^3}{\ell n \left(1 + \frac{4k}{\kappa^2} \right)} \, dw \tag{10}$$

where

$$B = \frac{64 \sqrt{\pi} \varepsilon^2 k_B^{3/2} T^{3/2}}{3\sqrt{m} N_o z^2 e^3} .$$

We now have

$$\frac{S_{\mu_n}}{\mu_n^2} = \frac{1}{f}\left(\frac{A'}{B^2}\right) \frac{\left\{\int_0^\infty e^{-2w} w^7 dw \Big/ \left[\ell n\left(1+\frac{4k^2}{\kappa^2}\right)\right]^4 \int_0^{\beta'} \frac{\tan^7\beta}{\sec^6\beta}\, d\beta\right\}}{\left[\int_0^\infty \frac{e^{-w}\, w^3 dw}{\ell n(1+4k^2/\kappa^2)}\right]^2}$$

$$\boxed{\frac{S_{\mu_n}}{\mu_n^2} = \frac{16\alpha k_B T}{3m^* \pi^2 c} \cdot \frac{1}{f} \frac{\left\{\int_0^\infty \frac{e^{-2w}\, w^7 dw}{[\ell n(1+4k^2/\kappa^2)]^4} \int_0^{\beta'} \frac{\tan^7\beta}{\sec^6\beta}\, d\beta\right\}}{\left\{\int_0^\infty \frac{e^{-w}\, w^3 dw}{\ell n(1+4k^2/\kappa^2)}\right\}^2}.} \qquad (11)$$

For nondegenerate silicon

$$\kappa^2 = \frac{4\pi e^2}{\varepsilon k_B T} n\left(2 - \frac{n}{N_D}\right)$$

where n is the number of conduction electrons and N_D is the donor concentration. ε the dielectric constant is 11.9 ε_o.

At temperatures in the 10° - 70°K range, not all donors are ionized. To find n, we solve the neutrality equation

$$p - n + N_D^+ = 0 \qquad (12)$$

where $N_D^+ = \frac{N_D n_1}{n_1 + n}$ and $n_1 = N_c \exp\left[\frac{E_F - E_c}{k_B T}\right]$. Therefore, the equation for n is

$$n^2 + n_1 n - N_D n_1 \simeq 0 \qquad (13)$$

neglecting terms with $n_i^2 \approx 0$. Figure 45 shows $S_{\mu_n} f/\mu_n^2$ vs. T.

In metals one uses the Thomas-Fermi screening

$$\kappa^2 = 4\pi e^2 \mathcal{N}(\varepsilon_F) \quad \text{(in CGS units)}$$

where $\mathcal{N}(\varepsilon_F)$; the density of states at the Fermi level,

$$\mathcal{N}(\varepsilon_F) = \frac{3}{2} \frac{N}{\varepsilon_F} .$$

For gold:

$$N = 5.9 \times 10^{22} \text{ cm}^{-3}$$

$$\varepsilon_F = k_B T_F = k_B \times 6.39 \times 10^4 \text{ ergs.}$$

and spherical energy surface ($k^2 = 2m\varepsilon/h^2$) have been used. $\frac{S_{\mu_n}}{\mu_n^2}$ vs. T for gold are shown in Figure 46.

Equation (11) implies $\frac{S_{\mu f}}{\mu^2}$, the noisiness, is not a strong function of the doping density in semiconductors. It is nearly a linear function of T in both Si and gold, in fact in semiconductors and metals.

The noise in gold (Fig. 45) is smaller, probably due to a much larger screening constant than in silicon. Thus the electron does not see the ion potential as strongly as in Si.

For a purely coulomb potential, we find $\tau \to 0$ and therefore

$$S_{\mu_n} \to 0 ;$$

also,

$$\mu_n \to 0, \text{ but } \frac{S_\mu}{\mu^2} \to \frac{\int \tau^4 \ldots dw}{\left[\int \tau \ldots dw\right]^2} \to 0.$$

III. Noise Out of Equilibrium*

by

Carolyn M. Van Vliet

Department of Electrical Engineering
University of Florida, Gainesville, 32611

and

Centre de Recherches Mathematiques
Universite de Montreal, Montreal, Quebec H3C3J7, Canada

Summary

We discuss six properties of stochastic processes which are generally valid only in thermal equilibrium systems. In Part A of this paper we discuss the first and most fundamental property, viz, the fluctuation-dissipation theorem. Kubo's and Van Vliet's quantum statistical mechanical derivations are reviewed. Next we discuss Gupta's thermodynamic theorem, which may hold for a class of nonequilibrium systems. In Part B we discuss the other properties which mainly center around the principles of mesoscopic reversibility and detailed balance, and the symmetrization property of the two terms in the generalized second moment relaxation theorem (also called generalized g-r theorem, generalized Einstein relation, or Λ-theorem). We then give two examples for which this symmetrization property does not hold. First we review Van Vliet's model of nonequilibrium optical pumping in photoconductors with traps. Finally, we review Tremblay's et al. derivation of Brillouin light scattering as an example of a nonequilibrium hydrodynamic steady state.

1. Thermal equilibrium properties

There are a number of properties which render the description of noise in thermal equilibrium considerably simpler than in a nonequilibrium, or driven equilibrium, steady state. The main features for fluctuation processes are as follows.

*Invited paper presented at the 7th International Symposium on Noise in Physical Systems, Montpellier, France, May, 1983.

1) Validity of the fluctuation-dissipation theorem

2) The principle of mesoscopic reversibility

3) The principle of detailed balance

4) The symmetrization property of the "generalized second moment relaxation theorem"

5) The equilibrium Einstein relation between generalized mobility and diffusivity

6) The Onsager relation for reciprocal flow problems.

The derivation of (1) will be briefly given below. The fluctuation-dissipation theorem is a genuine consequence of the existence of the micro-canonical or canonical ensemble to describe equilibrium properties. It can be derived from a purely thermodynamic point of view (Nyquist 1928, Callen and Greene 1952) or from a quantum statistical mechanical approach (Kubo 1957).

The other five properties are somewhat more subtle and have a less general form in that we must distinguish between a-variables, which are intrinsically time reversible, such as the position, and b-variables, which are odd, i.e., change sign under time reversal, such as the velocity (Casimir 1945). The details of this necessary distinction are often overlooked, and a number of errors occur even in recent literature. A much more careful consideration than hitherto given is necessary, and errors occur both in Lax (1960) and the author's papers (1965) in this respect. Since the space of this conference paper is limited, we shall make no attempt to rectify these errors hereby, restricting ourselves to a-variables. Some remarks on the other cases will be made in some instances. The five properties 2) to 6) all hang together in a unique way. One can show that the validity of any one of the five implies the validity of the others. Again, the writing of a comprehensive survey paper on this topic would be extremely useful, but space is lacking here since we have been asked to write on nonequilibrium.

This paper will therefore be divided as follows. In Section 2 we review the standard derivation due to Kubo, and its recent modification by Van Vliet (1978, 1979) of the fluctuation dissipation theory. We also discuss how a true general extension to nonequilibrium systems should be obtained. Lacking such a general extension at this moment, we review in Section 3 Gupta's thermodynamic attempt to obtain a meaningful extension for electric nonlinear circuits under a set of restricted but useful conditions (Gupta 1978, 1982).

In the rest of the paper we discuss the extensions for nonequilibrium when any of the properties 2) to 6) does not hold. This is relatively easier, since full solutions for Markovian nonequilibrium systems have existed since the initial work on optically excited generation-recombination statistics in semiconductors by Van Vliet and Blok in 1956 (a & b). The first true nonequilibrium example involving the "generalized nonequilibrium second order moment relaxation theorem" (also called generalized Einstein relation by Lax 1960, generalized g-r theorem by Van Vliet and Fassett 1965, and Λ-theorem by Van Vliet 1971) was given by Van Vliet in 1964. This is discussed in Sections 4 and 5.

In recent years renewed interest in the nonequilibrium problem arose from light scattering in the presence of a small temperature gradient, causing nonsymmetric Brillouin peaks. This problem was treated by a number of authors (Procaccia, Ronis and Oppenheim 1979, Kirkpatrick, Cohen and Dorfmann 1979, Tremblay, Siggia and Arai 1980). We will here present the treatment of the latter paper (Section 6). It will be shown that their example is another straightforward nonequilibrium application of the "generalized nonequilibrium second order moment relaxation theorem" as originally set forth by the author and coworkers (1954, 1965, 1971).

Part A. The fluctuation-dissipation theorem and extensions

2. Quantum statistical derivations

Kubo considers systems with a Hamiltonian

$$H_{total} = H - AF(t) \ . \tag{2.1}$$

Here H is the Hamiltonian of the system proper and -AF(t) the coupling to an external field. For electrical conductors, $F(t) \to q\underset{\sim}{E}(t)$ and $A = \sum_i \underset{\sim}{r}_i$, where $\underset{\sim}{r}_i$ are the position operators of all of the particles. The Von Neumann equation for the density operator now reads

$$\frac{\partial \rho}{\partial t} + \left(\frac{i}{\hbar}\right)[H,\rho] = \left(\frac{i}{\hbar}\right) u(t)F(t)\ [A,\rho] \tag{2.2}$$

where u(t) indicates that the field was switched on at t = 0. If we are now near a thermal equilibrium state, we can substitute $\rho \to \rho_{eq}$ in the r.h.s. of (2.2) where ρ_{eq} is the canonical density operator $\rho_{eq} = e^{-\beta H}/\mathrm{Tr}\ e^{-\beta H}$, $\beta = 1/kT$. The equation (2.2) can easily be solved for the average response of a flow quantity $\dot{B}$ where B is an operator in the system. One finds in a straightforward way (Van Vliet 1978)

$$\langle \Delta\dot{B}(t) \rangle = \mathrm{Tr}\ \rho(t)B - \mathrm{Tr}\ \rho_{eq}B = \int_0^t d\tau\ \phi_{\dot{B}A}(t-\tau)F(\tau) \ . \tag{2.3}$$

Here $\phi_{\dot{B}A}$ is the response function given by the commutator

$$\phi_{\dot{B}A}(t) = \frac{1}{\hbar i}\,\mathrm{Tr}\{[A,\dot{B}(t)]\rho_{eq}\} \tag{2.4}$$

where the time dependence of ρ (Schrödinger picture) was transferred to the time dependence of $\dot{B}$ (Heisenberg picture):

$$\dot{B}(t) = e^{i\mathcal{L}t}\,B^S = e^{iHt/\hbar}\,B^S\,e^{-iHt/\hbar} \tag{2.5}$$

where B^S is the Schrödinger operator (the superscript S will henceforth be omitted); $\mathcal{L}$ is the Liouville superoperator acting in the Liouville space that contains all operators A, B, ... In particular, let $\dot{B}$ be the current

$\underset{\sim}{J} = \dot{\underset{\sim}{B}} = \frac{q}{\Omega}\sum_i \dot{\underset{\sim}{r}}_i = \frac{q}{\Omega}\dot{\underset{\sim}{A}}$, where Ω is the sample volume. If we take the Fourier-Laplace transform of (2.3), then we have, denoting by ~ the transform,

$$\tilde{\underset{\sim}{J}}(i\omega) = q\underline{\underline{\tilde{\varphi}}}_{(q/\Omega)\dot{A},A}(i\omega)\cdot\tilde{\underset{\sim}{E}}(i\omega) \tag{2.6}$$

so that the conductivity becomes

$$\underline{\underline{\sigma}}(i\omega) = \frac{q^2}{\Omega}\frac{1}{\hbar i}\int_0^\infty dt\, e^{-i\omega t}\, \mathrm{Tr}\,\{[\underset{\sim}{A},\dot{\underset{\sim}{A}}(t)]\rho_{eq}$$

$$= \Omega\int_0^\infty dt\,\frac{e^{-i\omega t}-1}{\hbar\omega}\,\mathrm{Tr}\,\{[\underset{\sim}{J},\underset{\sim}{J}(t)]\rho_{eq}\}\ . \tag{2.7}$$

We have here the beginning of Nyquist's theorem: the conductivity is related to the correlation expression,

$$<[J,J(t)]> = <JJ(t)> - <J(t)J> \tag{2.8}$$

where $J \equiv J^S = J(0)$.

Now to obtain the correlation function proper, it must be defined as an anticommutator, since the product JJ(t) must be symmetrized:

$$:(t) = <[J,J(t)]_+>\ . \tag{2.9}$$

It is now possible to relate the commutator to the anticommutator with some transformations involving contour integration for the Fourier transforms. It is then possible to express the full (two-sided) Fourier transform of the correlation anticommutator into the single-sided Fourier transform given by (2.7). The result is the spectral expression

$$S_{J_\nu J_\mu}(\omega) = 4\mathcal{E}(\omega,T)\,\{[\sigma'_{\nu\mu}(\omega)]^S + i[\sigma''_{\nu\mu}(\omega)]^a\} \tag{2.10}$$

where ν and μ denote either two different (but correlated) currents or Cartesian current components, $\sigma = \sigma' + i\sigma''$, and

$$\sigma^s_{\nu\mu} = \frac{1}{2}[\sigma_{\nu\mu} + \sigma_{\mu\nu}],\ \sigma^a_{\nu\mu} = \frac{1}{2}[\sigma_{\nu\mu} - \sigma_{\mu\nu}];$$

further, $\mathcal{E}(\omega,T) = (\hbar\omega/2)\coth(\beta\hbar\omega/2)$ is the mean energy of a harmonic oscillator of frequency mode ω. Eq. (2.10) is the fluctuation-dissipation theorem in all its glory.

We have criticized Kubo's derivation in our 1978 paper, since nowhere was a form for the Hamiltonian H, commensurate with dissipation, introduced! In particular, the Heisenberg operators do not represent the required approach to equilibrium. As we indicated in our paper, a partitioning of the Hamiltonian is essential; i.e., instead of (2.1) we write

$$H_{total} = H^{o} + \lambda V - AF(t) \ . \tag{2.11}$$

Here H^{o} is the largest Hamiltonian that can be diagonalized for the many-body system, e.g., an electron-phonon system; λV represents the interactions which randomize the energy over the states of H^{o}. In the Van Hove limit ($\lambda \to 0$, t large, λ^{2}t finite) and large system limit, such randomization leads to irreversibility (The Poincaré cycle becomes "off limits" for observation in such a system). In our second paper on linear response theory we indicated that (2.2) now is carried over in an irreversible master equation, which for the reduced ρ^{R}(i.e., after the Van Hove limit) now reads

$$\frac{\partial \rho^{R}}{\partial t} + (\Lambda_{d} + i\mathcal{L}^{o})\rho^{R}(t) = F(t) \ [\text{times a functional of } \rho(t) \text{ and } A]. \tag{2.12}$$

Here Λ_{d} is the master operator

$$\Lambda_{d}K = -\sum_{\gamma\gamma'} |\gamma><\gamma|W_{\gamma\gamma'}[<\gamma'|K|\gamma'> - <\gamma|K|\gamma>]; \tag{2.13}$$

where $\{|\gamma>\}$ is the set of many-body states of H^{o}, $\mathcal{L}^{o}$ is the interaction Liouville operator $\mathcal{L}^{o}K = \hbar^{-1}[H^{o},K]$, and $W_{\gamma\gamma'}$ is the transition probability according to the golden rule, $W_{\gamma\gamma'} = (2\pi/\hbar)|<\gamma|V|\gamma'>|^{2}\delta(\mathcal{E}_{\gamma} - \mathcal{E}_{\gamma'})$. Equation (2.12) can be used similarly to (2.2) to obtain the transport coefficients σ, κ, and others, to be expressed in correlation functions involving

the reduced operators $J^R(t)J(0)$, where now $J^R(t) = \exp[-(\Lambda_d + i\mathcal{L}^o)t]J(0)$. The main problem with (2.12) is that the r.h.s. has so far only been evaluated for a near-thermal equilibrium state. For a driven equilibrium, the Hamiltonian (2.11) should be further partitioned:

$$H_{total} = H^o + \lambda V - AF - Af(t) - Fa(t) \ . \tag{2.14}$$

Here AF would be the steady driven equilibrium coupling to the sustaining field F_o, and f(t) would be a small time-dependent field perturbation. Could Equation (2.12) be reformulated for this Hamiltonian with only the part -Af(t) occurring in the r.h.s., then we could obtain a steady-state fluctuation-dissipation theorem. Such a program has not yet been carried out. One statement can be easily deduced from such a theory, however. We note that in the above the two Hamiltonians λV and AF are on an equal footing. The noise due to <u>both</u> is a function of the small signal transport coefficient caused by f(t). Since traditionally λV causes thermal dissipative noise and AF causes current or shot noise, it is clear, then, that in a generalized nonequilibrium fluctuation-dissipation theorem we will no longer be able to separate "thermal" and "shot noise"; both will be contained in the new fluctuation-dissipation theorem. This is born out by the theory due to Gupta, reviewed below.

3. <u>Gupta's thermodynamic result</u>

Since F is the driving parameter which is fixed, typically a large d.c. field, the entropy will contain intensive variables, as foreseen by Gibbs (1902), a fact overlooked by Callen in his well-known monograph (1962). Thus, properly the entropy is a Massieu-type Legendre transform of Callen's entropy. From (2.14) we arrive at a Gibbs entropy production

$$T\,d\dot{S} = d\dot{\mathcal{E}} - \dot{A}\,dF \tag{3.1}$$

where $Td\dot{S}$ represents the dissipation caused by λV. This form satisfies Gupta's thermodynamic theory. His basic assumptions are noted in his 1982

paper. The most important are:

a) The entropy depends, besides on $\mathcal{E}$, on another variable F, which can pass through the port of the system and which is fixed.

b) The system is purely resistive, so no energy is stored in $\dot{A}dF$. We should therefore be able to write $\dot{A}$ as a function of the instantaneous values of F: $\dot{A} = C_1 \langle F \rangle + C_2 \langle F^2 \rangle$, etc.

c) The system has no quantum correction. This is, in our case, born out by the use of the Λ operator.

For the present case of electrical conduction, $\dot{A}$ can again be interpreted as $(\Omega/q)J = IL/q$ where I is the current and $F = qE = Vq/L$. Thus $\dot{A}dF = IV$. Gupta's theorem for the noise now reads

$$S_{FF}(\omega) = 4kT\, P_{ex} / \overline{\dot{a}^2} \,, \tag{3.2}$$

or

$$S_{VV}(\omega) = 4kT\, P_{ex} / \overline{i^2} \,, \tag{3.3}$$

where P_{ex} is the excess power dissipation caused by the presence of a periodic zero average small signal a (or i) superimposed on the driven steady state. For a nonlinear resistor with $V = V(I)$

$$P_{ex} = \overline{(V_o + \frac{dV}{dI}\, i + \frac{1}{2}\frac{d^2V}{dI^2}\, i^2)\,(I_o + i)} - V_o I_o$$

$$= \left[\frac{dV}{dI}\,\overline{i^2} + \frac{1}{2}\,\frac{d^2V}{dI^2}\, I\,\overline{i^2}\right]_{I = I_o} \,, \tag{3.4}$$

where the overhead bar means time averaging. Clearly, from (3.3) and (3.4)

$$S_{VV}(\omega) = 4kT\left[\frac{dV}{dI} + \frac{1}{2}\, I\, \frac{d^2V}{dI^2}\right]_{I_o} \,. \tag{3.5}$$

Similarly, one finds

$$S_{II}(\omega) = S_{VV}(\omega)(dI/dV)^2 = 4kT\left[\frac{dI}{dV} - \frac{1}{2}\, I\, \frac{d^2I}{dV^2} \Big/ \frac{dI}{dV}\right]_{I_o} \tag{3.6}$$

Define now

$$\beta = \frac{1}{2}\left[\frac{d^2I}{dV^2}\Big/\frac{dI}{dV}\right]_{I_o} . \tag{3.7}$$

Then (3.6) reads

$$S_{II}(\omega) = 4kT\,[g(I_T) - \beta I_T] \tag{3.8}$$

where we replaced I_o by the more useful symbol I_T (for total average current).

Application: Schottky barrier diodes or p-n junctions at low frequencies (no energy storage in extra term). Then

$$I = I_1(e^{qV/kT} - 1) \tag{3.9}$$

$$g(I_T) = (dI/dV)_{I_T} = (q/kT)(I_T + I_1) \tag{3.10}$$

$$\beta I_T = (q/2kT)I_T .$$

Thus (3.8) reads

$$S_{II}(\omega) = 2q\,[\,(I_T + I_1) + I_1\,] , \tag{3.11}$$

indicating shot noise of forward and reverse current. Clearly, this comprises the thermal noise, for at zero bias

$$S_{II}(\omega)\big|_{V=0} = 4qI_1 = 4kTg\big|_{V=0} . \tag{3.12}$$

As we noted before, no distinction can be made between thermal noise "proper" and shot noise.

Whereas Gupta's theory is highly specialized, it has opened the way to show that steady state dissipation fluctuation theorems do exist, contrary to previous pessimistic claims (for a survey see van Kampen 1965). Gupta's result (3.6) or (3.8) is not a trivial result. Others have tried to generalize

the fluctuation-dissipation-theorem on more heuristic grounds. Van der Ziel (1973) considered the following possibilities for Nyquist's theorem in non-linear devices:

a) $\langle v_n^2(f)\rangle = 4kT\,B(V/I)$: $\langle i_n^2(f)\rangle = 4kT\,B(V/I)|y(f)|^2$

b) $\langle i_n^2(f)\rangle = 4kT\,B(I/V)$; $\langle v_n^2(f)\rangle = 4kT\,B(I/V)\,/\,|y(f)|^2$

c) $\langle v_n^2(f)\rangle = 4kT\,B(dV/dI)$; $\langle i_n^2(f)\rangle = 4kT\,B(dV/dI)|y(f)|^2$

d) $\langle i_n^2(f)\rangle = 4kT\,B(dI/dV)$; $\langle v_n^2(f)\rangle = 4kT\,B(dI/dV)\,/\,|y(f)|^2$

e) none of the above

In view of Gupta's result, possibility e) is the answer to this multiple choice question, even though it can be shown that some devices satisfy some of the other possibilities (which then must be equivalent to (3.6) or (3.8)).

Part B. The generalized nonequilibrium second moment relaxation theorem (generalized g-r theorem, generalized Einstein relation, or Λ-theorem)

4. The mesoscopic Markov process

In statistical mechanics the variables are the microscopic variables p_i and q_i or their quantum operators. In stochastic processes we deal, however, with much more coarse-grained variables, which are averages over large ranges of quantum states, even though the fluctuations in these variables cannot be seen until after suitable amplification. Brownian motion and fluctuations in carrier populations (conduction band, traps) are typical examples. We call these variables mesoscopic (term of van Kampen 1962). They can be pictured in "a-space" (De Groot and Mazur, 1962).

From the microscopic master equation, see (2.12), one can derive a mesoscopic master equation. The equation reads

$$\frac{\partial P(a,t|a')}{\partial t} = \int d^s a''\,[P(a'',t|a')Q_{a''a} - P(a,t|a')Q_{aa''}] \qquad (4.1)$$

where $Q_{a''a}$ is the transition probability per unit time for a change $a'' \to a$. Assuming that $\underset{\sim}{a}$ is a set of variables on $(0,\infty)$, one can Laplace transform the master equation, and one easily finds for the characteristic function (Van Vliet 1983)

$$\frac{\partial}{\partial t} \langle e^{-\underset{\sim}{s}\cdot\underset{\sim}{a}(t)} \rangle_{\underset{\sim}{a}'} = \sum_{n=1}^{\infty} \langle e^{-\underset{\sim}{s}\cdot\underset{\sim}{a}(t)} \frac{(-1)^n}{n=1} s^n : F_n(\underset{\sim}{a}(t)) \rangle_{\underset{\sim}{a}'} \tag{4.2}$$

where F_n is the nth order Fokker-Planck tensor

$$F_n(\underset{\sim}{a}'') = \int (\underset{\sim}{a} - \underset{\sim}{a}'')^n Q_{\underset{\sim}{a}''\underset{\sim}{a}} d^S a = \langle \underset{\sim}{a}(\Delta t) - \underset{\sim}{a}'' \rangle^n_{\underset{\sim}{a}''} / \Delta t \ . \tag{4.3}$$

Differentiating now repeatedly with respect to s, and setting s = 0, one finds the moment equations. The first moment equation is the phenomenological equation

$$\frac{\partial}{\partial t} \langle \Delta\underset{\sim}{a}(t) \rangle_{\underset{\sim}{a}'} = -\underline{\underline{M}} \langle \Delta\underset{\sim}{a}(t) \rangle_{\underset{\sim}{a}'} \tag{4.4}$$

(sub $\underset{\sim}{a}'$ means a conditional average in an ensemble with $\underset{\sim}{a}(0) = \underset{\sim}{a}'$ fixed); $\underline{\underline{M}}$ is the phenomenological relaxation matrix; it is defined by

$$M_{ij} = -\left[\frac{\partial}{\partial a''_j} \sum_{\underset{\sim}{a}} (a_i - a''_i) Q_{\underset{\sim}{a}''\underset{\sim}{a}} \right]_{\underset{\sim}{a}'' = \underset{\sim}{a}^o} \ , \tag{4.5}$$

where $\underset{\sim}{a}_o \equiv \langle \underset{\sim}{a} \rangle$, the unconditional stationary average. By differentiating twice to s, setting s = 0 and letting $t \to \infty$, one finds from (4.2) the generalized nonequilibrium second moment relaxation theorem:

$$\langle \Delta\underset{\sim}{a} \Delta\tilde{a} \rangle \tilde{\underline{\underline{M}}} + \underline{\underline{M}} \langle \Delta\underset{\sim}{a} \Delta\tilde{a} \rangle = \underline{\underline{B}}(a^o) \tag{4.6}$$

where $\underline{\underline{B}}$ is the second order Fokker Planck moment; $\tilde{\underline{\underline{M}}}$ is the transpose, $\Delta\underset{\sim}{a}$ is a column matrix and $\Delta\tilde{a}$ a row matrix.

The theorem was first derived for generation-recombination noise in multilevel semiconductors or photoconductors (note that the theorem holds out of equilibrium as in a photoconductor!); in this case $\underset{\sim}{a}$ represents the various

populations of carriers, $\underset{\sim}{a} = \{n_1 n_2 \ldots n_s\}$. The theorem was called the generalized g-r theorem (Van Vliet-Blok 1956a). For three-dimensional Brownian motion the theorem takes a special form (M.C. Wang and Uhlenbeck 1943). The phenomenological equation for this type is $d\underset{\sim}{v}/dt = -\beta\underset{\sim}{v}$. Thus M→B. The second-order Fokker-Planck moment is easily found to be $\underline{\underline{B}} = 2D\beta^2\underline{\underline{I}}$, where $\underline{\underline{I}}$ is the unit tensor, D is the diffusivity. Further, $<\Delta v\Delta\tilde{v}> = (kT/m)\underline{\underline{I}}$. Thus (4.6) leads to $mD = kT/\beta$, which is the Einstein relation for Brownian motion. (For carrier motion in a simple semiconductor model $\beta = 1/\tau$, $\mu = q\tau/m$, so the above leads to $qD = \mu kT$.) For this reason some authors (Lax 1960) have called (4.6) the generalized Einstein relation. When dealing with transport processes, $<\Delta a\Delta\tilde{a}>$ is to be replaced by the covariance kernel $<\Delta a(r)\Delta\tilde{a}(r')>$ and the corresponding theorem has been called the Λ-theorem (Van Vliet 1971). To us, at present, the name "generalized nonequilibrium second moment relaxation theorem" seems most appropriate.

We now state the equilibrium properties 2) - 6) mentioned in the introduction.

a) Microscopic reversibility $W_{\gamma\gamma'} = W_{\gamma'\gamma}$ follows from the golden rule in quantum mechanics. The mesoscopic transition probabilities will be denoted by $Q_{aa'}$. Let now $\chi(\underset{\sim}{a})\,d\underset{\sim}{a}$ be the number of quantum states $|\gamma>$ when $\underset{\sim}{a}$ varies between $\underset{\sim}{a}$ and $\underset{\sim}{a} + d\underset{\sim}{a}$. We then clearly have, since $\sum_{\gamma} \to \int \chi(\underset{\sim}{a})\,da$,

$$\chi(a'')Q_{a''a} = \chi(a)Q_{aa''} \,. \tag{4.7}$$

This is the principle of mesoscopic reversibility. In the microcanonical or canonical equilibrium ensemble the probability $W(\underset{\sim}{a})d\underset{\sim}{a}$ is proportional to the number of accessible quantum states in $d\underset{\sim}{a}$, i.e., $\chi(\underset{\sim}{a})d\underset{\sim}{a}$. Thus (4.7) leads to the property of "mesoscopic reversibility"

$$W(a'')Q_{a''a} = W(a)Q_{aa''} \,. \tag{4.8}$$

b) The above leads to detailed balance (Van Vliet 1964). Consider that $\underset{\sim}{a}$ labels the occupancy of a set of quantum levels, i.e., let $\underset{\sim}{a} = \underset{\sim}{m}$, $\underset{\sim}{n}$, or $\underset{\sim}{k}$, which represent discrete population vectors. In particular, we consider transitions $\underset{\sim}{k} \leftrightarrow \underset{\sim}{m}$ such that

$$\{k_1 \dots k_i,\ k_j \dots k_s\} \leftrightarrow \{m_1 \dots m_i,\ m_j \dots m_s\} = \{k_1 \dots k_i + 1,\ k_j - 1, \dots k_s\}. \tag{4.9}$$

Let p_{ij} be the transition rate from levels $\mathcal{E}_i$ to levels $\mathcal{E}_j$ (governed by mass action laws or similar rates). Then

$$Q_{\underset{\sim}{k}\underset{\sim}{m}} = p_{ji}(\underset{\sim}{k}) \ ; \quad Q_{\underset{\sim}{m}\underset{\sim}{k}} = p_{ij}(\underset{\sim}{m}) \ . \tag{4.10}$$

Eq. (4.8) reads in this notation

$$W(\underset{\sim}{k})Q_{\underset{\sim}{k}\underset{\sim}{m}} = W(\underset{\sim}{m})Q_{\underset{\sim}{m}\underset{\sim}{k}} \ . \tag{4.11}$$

We sum this result over all $\underset{\sim}{m}$. Then from (4.9) and (4.10)

$$\sum_{k_1=0}^{\infty} \cdots \sum_{k_i=0}^{\infty} \sum_{k_j=1}^{\infty} \cdots \sum_{k_s=0}^{\infty} W(\underset{\sim}{k})p_{ji}(\underset{\sim}{k})$$

$$= \sum_{m_1=0}^{\infty} \cdots \sum_{m_i=1}^{\infty} \sum_{m_j=0}^{\infty} \cdots \sum_{m_s=0}^{\infty} W(\underset{\sim}{m})p_{ij}(\underset{\sim}{m}) \tag{4.12}$$

or also

$$\langle p_{ji}(\underset{\sim}{k}) \rangle = \langle p_{ij}(\underset{\sim}{m}) \rangle . \tag{4.13}$$

The variables $\underset{\sim}{k}$ and $\underset{\sim}{m}$ are dummy variables; thus (4.13) simply says $\langle p_{ji} \rangle = \langle p_{ij} \rangle$. This is detailed balance for the rates between any two sets of quantum states in the system.

c) From Bayes' theorem one easily shows that (4.8) leads to the symmetry of the pair correlation function for small intervals Δt

$$W_2(\underset{\sim}{a},\Delta t;\ \underset{\sim}{a}'',0) = W_2(\underset{\sim}{a}'',\Delta t;\ \underset{\sim}{a},0) \ . \tag{4.14}$$

With the linearized phenomenological equation this leads to

$$\langle \underset{\sim}{a}(\Delta t)\tilde{\underset{\sim}{a}}(0)\rangle = \langle \underset{\sim}{\underset{\sim}{aa}}\rangle - \underset{\approx}{M}\langle \Delta\underset{\sim}{a}\Delta\underset{\sim}{a}\rangle \Delta t \tag{4.15}$$

and

$$\langle \underset{\sim}{a}(0)\tilde{\underset{\sim}{a}}(\Delta t)\rangle = \langle \underset{\sim}{\underset{\sim}{aa}}\rangle - \langle \Delta\underset{\sim}{a}\Delta\underset{\sim}{a}\rangle \underset{\approx}{M}\Delta t \ . \tag{4.16}$$

When in (4.14) we multiply by $\underset{\sim}{a}\tilde{\underset{\sim}{a}}''$ and sum over both variables, we easily see that the l.h. sides of Eqs. (4.15) and (4.16) are equal. Thus, in thermal equilibrium the r.h. sides of (4.15) and (4.16) must also be equal, which is the symmetrization postulate of the "generalized second moment relaxation theorem"; in (4.6) both sides are now equal

$$\langle \Delta\underset{\sim}{a}\Delta\tilde{\underset{\sim}{a}}\rangle \underset{\approx}{M} = \underset{\approx}{M}\langle \Delta\underset{\sim}{a}\Delta\tilde{\underset{\sim}{a}}\rangle \ . \tag{4.17}$$

This property gives a tremendous simplification for thermal equilibrium processes; for now (4.6) can at once be solved

$$\underset{\approx}{M}\langle \Delta\underset{\sim}{a}\Delta\tilde{\underset{\sim}{a}}\rangle = \frac{1}{2}\,\underset{\approx}{B}(\underset{\sim}{a}^{o}) \tag{4.18}$$

or

$$\langle \Delta\underset{\sim}{a}\Delta\tilde{\underset{\sim}{a}}\rangle = \frac{1}{2}\,\underset{\approx}{M}^{-1}\,\underset{\approx}{B}(\underset{\sim}{a}^{o}) \ . \tag{4.19}$$

Since (4.18) is for Brownian motion, nothing but the Einstein relation between mobility and diffusivity, it is clear that some authors (Lax) refer to the full theorem (4.6) as the nonequilibrium generalized Einstein relation. Well, whatever the name of Eq. (4.6), we do note that (4.6) is a genuine nonequilibrium result, while (4.18) or (4.19) is an equilibrium result. Thus, the properties

$$\langle \Delta\underset{\sim}{a}\Delta\tilde{\underset{\sim}{a}}\rangle \underset{\approx}{M} = \underset{\approx}{M}\langle \Delta\underset{\sim}{a}\Delta\tilde{\underset{\sim}{a}}\rangle \tag{4.20a}$$

$$\langle \Delta\underset{\sim}{a}\Delta\tilde{\underset{\sim}{a}}\rangle \underset{\approx}{M} \neq \underset{\approx}{M}\langle \Delta\underset{\sim}{a}\Delta\tilde{\underset{\sim}{a}}\rangle \tag{4.20b}$$

delineate clearly between equilibrium and nonequilibrium behavior.

We still mention the analog for transport processes (Van Vliet 1971). Suppose we have a stochastic variable depending on a (vector) parameter y,

which is continuous in $D(-\infty,\infty)^s$. The stochastic process $\underset{\sim}{a}(y,t)$ is then infinite dimensional, though we assume it to be still Markovian. The Langevin equation is of the matrix operator form

$$\frac{\partial \underset{\sim}{a}(y,t)}{\partial t} + \underset{\approx}{\Lambda}_y \underset{\sim}{a}(y,t) = \underset{\sim}{\xi}(y,t) \ . \tag{4.21}$$

where $\underset{\approx}{\Lambda}$ is some (matrix) integral or differential operator describing the transport process. Let the covariance matrix kernel be

$$\underset{\approx}{\Gamma}(y,y') = <\Delta \underset{\sim}{a}(y) \Delta \tilde{\underset{\sim}{a}}(y')> . \tag{4.22}$$

The analog of the matrix theorem (4.6) is now the Λ-theorem

$$\underset{\approx}{\Lambda}_y \underset{\approx}{\Gamma}(y,y') + \underset{\approx}{\Gamma}(y,y') \underset{\approx}{\Lambda}^{tr}_{y'} = \frac{1}{2} \underset{\approx}{S}_{\xi}(y,y') \tag{4.23}$$

where Λ^{tr} acts from the right on Γ. This theorem was proven using Hilbert-space methods by the author. Notice that S_{ξ} is the white spectral density of the Langevin sources. Again, when both terms on the l.h.s. of the Λ-theorem (4.23) are unequal, we deal with a true nonequilibrium state.

In the next two sections we give both a matrix and a transport example of a true nonequilibrium situation, which, moreover, has been experimentally verified.

5. Optical pumping in a nonequilibrium steady state

In 1964 we considered a model of a photoconductor in which free electron hole pairs were created by optical absorption, whereas all of the recombination was occurring via intermediate states, see Figure 1.

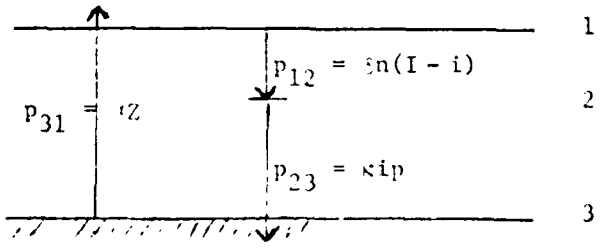

Figure 1

δ and κ are capture constants. Clearly, there is no detailed balance, so we

have a genuine nonequilibrium state. The M matrix follows from the linearized mass action type kinetic equations for $d\Delta n/dt$ and $d\Delta i/dt$ ($\Delta p = \Delta i + \Delta n$ is a dependent variable). One obtains

$$\left.\begin{aligned} M_{11} &= \delta(I - i_o), \quad M_{12} = -\delta n_o \\ M_{21} &= -\delta I + \delta i_o + \kappa i_o, \quad M_{22} = \delta n_o + \kappa n_o + 2\kappa i_o \ . \end{aligned}\right\} \tag{5.1}$$

For the B-matrix one finds, likewise,

$$\left.\begin{aligned} B_{11} &= 2\delta n_o(I - i_o) \\ B_{12} &= B_{21} = -\delta n_o(I - i_o) \\ B_{22} &= 2\delta n_o(I - i_o) \ . \end{aligned}\right\} \tag{5.2}$$

Moreover, in the steady state one has

$$\alpha Z = \delta n_o(I - i_o) = \kappa i_o(n_o + i_o) \ . \tag{5.3}$$

One can now solve the nonequilibrium moment relation (4.6), expressing i_o into n_o via (5.3). Since (4.6) is homogeneous in δ/κ, the relative variance $<\Delta n^2>/n_o$ can be computed as a function of $\alpha Z (= \mathcal{L})$ for various values of the ratio $y = \kappa/\delta$. The results are given in Figure 2 below.

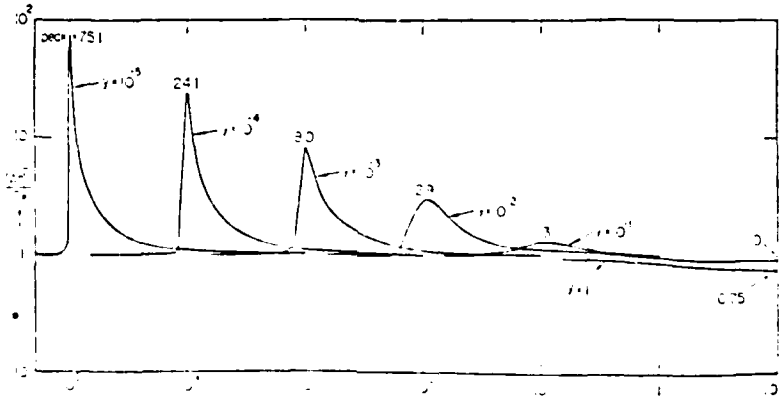

Fig. 4. The relative variance $<\Delta n^2>/n_o$ vs. $\mathcal{L}$.

The pecularity of this model is that $<\Delta n^2>/n_o$ may attain values $>> 1$, as are indeed experimentally observed in cadmium sulfide. For a thermal equilibrium situation, on the contrary, we always have $<\Delta n^2>/n_o \leq 1$, according to ermi-Dirac statistics. Thus, the model of this section represents a true nonequilibrium situation, in which familiar concepts like Fermi-Dirac statistics are entirely eclipsed.

6. Brillouin scattering as an example of fluctuations about a hydrodynamic nonequilibrium state

Tremblay et al. (1980) considered fluctuations in hydrodynamic modes A(k) governed by a Langevin matrix equation

$$\frac{\partial \underset{\sim}{A}(\underset{\sim}{k},t)}{\partial t} + \underline{\underline{M}}(\underset{\sim}{k})\cdot\underset{\sim}{A}(\underset{\sim}{k}) = \underset{\sim}{\xi}(\underset{\sim}{k},t) \ . \tag{6.1}$$

Notice that $\underline{\underline{M}}(\underset{\sim}{k})$ is the Λ operator of the last part of Section 4. This is an example of our transport formalism for infinite dimensional stochastic processes $(y \to \underset{\sim}{k})$ as considered in detail in our 1971 paper. For the Langevin forces correlation we write as usual

$$<\underset{\sim}{\xi}(\underset{\sim}{k},t)\underset{\sim}{\xi}(\underset{\sim}{k}',t')> = \frac{1}{2}\,\underline{\underline{S}}_{\xi}(\underset{\sim}{k},\underset{\sim}{k}')\delta(t-t') \equiv \underline{\underline{D}}(\underset{\sim}{k},\underset{\sim}{k}')\delta(t-t') \ . \tag{6.2}$$

Solving from the Langevin equation for the spectrum, one finds

$$\underline{\underline{S}}_{A}(\underset{\sim}{k},\underset{\sim}{k}',\omega) = 2[\underline{\underline{M}}(\underset{\sim}{k}) + i\omega\underline{\underline{I}}]^{-1}\underline{\underline{\Gamma}}(\underset{\sim}{k},\underset{\sim}{k}') + 2\underline{\underline{\Gamma}}(\underset{\sim}{k},\underset{\sim}{k}')[\tilde{\underline{\underline{M}}}(\underset{\sim}{k}) - i\omega\underline{\underline{I}}]^{-1} \ . \tag{6.3}$$

In a nonequilibrium state Γ can be eliminated by pre- and post-multiplying with the resolvent; hence

$$[\underline{\underline{M}}(\underset{\sim}{k}) + i\omega\underline{\underline{I}}]\underline{\underline{S}}_{A}(\underset{\sim}{k},\underset{\sim}{k}',\omega)[\tilde{\underline{\underline{M}}}(\underset{\sim}{k}) - i\omega\underline{\underline{I}}] = 2\underline{\underline{\Gamma}}(\underset{\sim}{k},\underset{\sim}{k}')\tilde{\underline{\underline{M}}}(\underset{\sim}{k})$$

$$+ 2\underline{\underline{M}}(\underset{\sim}{k})\underline{\underline{\Gamma}}(\underset{\sim}{k},\underset{\sim}{k}') = 2\underline{\underline{D}}(\underset{\sim}{k},\underset{\sim}{k}') \tag{6.4}$$

where we used the full nonequilibrium second moment relaxation theorem (4.23). Inverting (6.3) we have

$$\underline{\underline{S}}_{A}(\underset{\sim}{k},\underset{\sim}{k}',\omega) = 2[\underline{\underline{M}}(\underset{\sim}{k}) + i\omega\underline{\underline{I}}]^{-1}\underline{\underline{D}}(\underset{\sim}{k},\underset{\sim}{k}')[\tilde{\underline{\underline{M}}}(\underset{\sim}{k}) - i\omega\underline{\underline{I}}]^{-1} \ . \tag{6.5}$$

(For comparison with Tremblay et al., notice our $\underline{\underline{S}}_A(\underset{\sim}{k},\underset{\sim}{k}',\omega)$ is their $2\underline{\underline{\chi}}^{\omega}(k,k')$ with $\underline{\underline{\chi}} = \| \chi_{\alpha\beta} \|$; our Eq. (6.5) is their Eq. (7).)

We now come to their specific model. They consider a fluid with a fluctuating stress tensor, in a small temperature gradient. The linearized hydrodynamic equations for such a fluid are

$$\frac{\partial p(\underset{\sim}{k},t)}{\partial t} = -i\rho c \underset{\sim}{k}\cdot\underset{\sim}{v} \tag{6.6}$$

$$\frac{\partial \underset{\sim}{k}\cdot\underset{\sim}{v}}{\partial t} = -i(k^2/\rho)p - [(\zeta + 4\eta/3)/\rho]k^2(\underset{\sim}{k}\cdot\underset{\sim}{v}) + (i/\rho)\underset{\sim}{k}\cdot\underline{\underline{S}}\cdot\underset{\sim}{k} \tag{6.7}$$

where p is the pressure, ρ is the density, c is the sound velocity, ζ the bulk and η the shear viscosity. There is no Langevin force associated with (6.6), but there is with (6.7), see their Eq. (9). Equations (6.6) and (6.7), taken together as a column matrix equation, are of the form (6.1), though the details are quite complex. One can thus solve for $S_{pp}(\underset{\sim}{k}',\underset{\sim}{k}'',\omega)$. They obtain

$$S_{pp}(\underset{\sim}{k}',\underset{\sim}{k}'',\omega) = \frac{c^4 2T(k'-k'')[2\eta(\underset{\sim}{k}'\cdot\underset{\sim}{k}'')^2 + (\zeta - 2\eta/3)k'^2k''^2]}{(\omega^2 - c^2k'^2 + i\omega D_\ell k'^2)(\omega^2 - c^2k''^2 - i\omega D_\ell k''^2)} \tag{6.8}$$

where $D_\ell \equiv (\zeta + 4\eta/3)/\rho$. Due to the temperature gradient contained in $T = T(\underset{\sim}{r})$, the two Brillouin light-scattering peaks obtain an asymmetrical height. One finds a difference spectrum $\delta S_{pp}(\omega)$ for the peaks located at $|\omega| = ck$, see Tremblay et al., Eq. (14). The experimental values observed are in agreement with the theory, thus once more confirming the basic nonequilibrium result (4.6) or (4.23).

Acknowledgements

This review paper was written and its production supported by AFOSR contract #82-0226 and by grant A9522 from NSERC, Ottawa.

References

1. H.B. Callen (1960), Thermodynamics, John Wiley, N.Y.

2. H.B.G. Casimir (1945), Revs. Mod. Phys. 17, 343.

3. S.R. de Groot and P. Mazur (1962), Nonequilibrium Thermodynamics, North Holland Publishing Co.

4. J.W. Gibbs (1902), Elementary Principles in Statistical Mechanics, reprinted Dover.

5. R.F. Greene and H.B. Callen (1951), Phys. Rev. 83, 1231.

6. M.S. Gupta (1978), Phys. Rev. A 18, 2725.

7. M.S. Gupta (1982), Proc. IEEE 70, 788.

8. T. Kirkpatrick, E.G.D. Cohen and J.R. Dorfman (1979), Phys. Rev. Lett. 42, 862.

9. R. Kubo (1957), J. Phys. Soc. Japan 12, 570.

10. M. Lax (1960), Revs. Mod. Phys. 32, 110.

11. H. Nyquist (1928), Phys. Rev. 32, 110.

12. I. Procaccia, D. Ronis, and I. Oppenheim (1979), Phys. Rev. Lett. 42, 287.

13. A.-M.S. Tremblay, E.D. Siggia and M.R. Arai (1980), Phys. Lett. 76A, 57.

14. A. van der Ziel (1973), Solid State Electr. 16, 751.

15. N.G. van Kampen (1962), in Fundamental Problems in Statistical Mechanics (E.G.D. Cohen, ed.), North Holland Publishing Co., p. 173.

16. N.G. van Kampen (1965), in Fluctuation Phenomena in Solids (R.E. Burgess, ed.), Acad. Press, p. 139.

17. K.M. van Vliet and J. Blok (1956a), Physica 22, 231.

18. K.M. van Vliet and J. Blok (1956b), Physica 22, 525.

19. K.M. van Vliet (1964), Phys. Rev. 133 A 1182 (corrected in Phys. Rev. 138, 3 AB (1965)).

20. K.M. van Vliet and J.R. Fassett (1965), in Fluctuation Phenomena in Solids (R.E. Burgess, ed.), Acad. Press, p. 267.

21. K.M. van Vliet (1971), J. Math. Phys. 12, 1981.

22. K.M. van Vliet (1978), J. Math. Phys. 19, 1345.

23. K.M. van Vliet (1979), J. Math. Phys. 20, 2573.

24. C.M. Van Vliet (1983), "Fluctuation Phenomena," lecture notes U. of Florida.

25. M.C. Wang and G.E. Uhlenbeck (1945), Revs. Mod. Phys. 17, 323.

D. PAPERS AND THESES PUBLISHED UNDER THE CONTRACT

I. Theses produced during this period

1. Jeng Gong, PhD thesis: Noise associated with electron statistics in avalanche photodiodes and emission statistics of α-particles, U. of Florida, 1983.
2. Robert R. Schmidt, PhD thesis: Noise and current-voltage characteristics of near-ballistic GaAs devices, U. of Florida, 1983.
3. Ching-Jinn Hsieh, Engineer's thesis: 1/f cathode noise and partition noise compensation in pentodes, U. of Florida, 1983.

II. Papers published under contract during this period

1. R.R. Schmidt, G. Bosman, C.M. Van Vliet, L.F. Eastman, and M. Hollis: Noise in near-ballistic n^+nn^+ and n^+pn^+ gallium arsenide submicron diodes, Solid State Electr. 26, 437-444, 1983.
2. J. Gong, C.M. Van Vliet, W.H. Ellis, and G. Bosman: 1/f fluctuations in alpha particle radioactive decay from ^{241}Am, submitted to Phys. Rev. A.
3. A. van der Ziel and C.M. Van Vliet: 1/f noise and mobility fluctuations and the Boltzmann equation, submitted to Physica B.
4. J. Kilmer, C.M. Van Vliet, G. Bosman, and A. van der Ziel: Evidence of electromagnetic quantum 1/f noise in gold films, submitted to Physica Status Solidi (b).

The following papers were accepted for the Proceedings of the 7th International Symposium of Noise in Physical Systems and the 3rd International Symposium on 1/f Noise, Montpellier, France (May, 1983). These proceedings are being published by North Holland Publishing Company.

1. C.M. Van Vliet: Noise out of equilibrium (invited survey paper), see Section C-III.

2. C.M. Van Vliet and P.H. Handel: A new transform theorem linking spectral density and Allan variance.

3. R.R. Schmidt, G. Bosman, C.M. Van Vliet, and A. van der Ziel: Noise in near-ballistic n^+nn^+ and n^+pn^+ gallium arsenide submicron devices.

4. J. Gong, C.M. Van Vliet, W.H. Ellis, G. Bosman, and P.H. Handel: 1/f noise fluctuations in α-particle radioactive decay of 95 Americium 241.

5. J. Kilmer, G. Bosman, C.M. Van Vliet, and A. van der Ziel: 1/f noise in metal films of submicron dimensions.

E. FIGURES

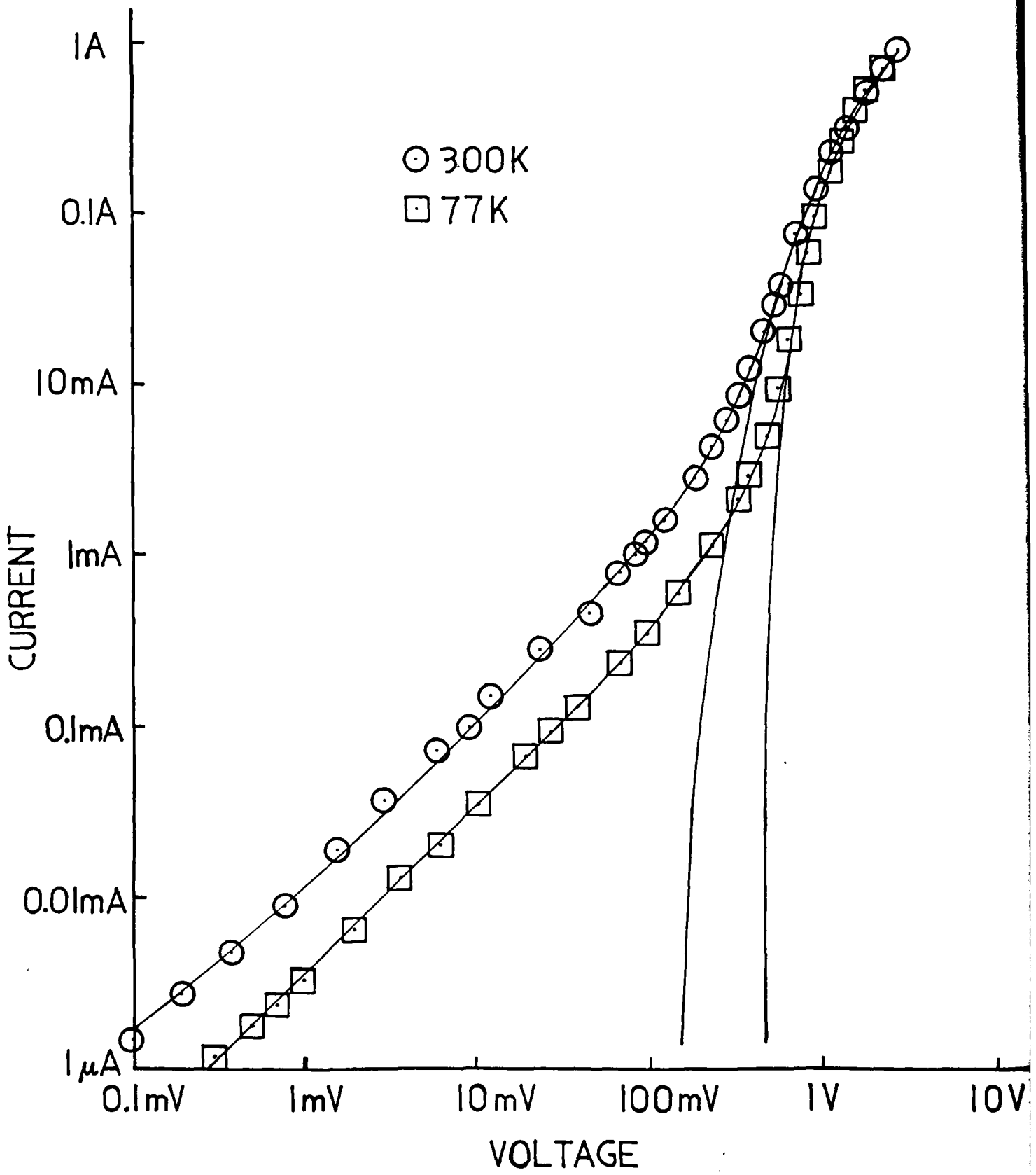
1A
0.1A
10mA
1mA
0.1mA
0.01mA
1μA
CURRENT
300K
77K
0.1mV
1mV
10mV
100mV
1V
10V
VOLTAGE

Figure 1

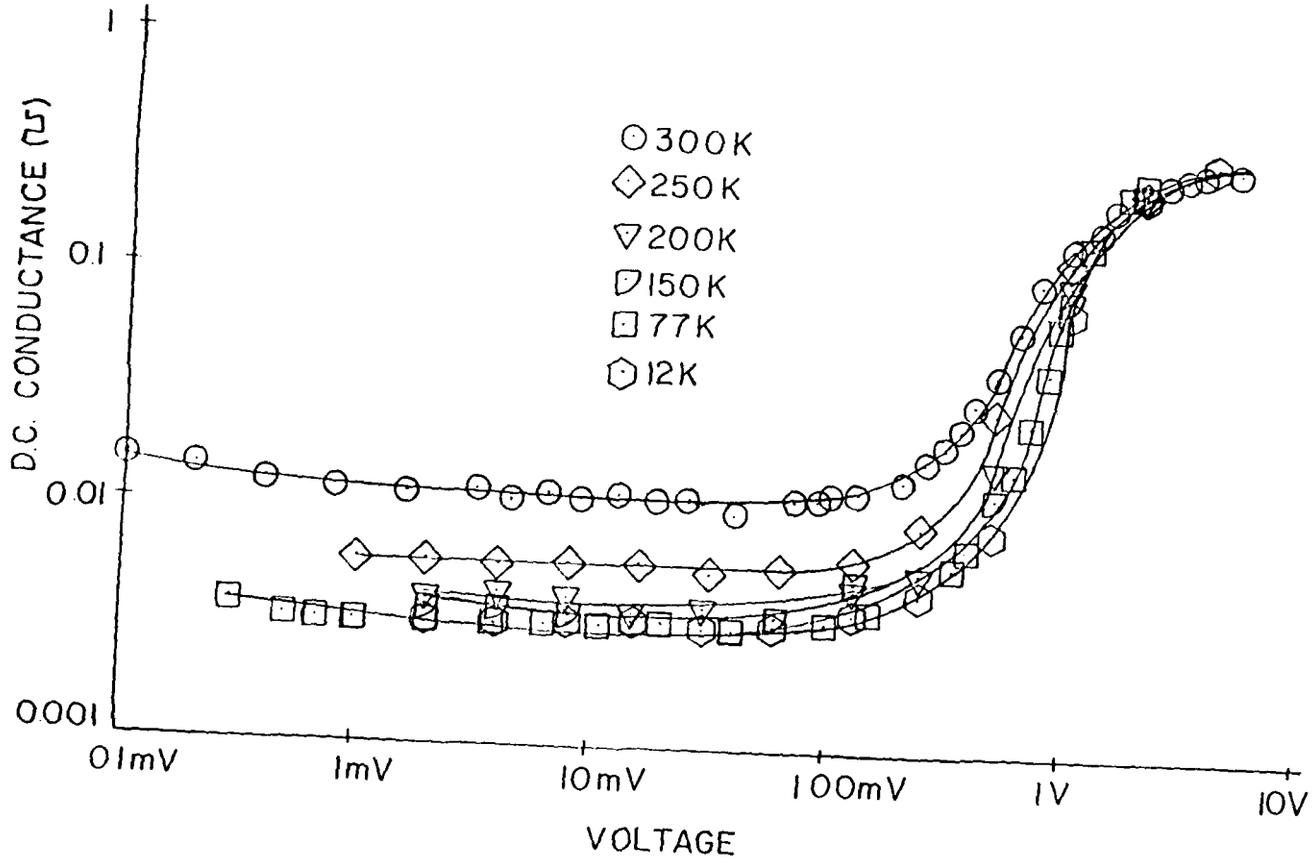
1
0.1
0.01
0.001
D.C. CONDUCTANCE (Ω⁻¹)
300K
250K
200K
150K
77K
12K
0.1mV
1mV
10mV
100mV
1V
10V
VOLTAGE

Figure 2

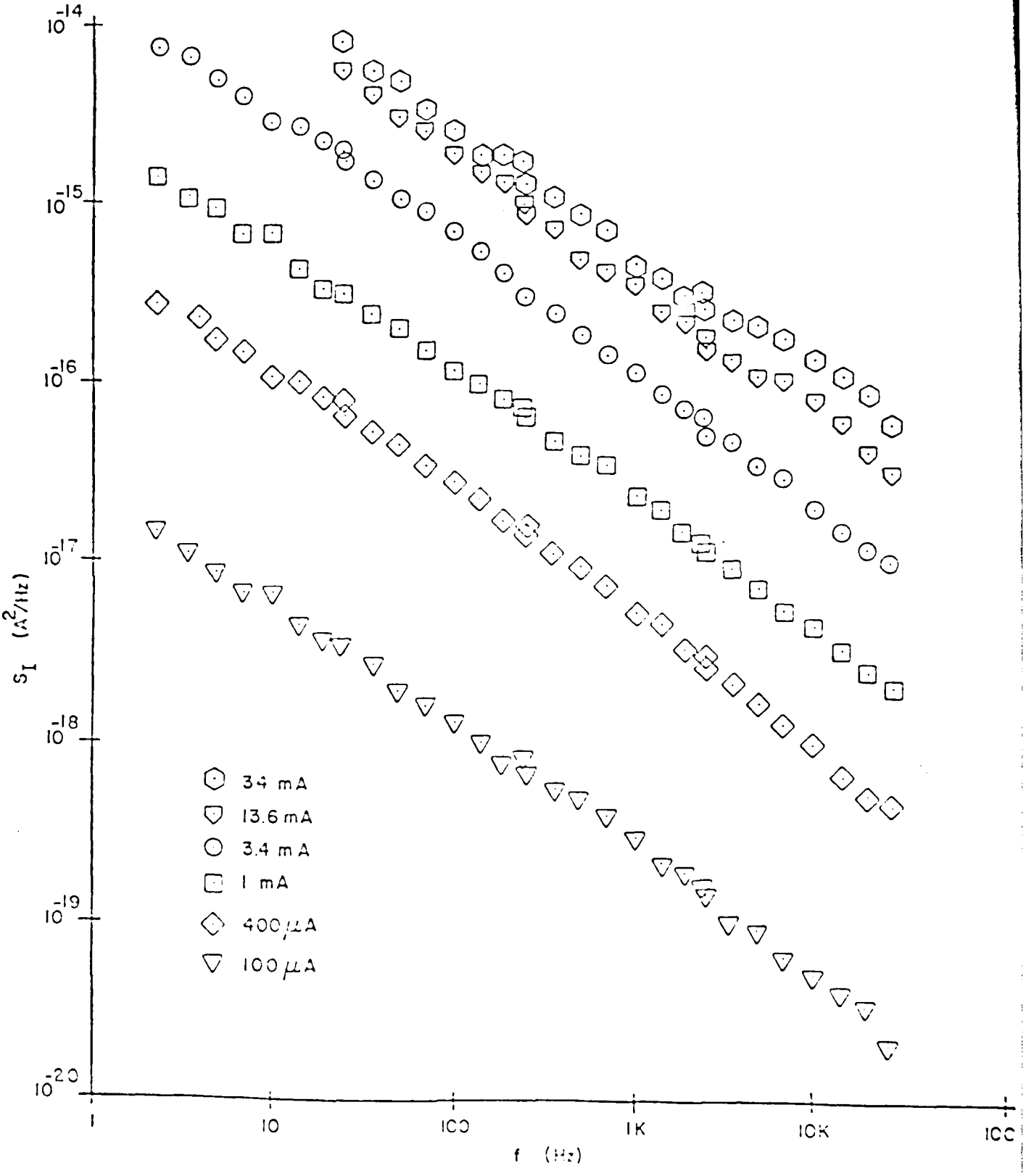
10^{-14}
10^{-15}
10^{-16}
10^{-17}
10^{-18}
10^{-19}
10^{-20}
S_I (A^2/Hz)
3.4 mA
13.6 mA
3.4 mA
1 mA
400 μA
100 μA
1
10
100
1K
10K
100
f (Hz)

Figure 3

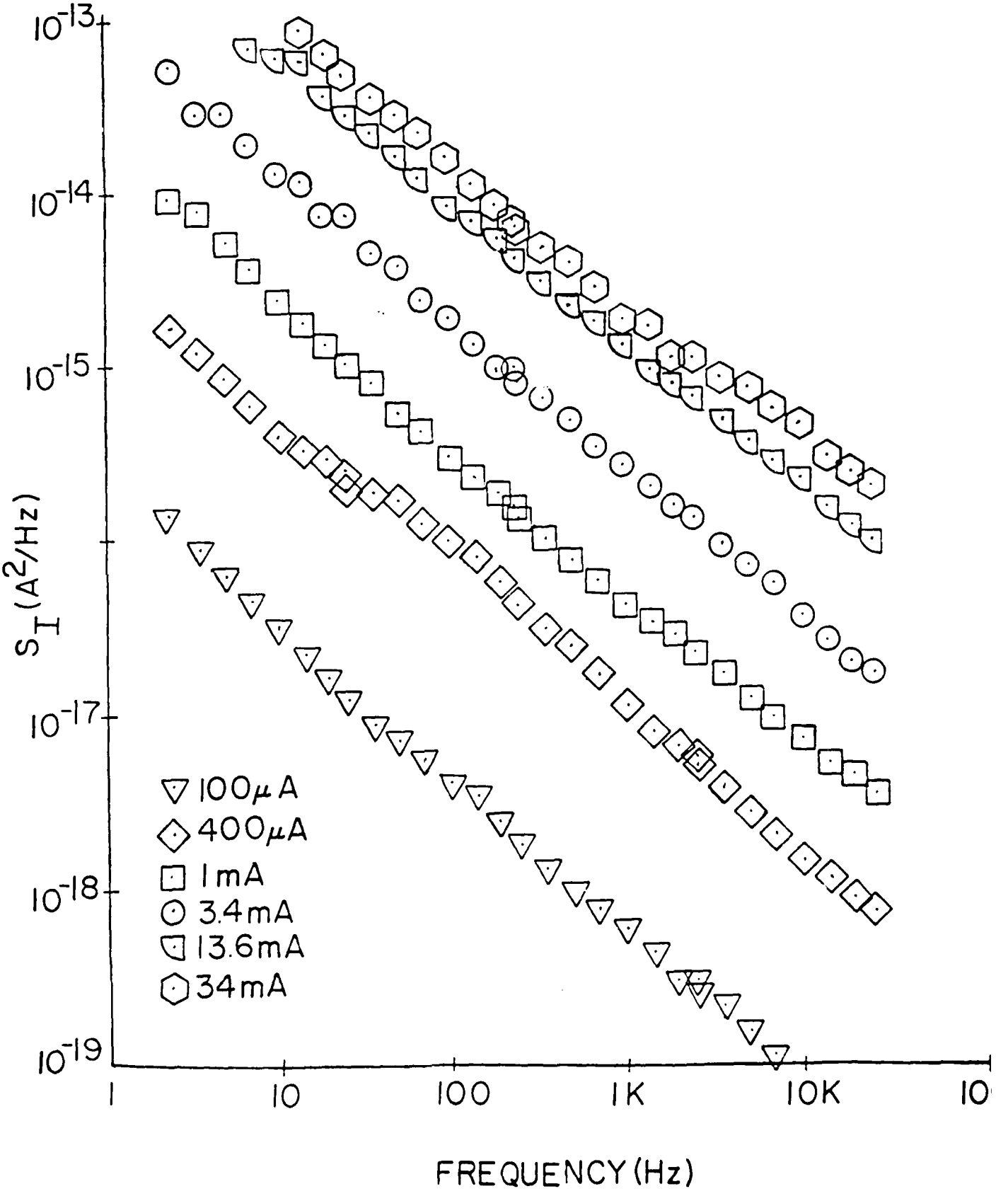
10^{-13}
10^{-14}
10^{-15}
10^{-17}
10^{-18}
10^{-19}
$S_I (A^2/Hz)$
100μA
400μA
1mA
3.4mA
13.6mA
34mA
1
10
100
1K
10K
FREQUENCY (Hz)

Figure 3

AD-A133 856 STUDY OF 1/F NOISE IN SOLIDS(U) FLORIDA UNIV GAINESVILLE DEPT OF ELECTRICAL ENGINEERING C M VAN VLIET ET AL. 1983 AFOSR-TR-83-0798

UNCLASSIFIED AFOSR-82-0226 F/G 20/12 NL

2/2

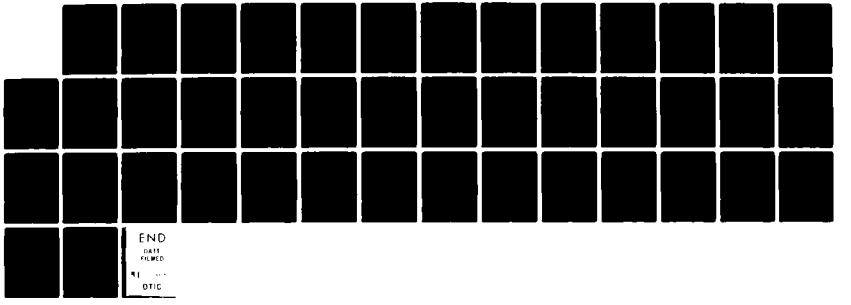

END

DATE FILMED

DTIC

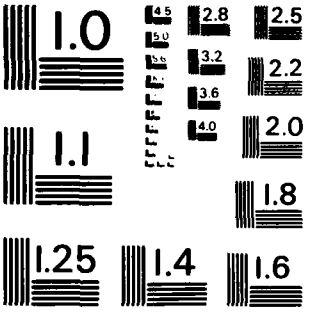

MICROCOPY RESOLUTION TEST CHART
NATIONAL BUREAU OF STANDARDS - 1963 - A

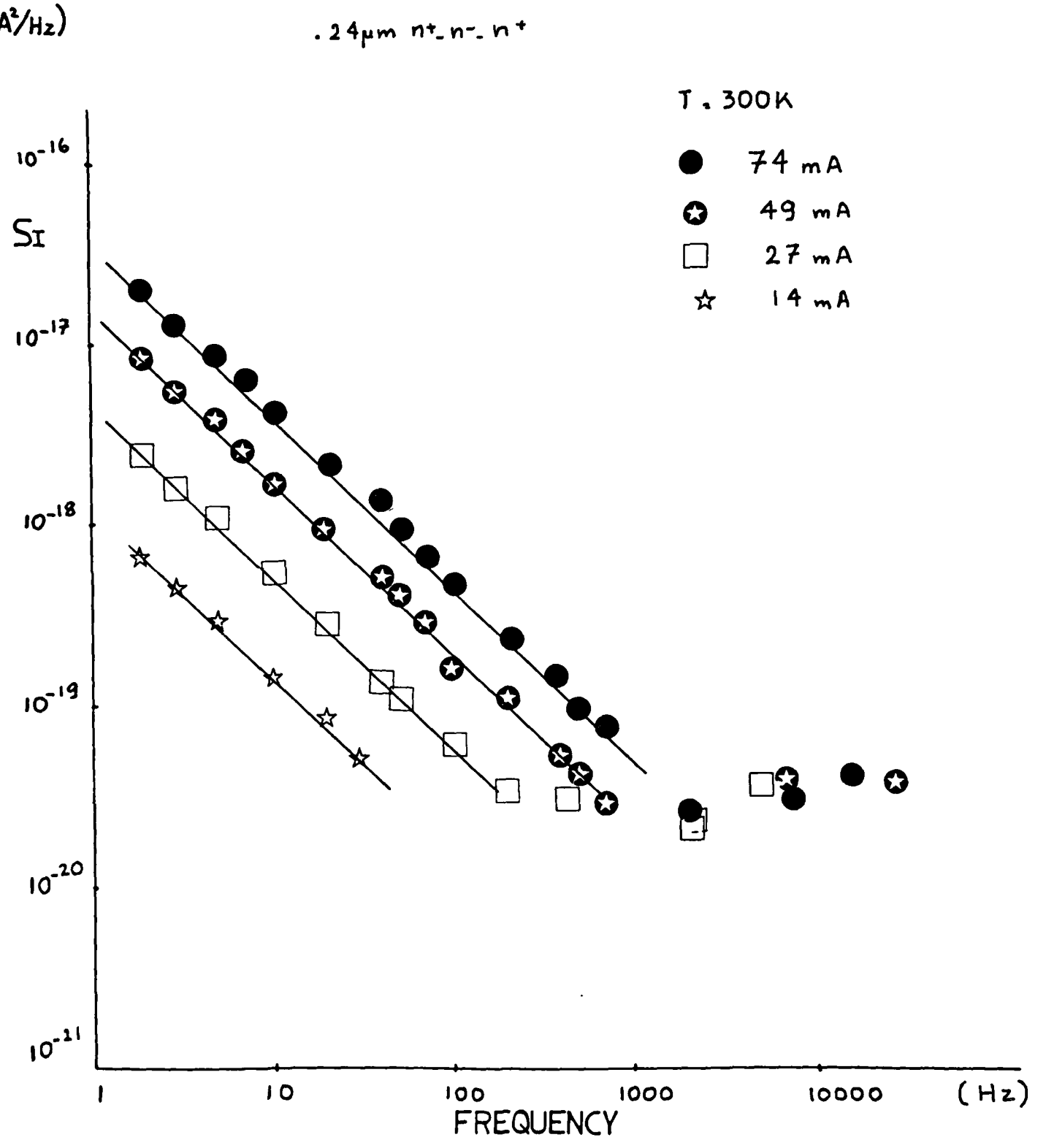
(A²/Hz)
.24μm n+_n-_n+
T . 300K
74 mA
49 mA
27 mA
14 mA
SI
10-16
10-17
10-18
10-19
10-20
10-21
1
10
100
1000
10000
(Hz)
FREQUENCY

Figure 5

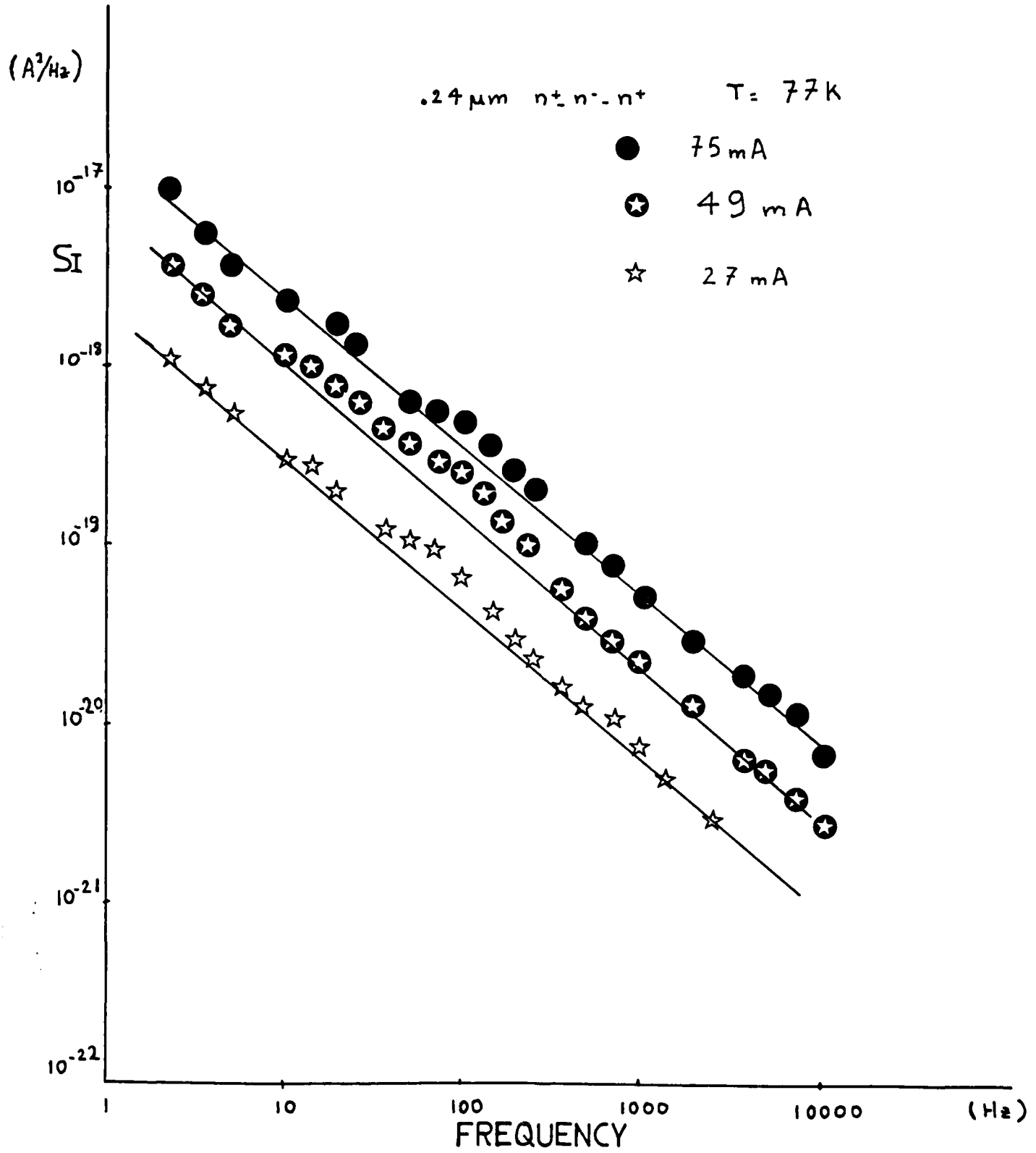
(A²/Hz)
.24 μm n+ n- n+
T= 77K
75 mA
49 mA
27 mA
SI
10⁻¹⁷
10⁻¹⁸
10⁻¹⁹
10⁻²⁰
10⁻²¹
10⁻²²
1
10
100
1000
10000
(Hz)
FREQUENCY

Figure 6

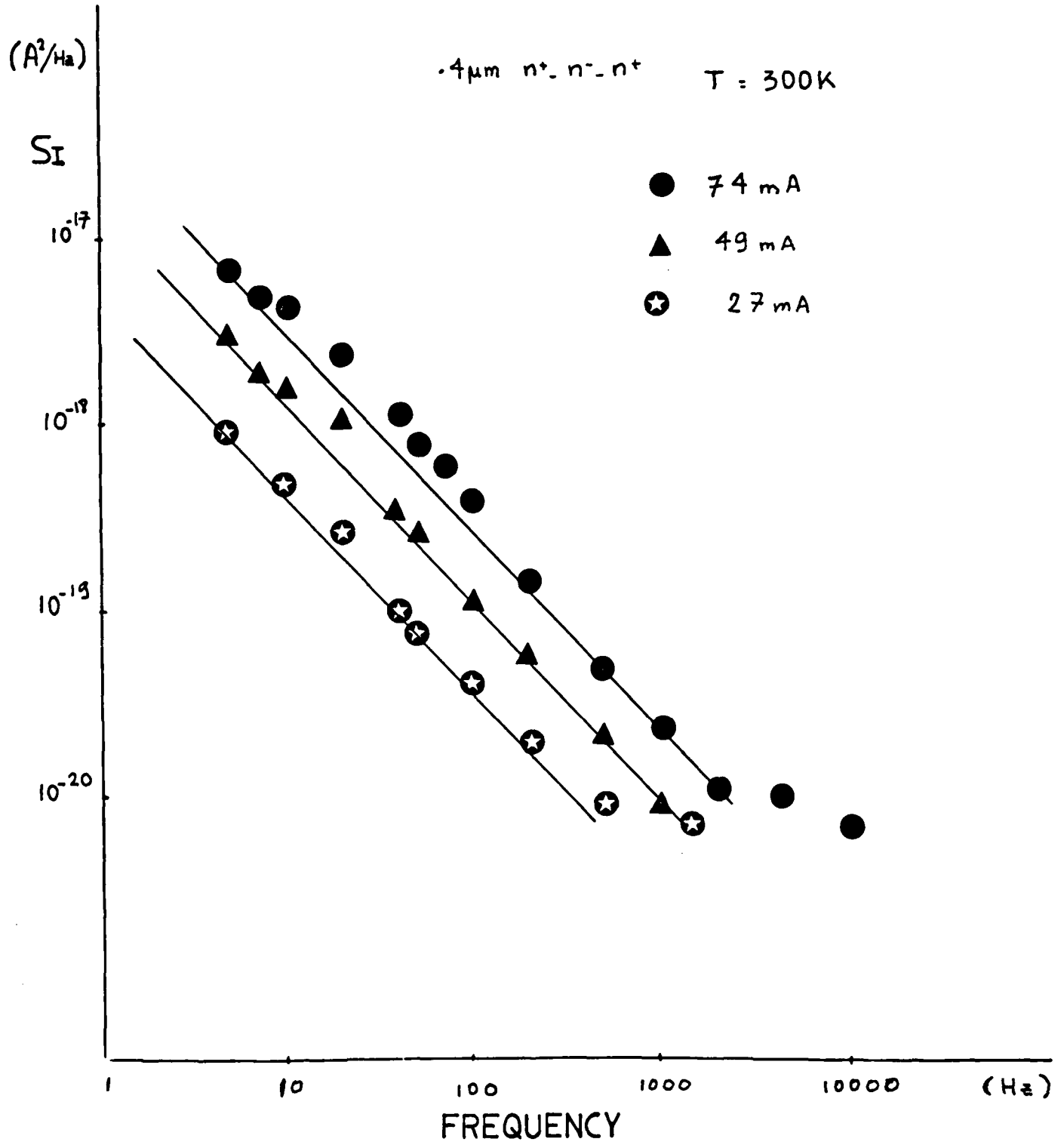
(A²/Hz)
SI
.4μm n+_n-_n+
T = 300K
74 mA
49 mA
27 mA
10^-17
10^-18
10^-19
10^-20
1
10
100
1000
10000
(Hz)
FREQUENCY

Figure 7

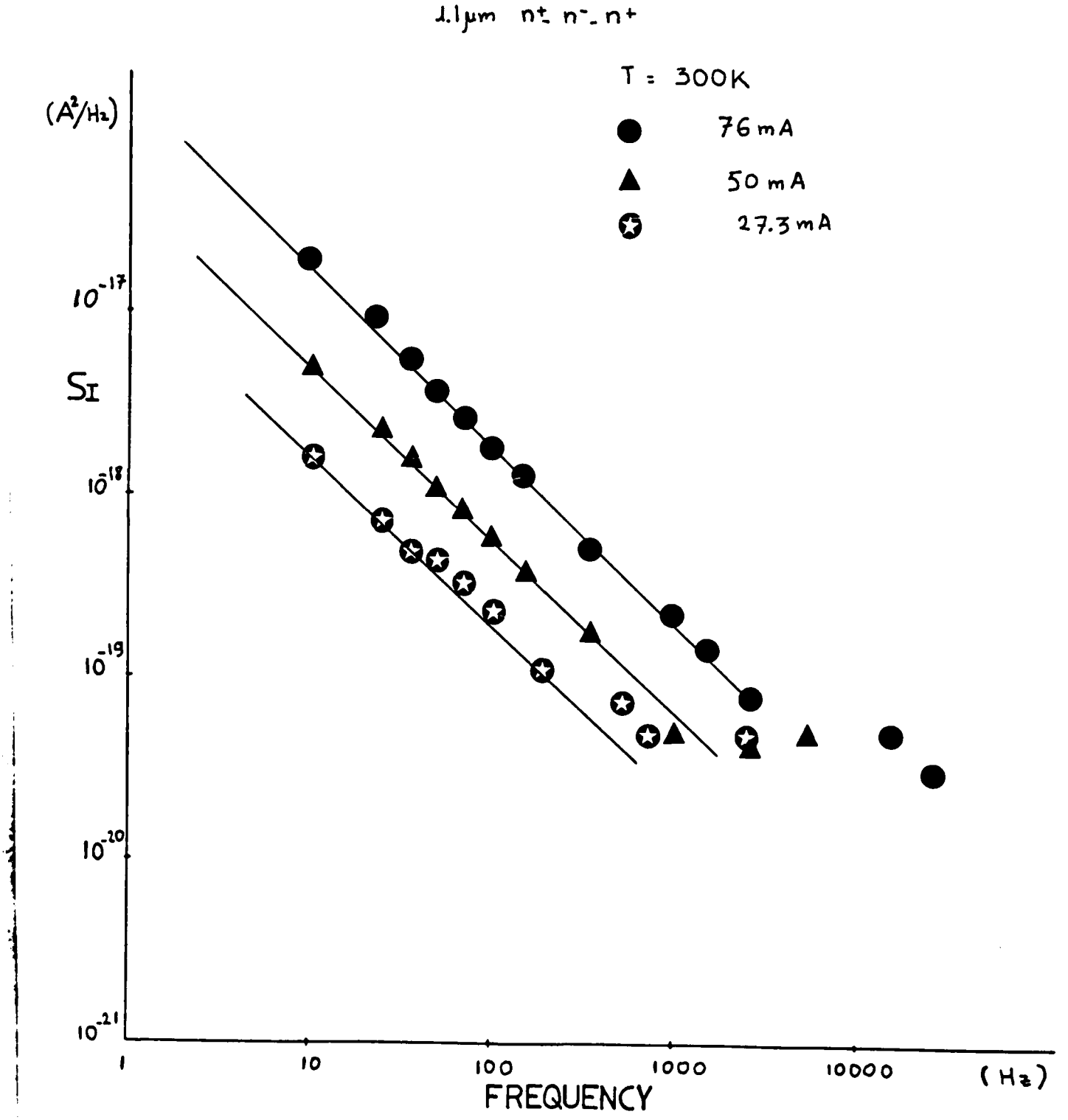
1.1μm n+ n⁻ n+
T = 300K
76 mA
50 mA
27.3 mA
(A²/Hz)
SI
10⁻¹⁷
10⁻¹⁸
10⁻¹⁹
10⁻²⁰
10⁻²¹
1
10
100
1000
10000
(Hz)
FREQUENCY

Figure 8

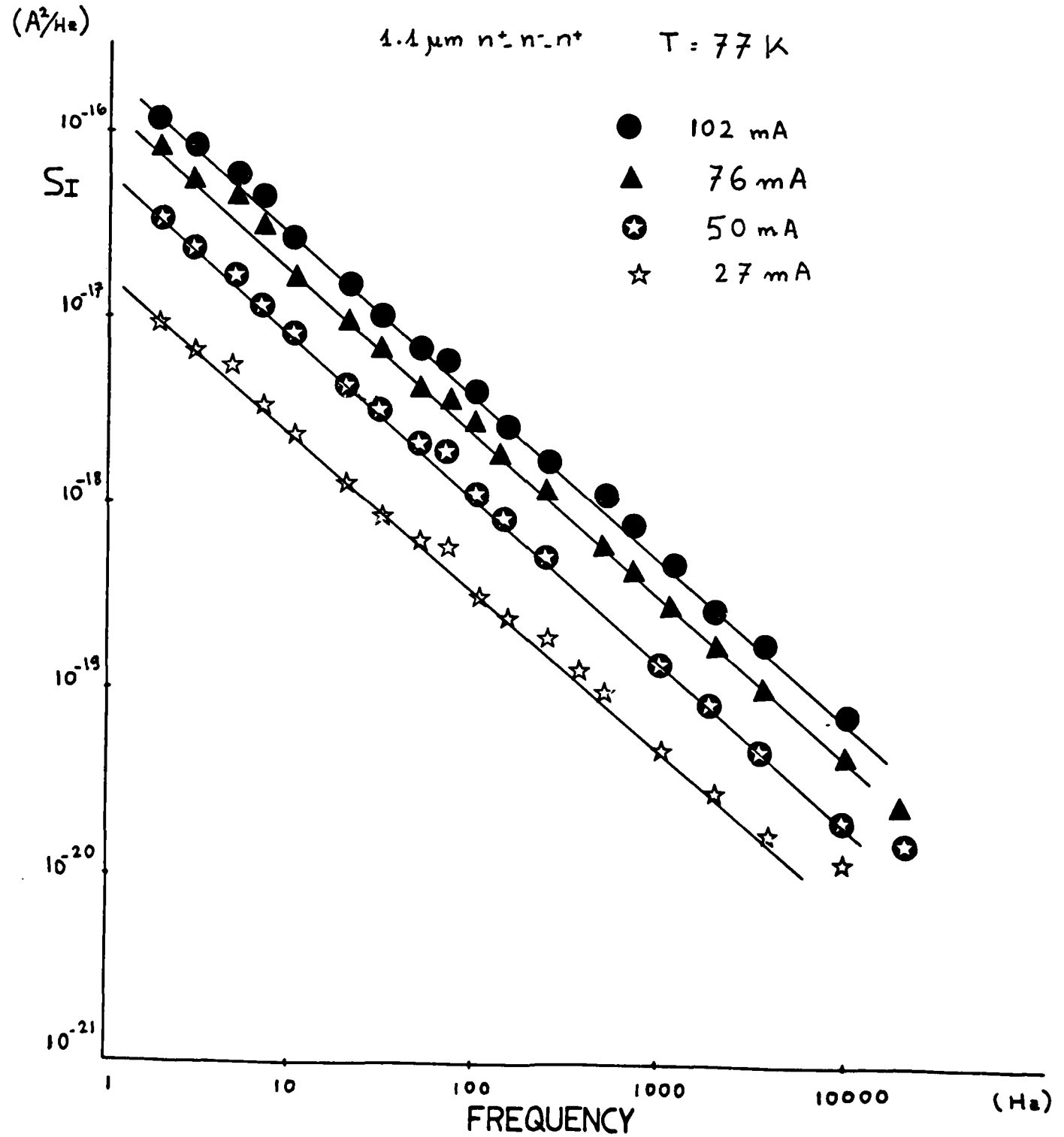
(A²/Hz)
1.1 μm n⁺-n⁻-n⁺
T = 77 K
102 mA
76 mA
50 mA
27 mA
SI
10⁻¹⁶
10⁻¹⁷
10⁻¹⁸
10⁻¹⁹
10⁻²⁰
10⁻²¹
1
10
100
1000
10000
(Hz)
FREQUENCY

Figure 9

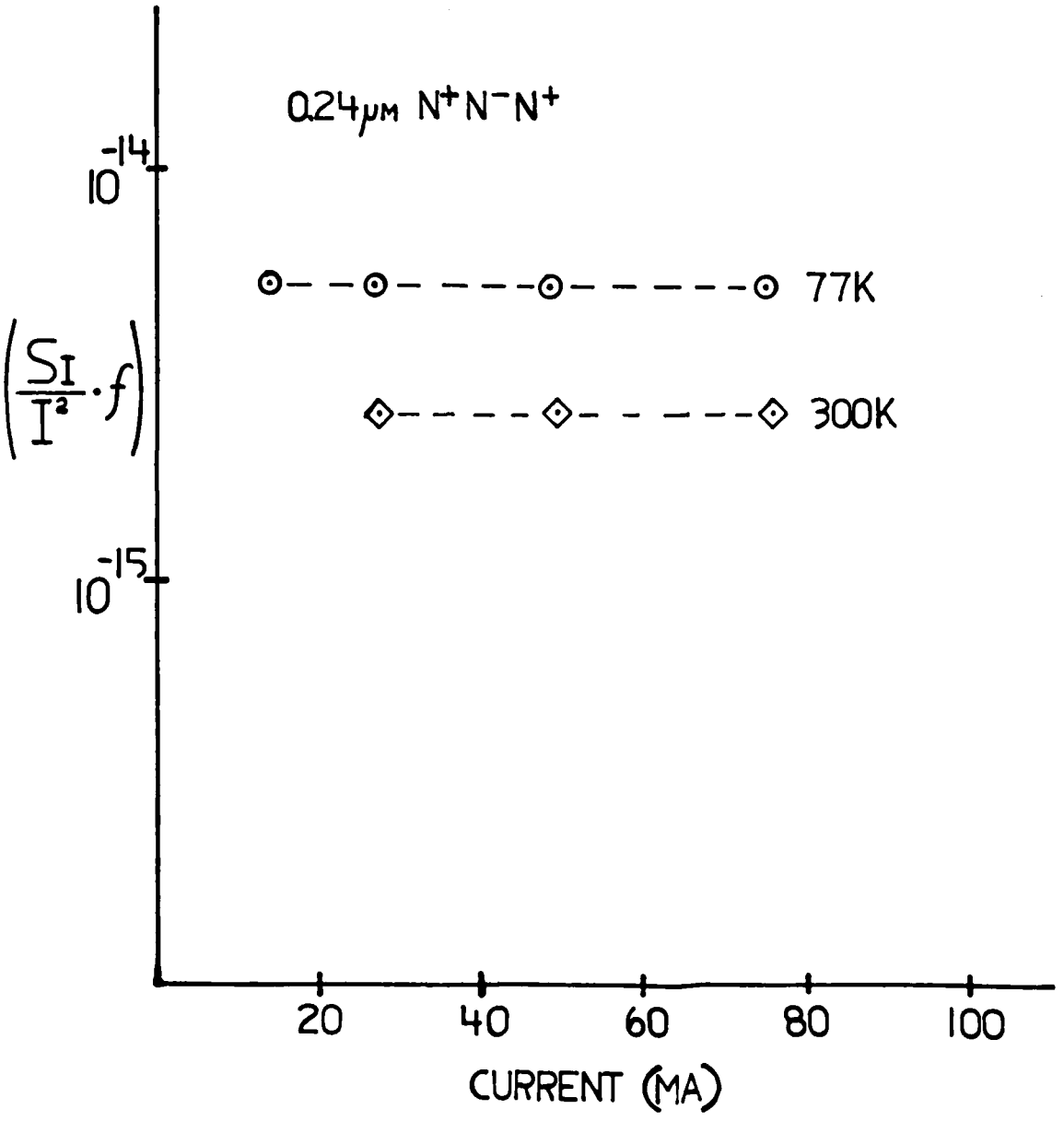

Figure 10

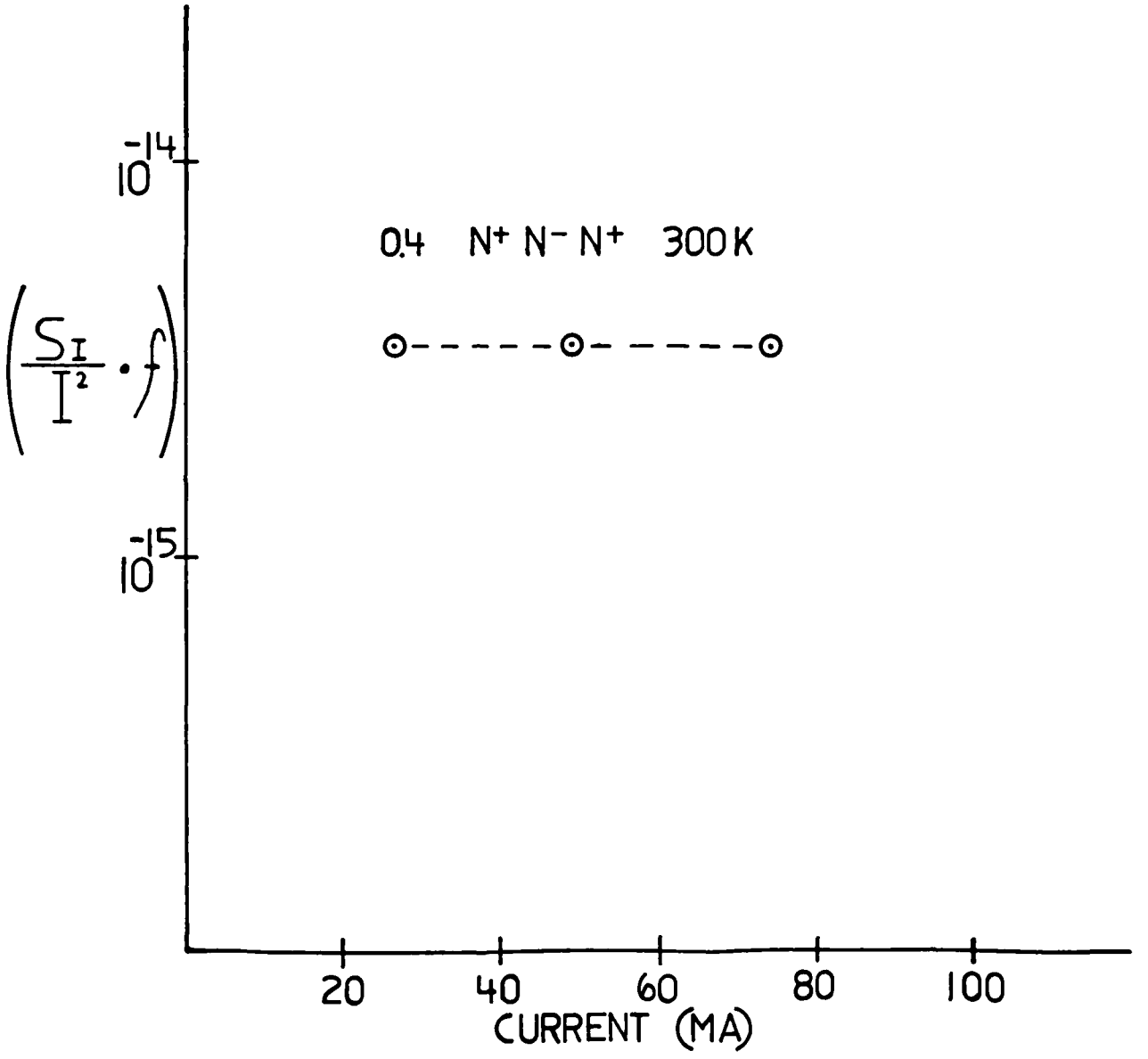
10^{-14}
10^{-15}
$\left(\frac{S_I}{I^2} \cdot f\right)$
0.4 N+ N- N+ 300K
20
40
60
80
100
CURRENT (MA)

Figure 11

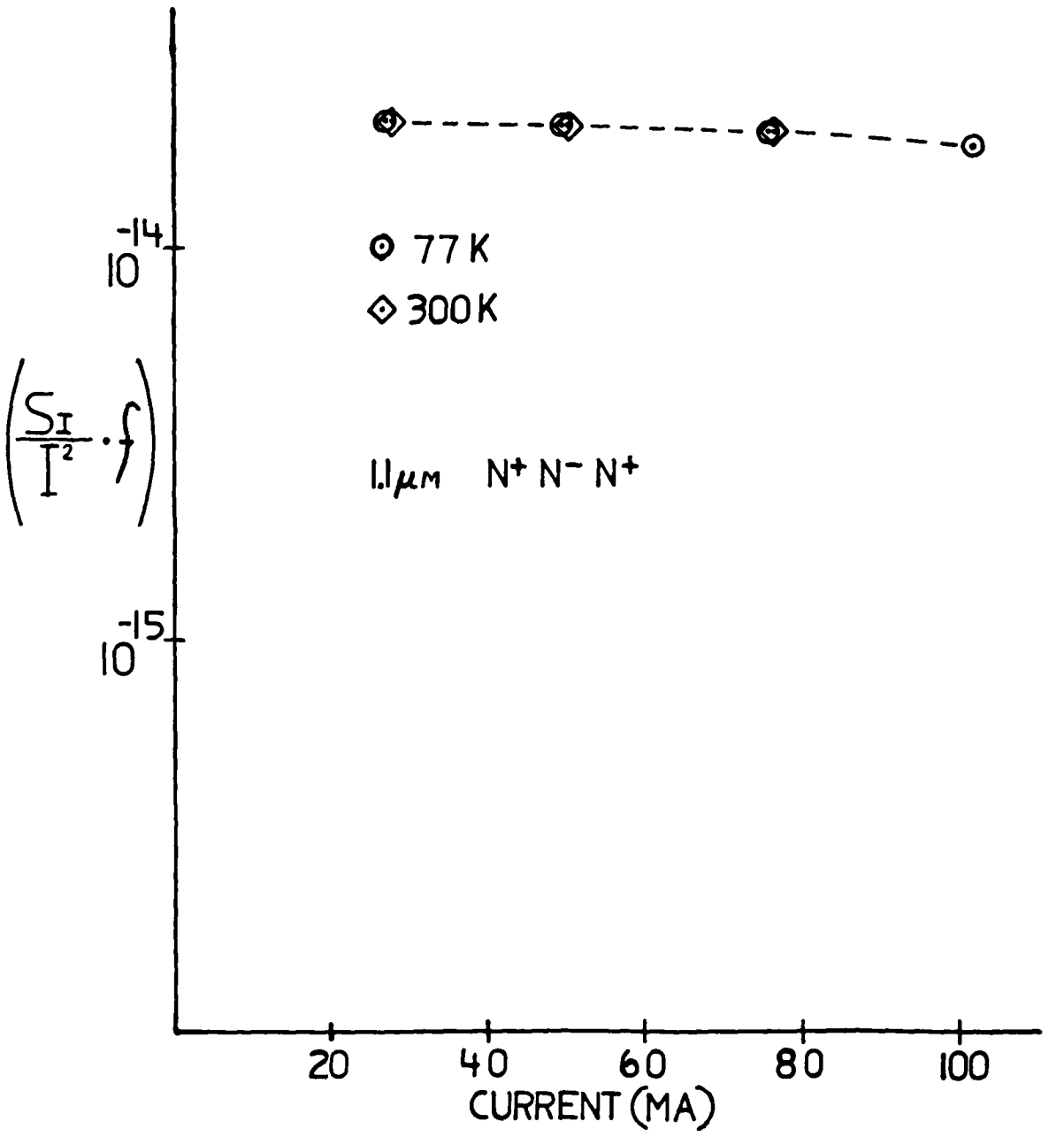
10^{-14}
10^{-15}
$\left(\frac{S_I}{I^2} \cdot f\right)$
77 K
300 K
1.1μm N+ N− N+
20
40
60
80
100
CURRENT (MA)

Figure 12

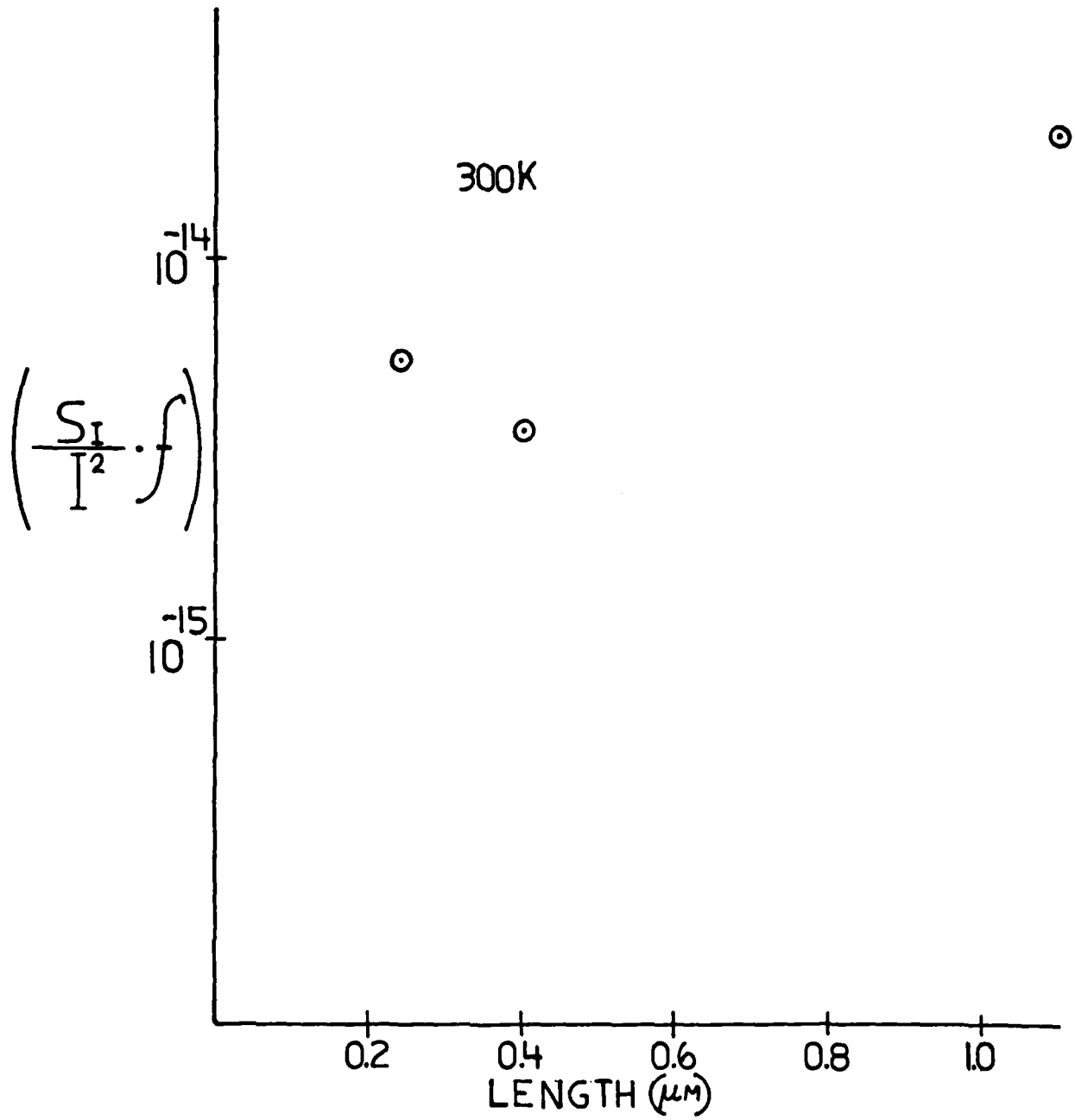
300K
10^{-14}
$\left(\frac{S_I}{I^2} \cdot f\right)$
10^{-15}
0.2
0.4
0.6
0.8
1.0
LENGTH (μM)

Figure 13

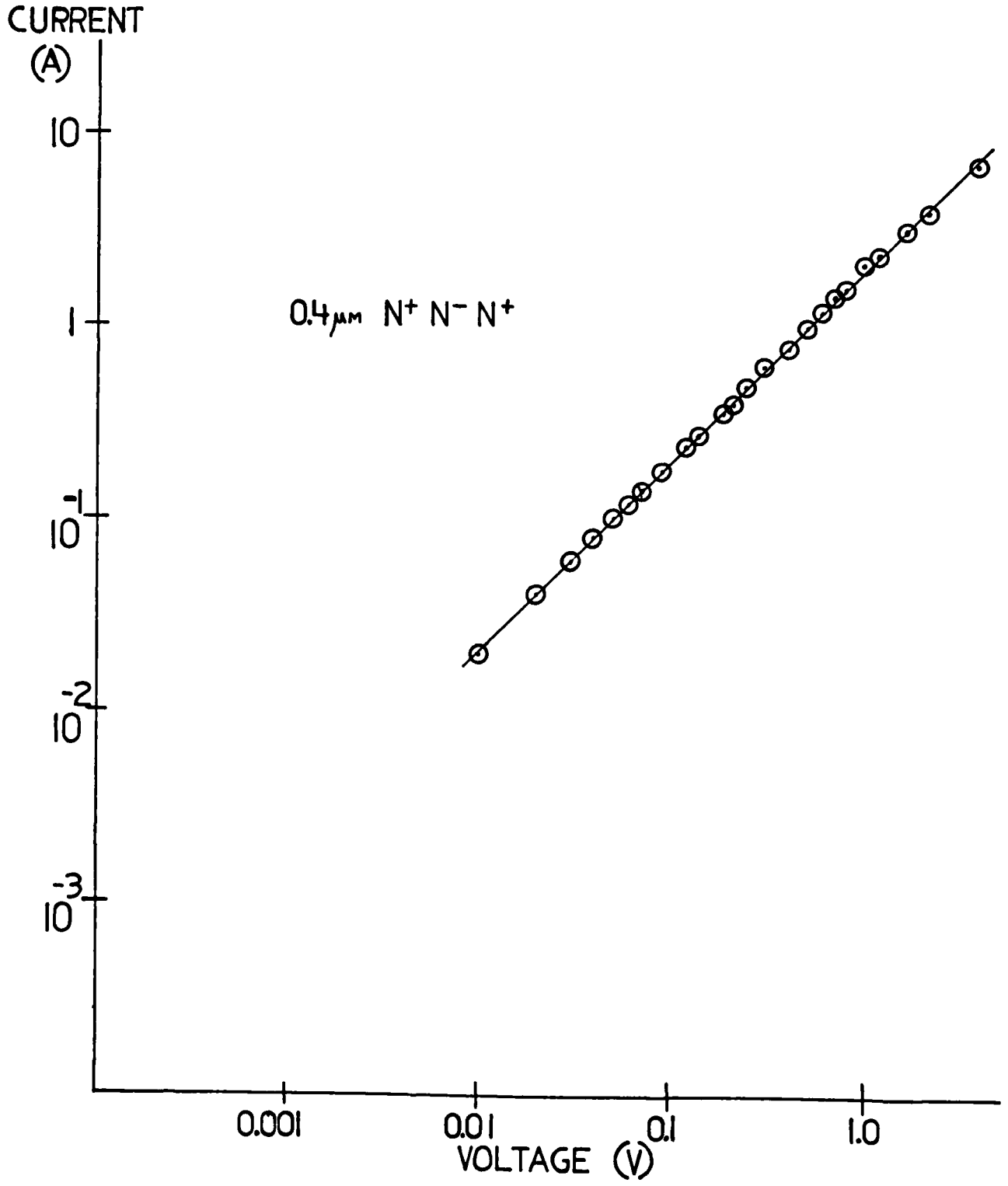

Figure 14

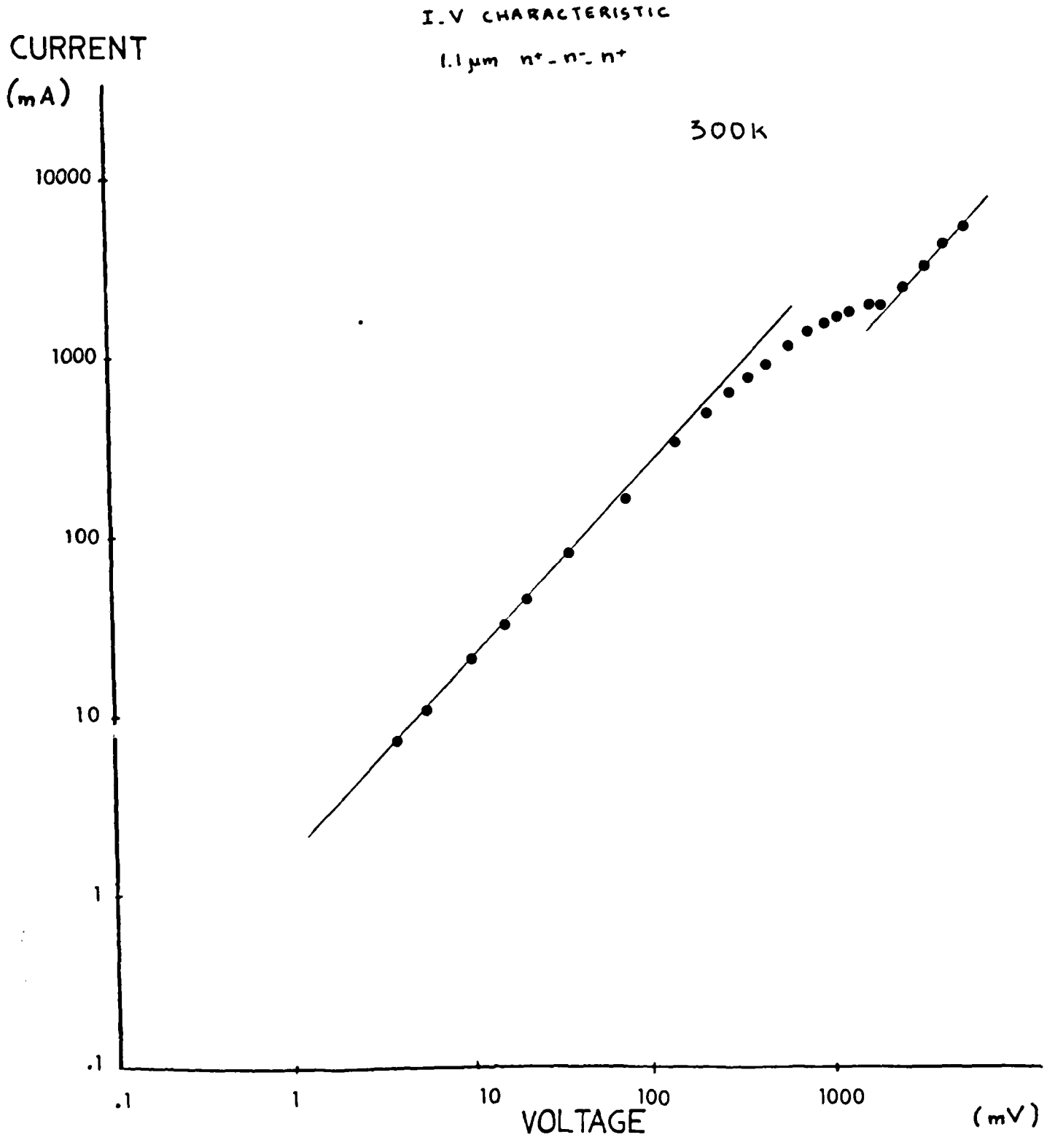
I.V CHARACTERISTIC
1.1 μm n⁺ - n⁻ - n⁺
300K
CURRENT
(mA)
10000
1000
100
10
1
.1
.1
1
10
100
1000
VOLTAGE
(mV)

Figure 15

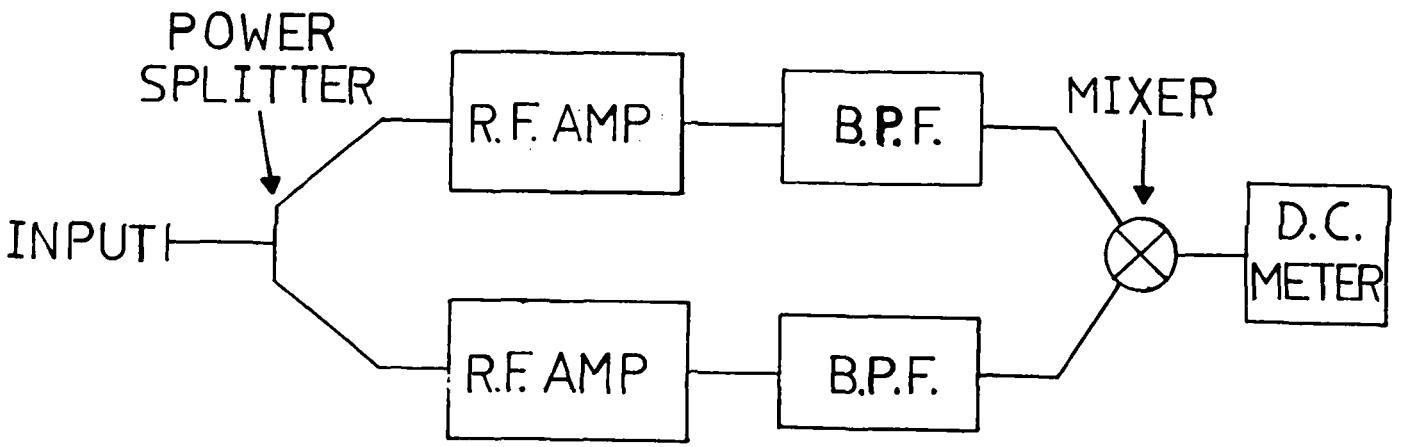

Figure 16

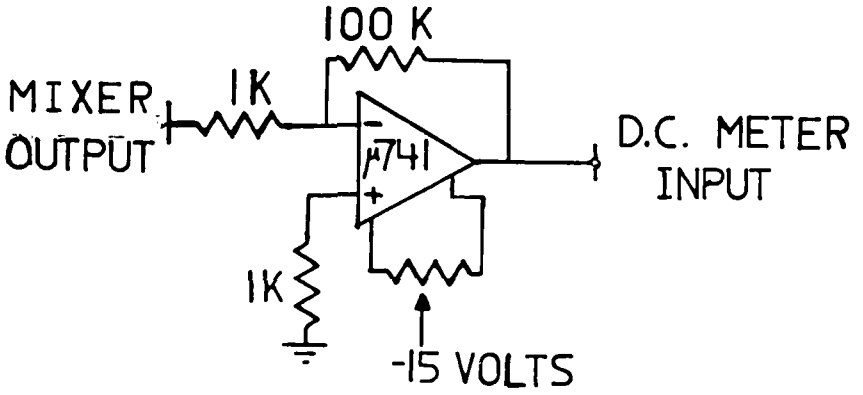

Figure 17

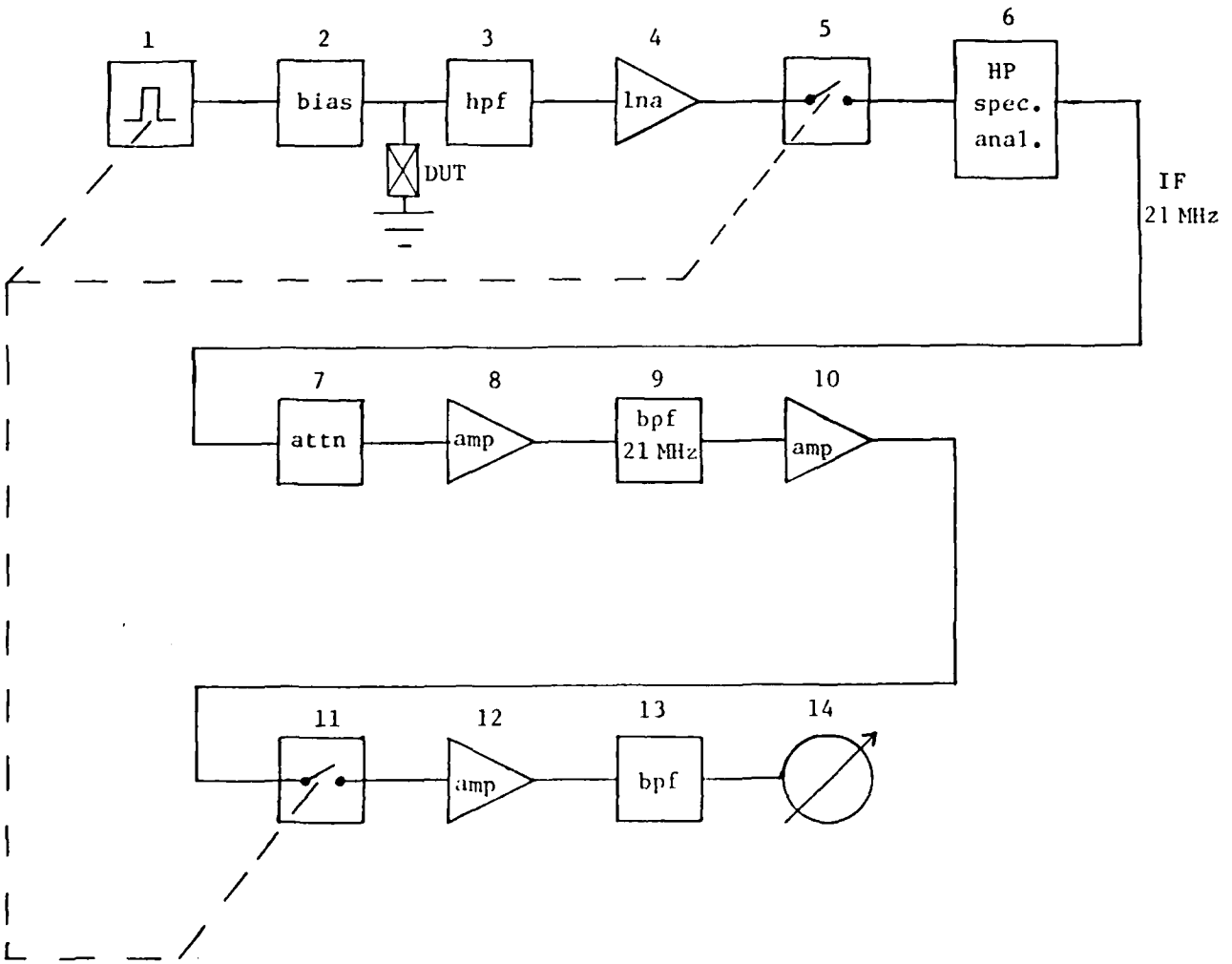
1
2
3
4
5
6
bias
hpf
lna
HP
spec.
anal.
DUT
IF
21 MHz
7
8
9
10
attn
amp
bpf
21 MHz
amp
11
12
13
14
amp
bpf

Figure 18

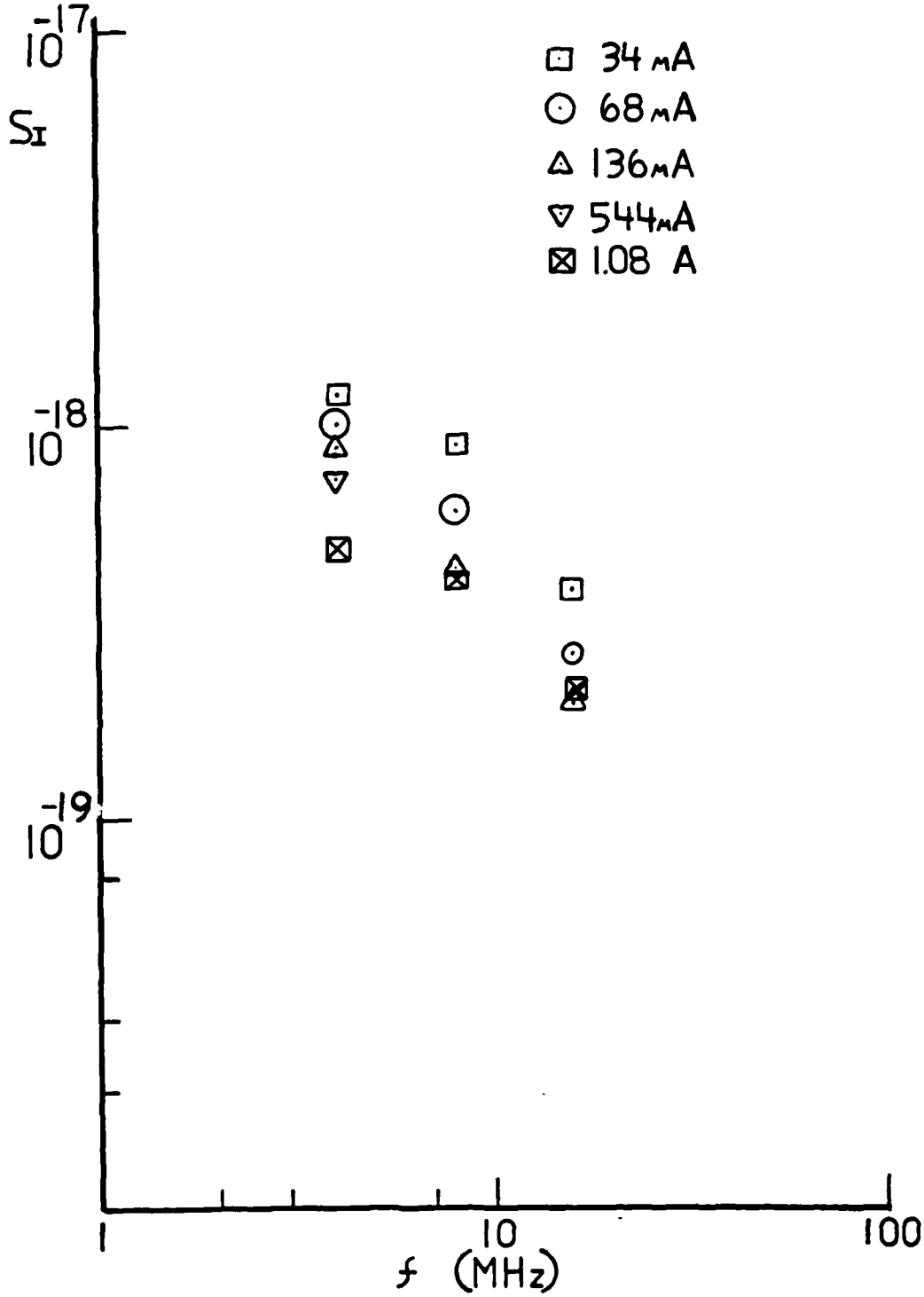

Figure 19

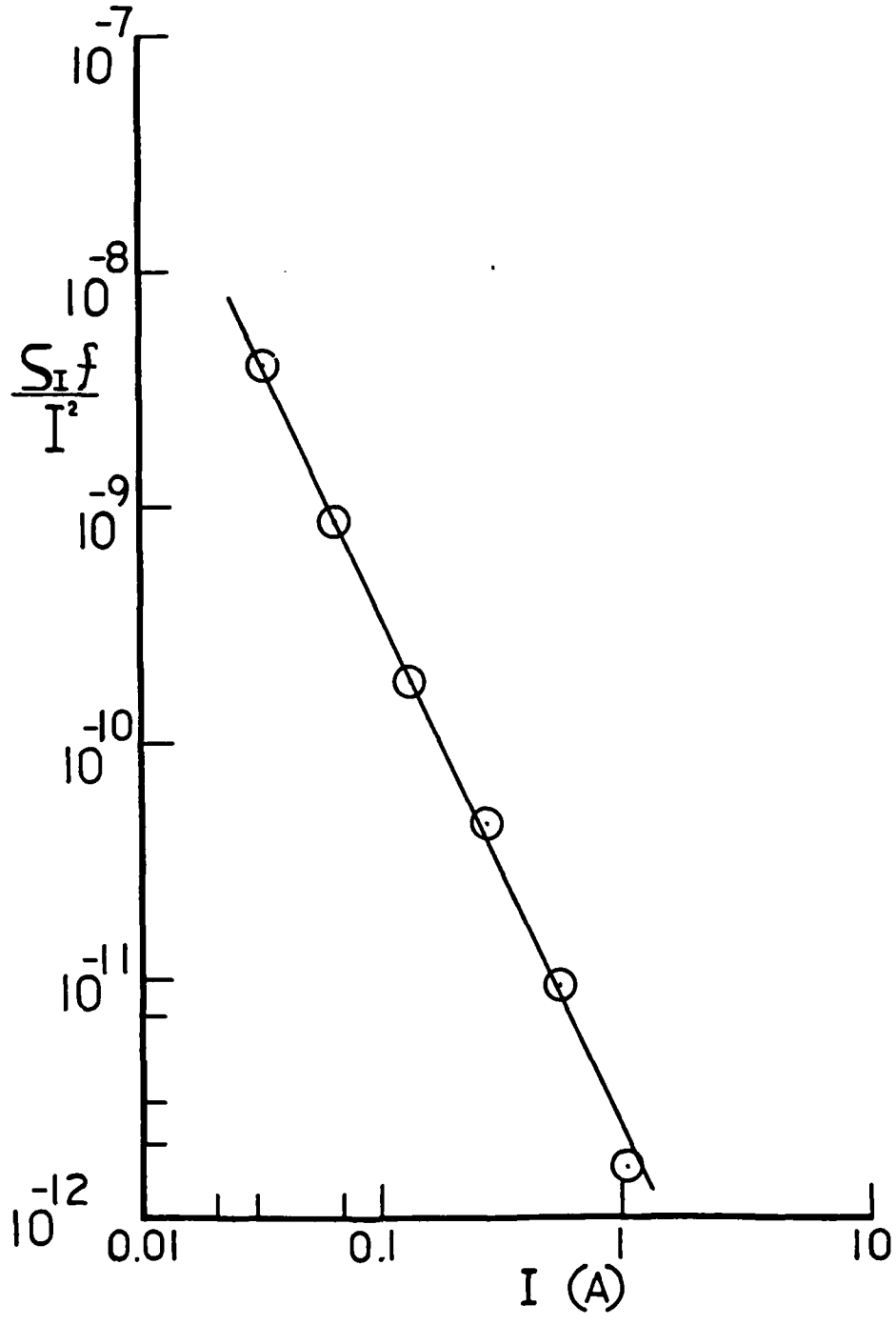

Figure 20

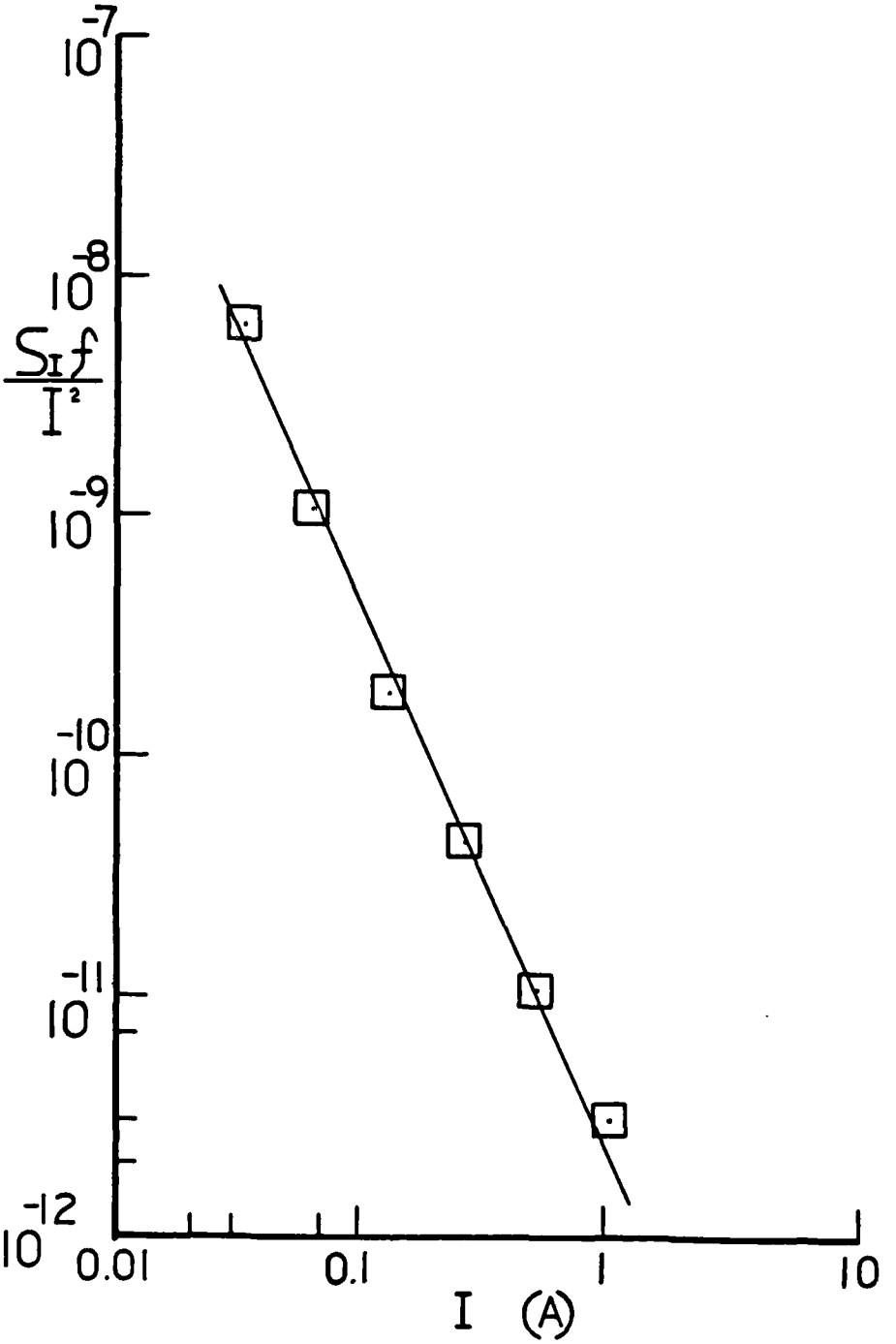

Figure 21

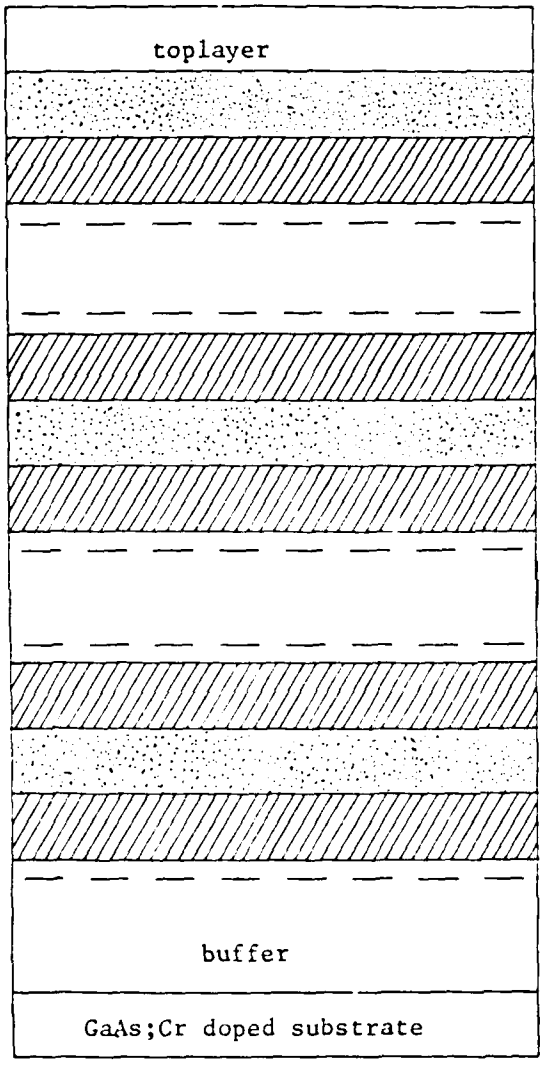

Layered structure of the Heterostructure

= GaAs;undoped. =$Al_xGa_{1-x}As$;undoped

=$Al_xGa_{1-x}As$; Si doped. = 2 DEG

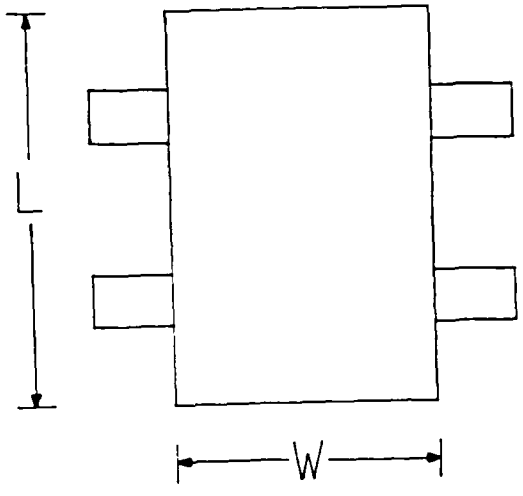

Hall-bar device pattern

(topview)

Figure 22

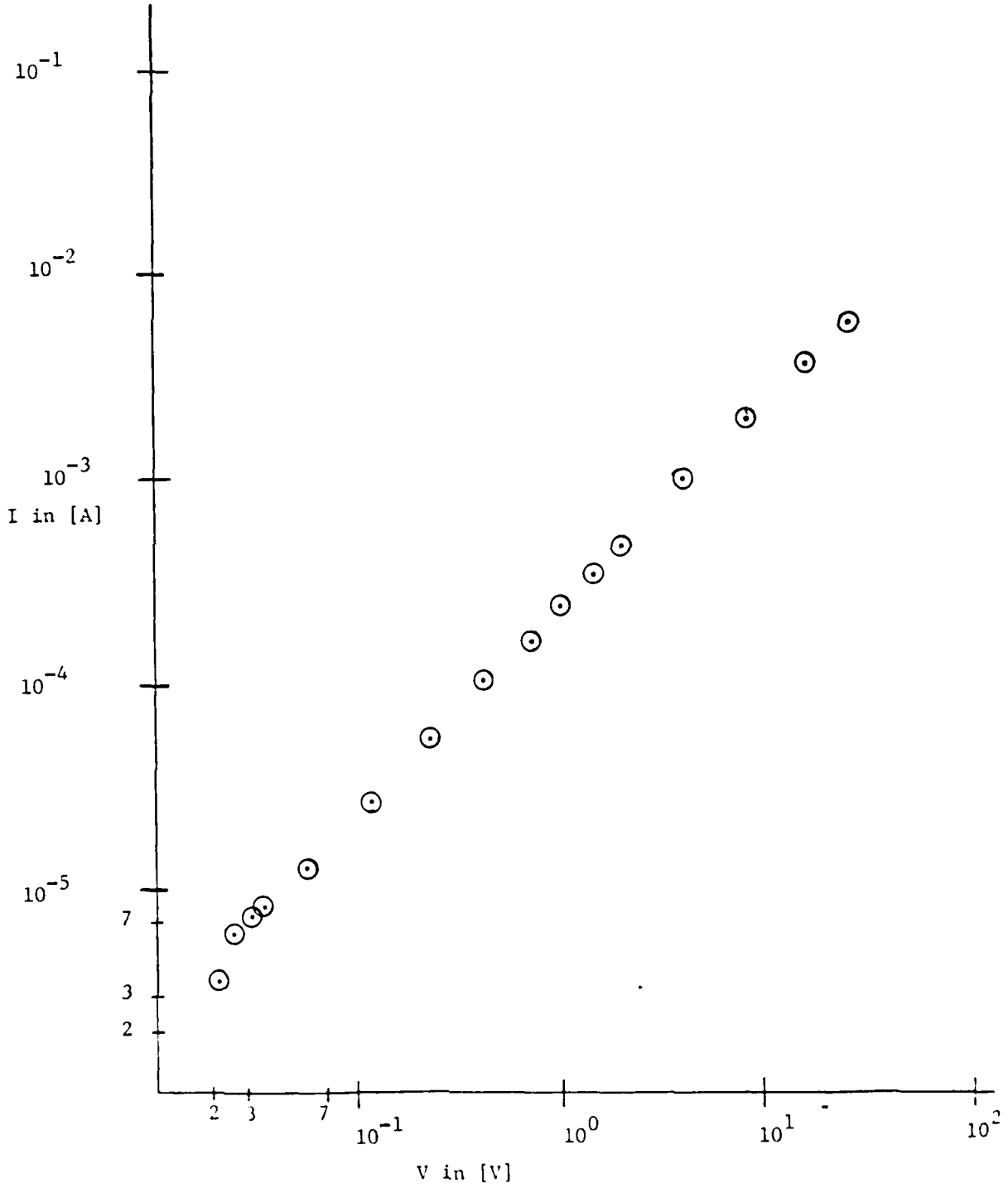

Figure 23

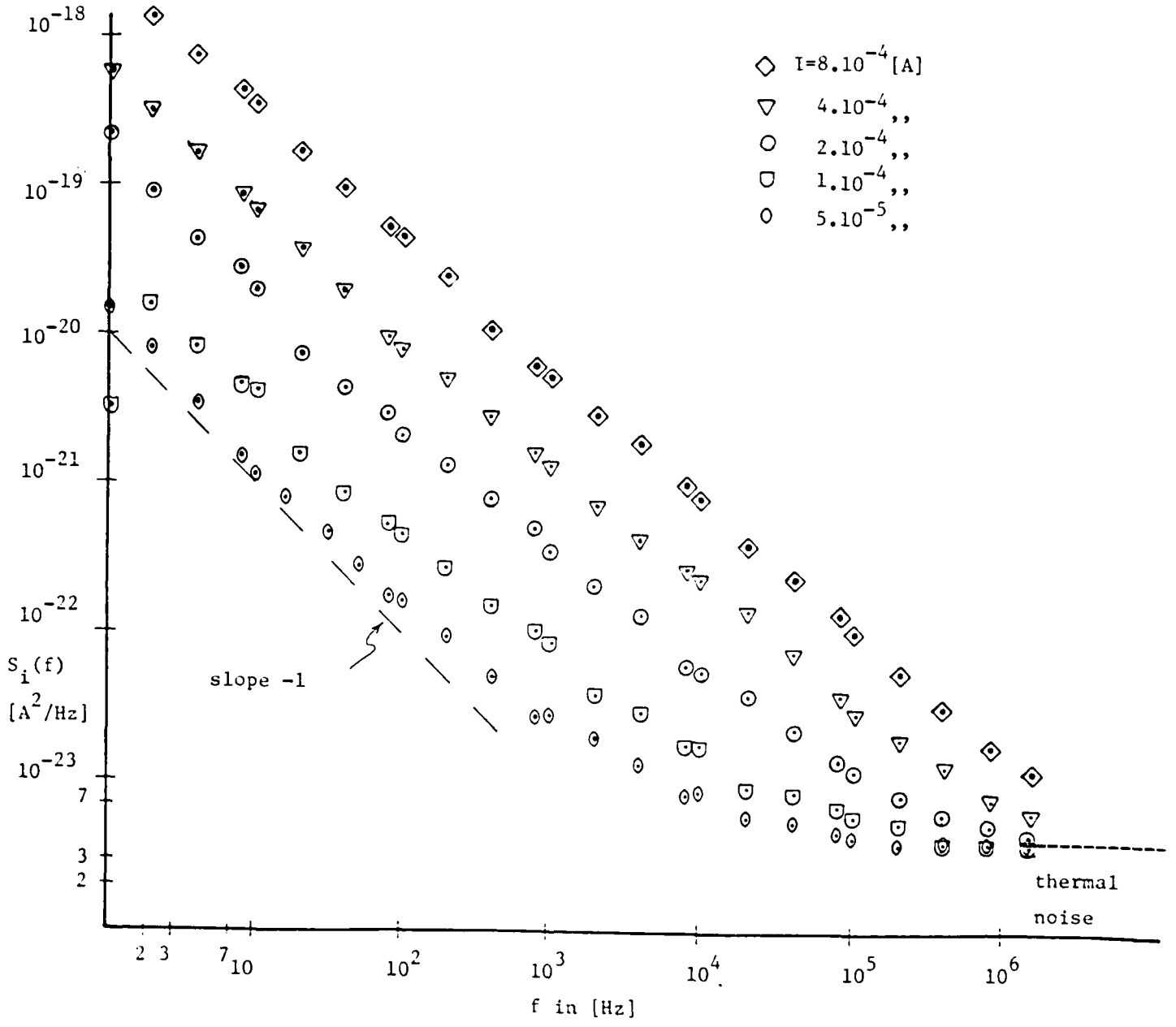
10^{-18}
10^{-19}
10^{-20}
10^{-21}
10^{-22}
10^{-23}
7
3
2
$S_i(f)$
$[A^2/Hz]$
slope -1
$I=8.10^{-4}$[A]
4.10^{-4},,
2.10^{-4},,
1.10^{-4},,
5.10^{-5},,
thermal
noise
2 3 7 10 10^2 10^3 10^4 10^5 10^6
f in [Hz]

Figure 24

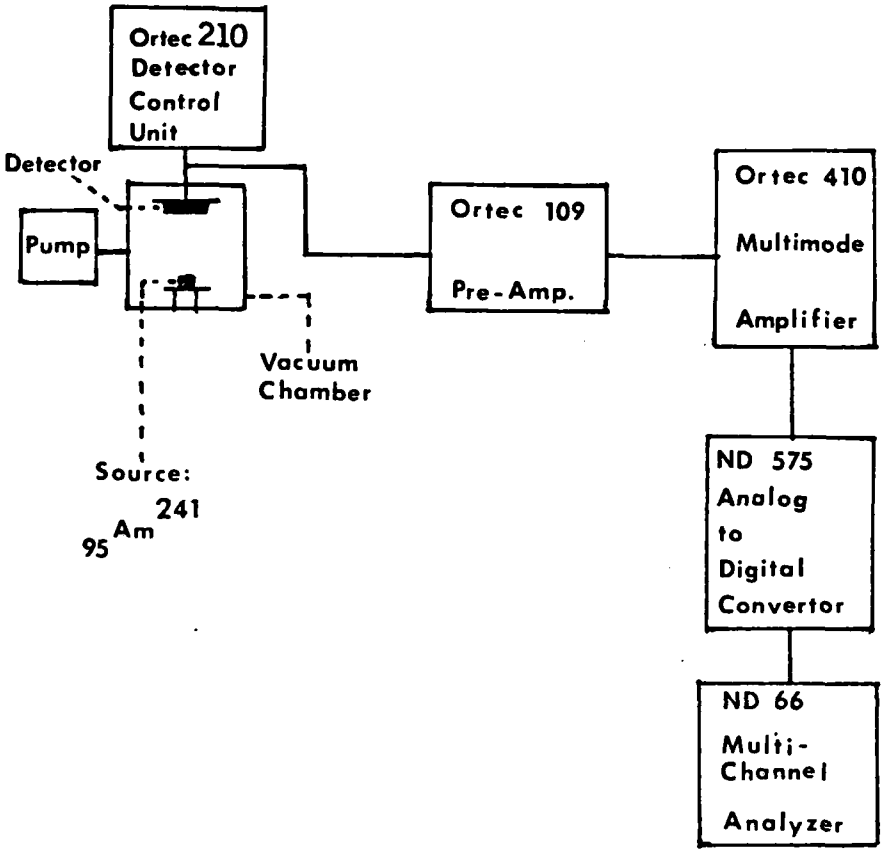

Figure 25. Block diagram of the counting system

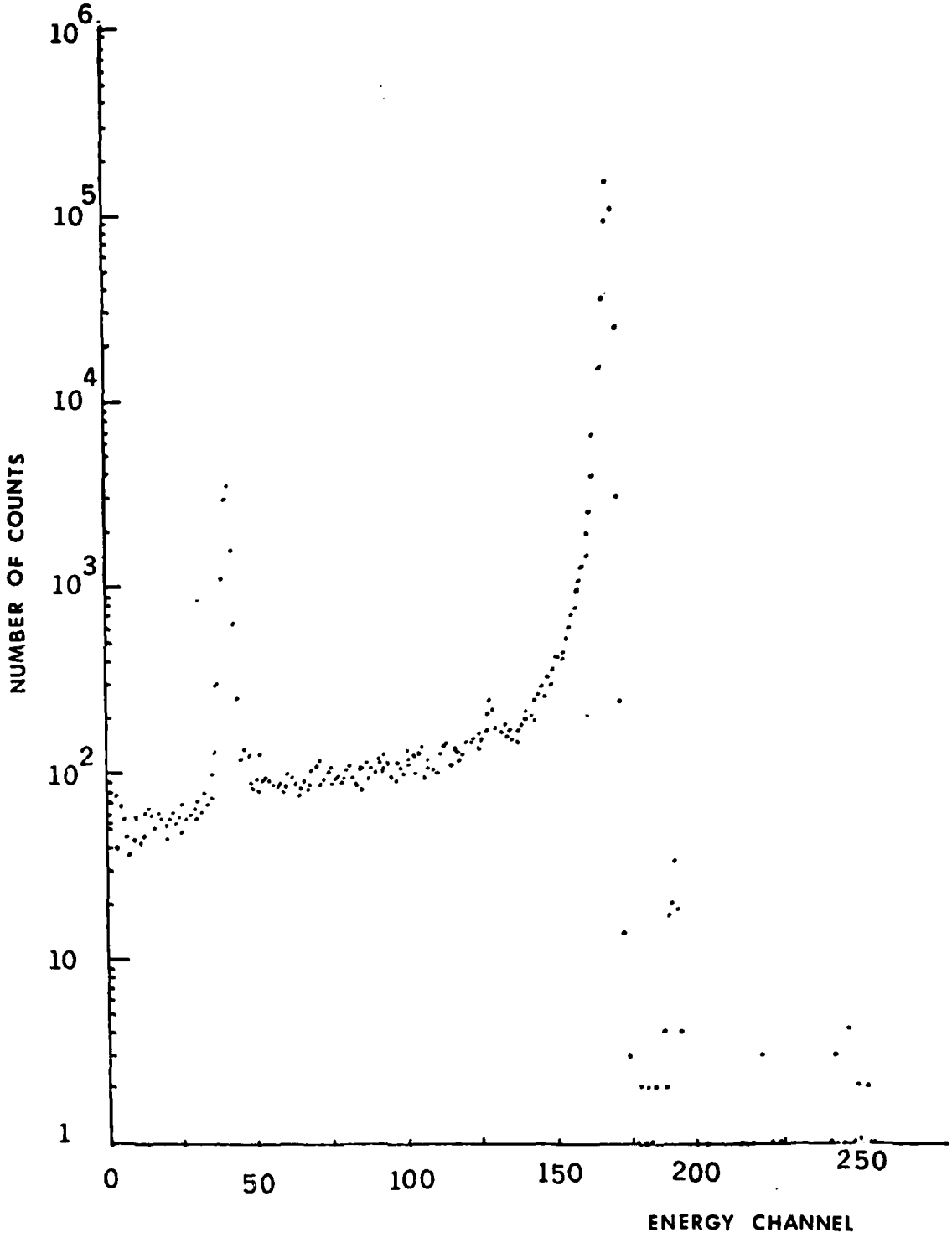

Figure 26. Typical full-energy spectrum.

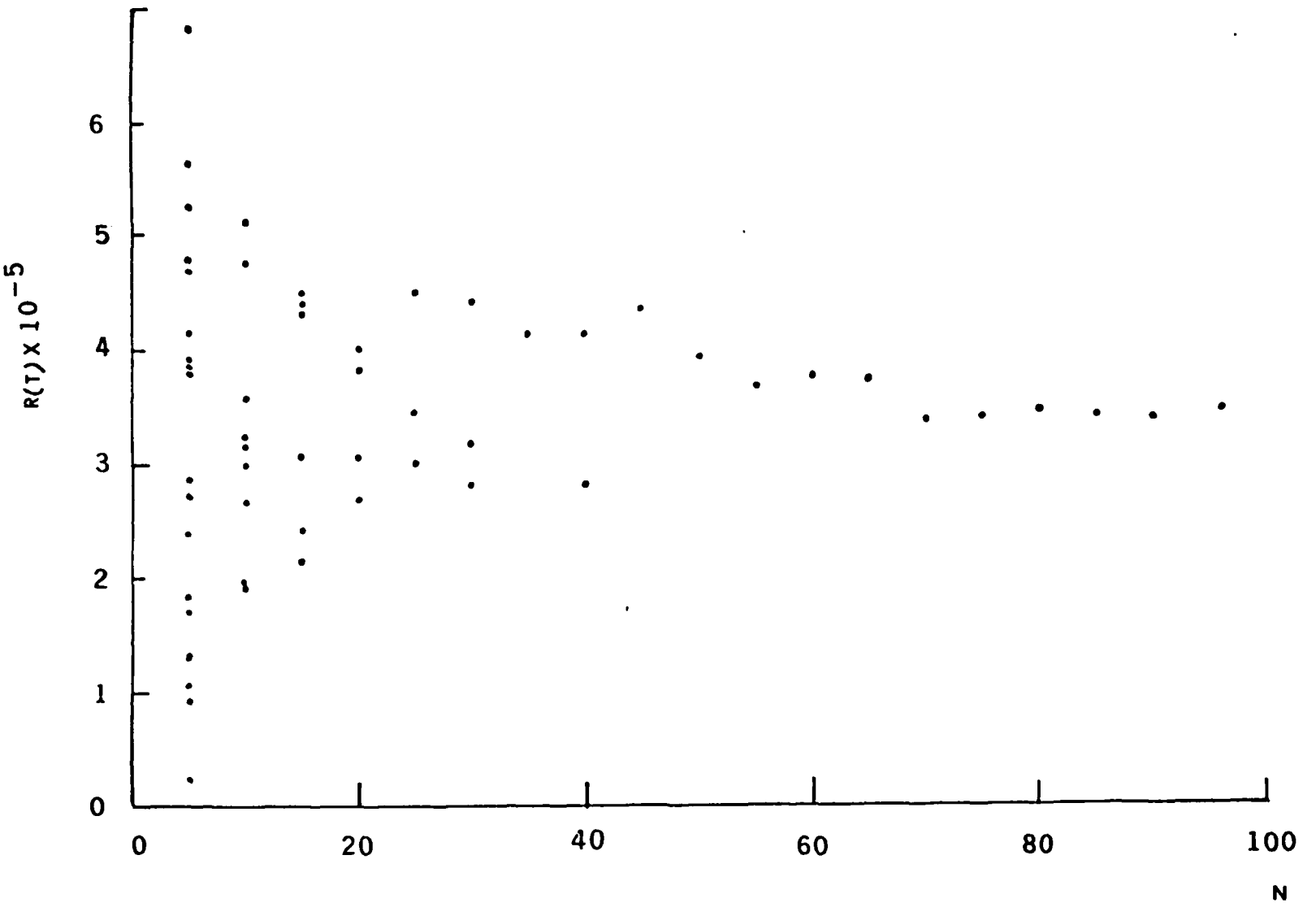

Figure 27. R(T) vs. N for T = 1 min.

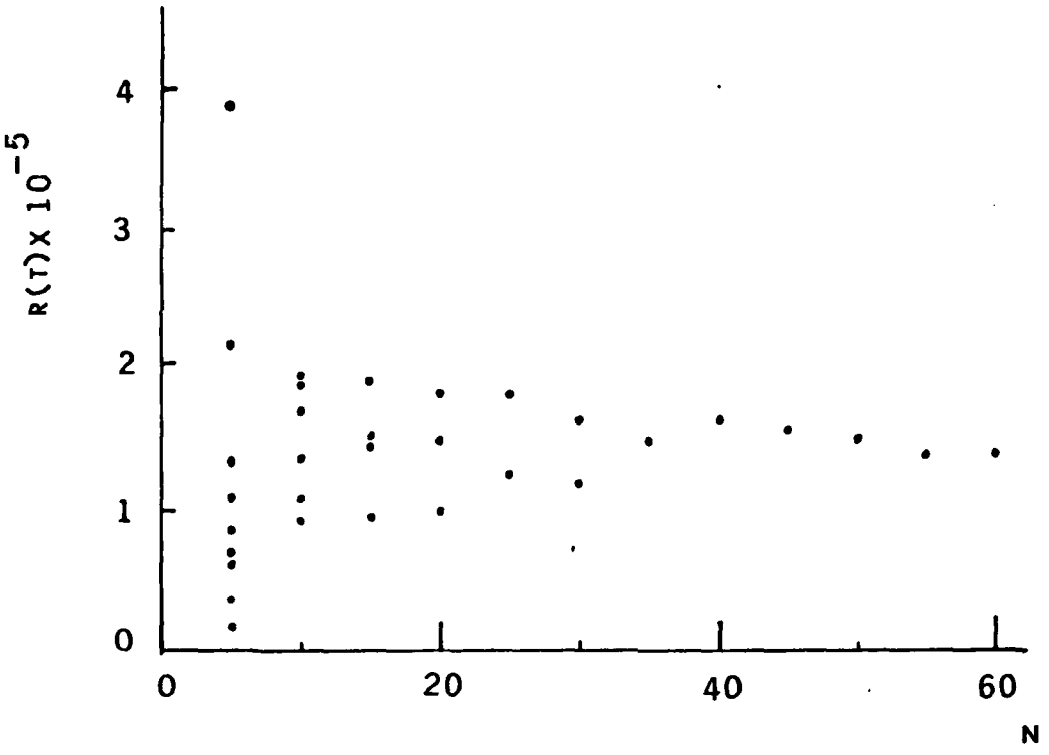

Figure 28. R(T) vs. N for T = 3 min.

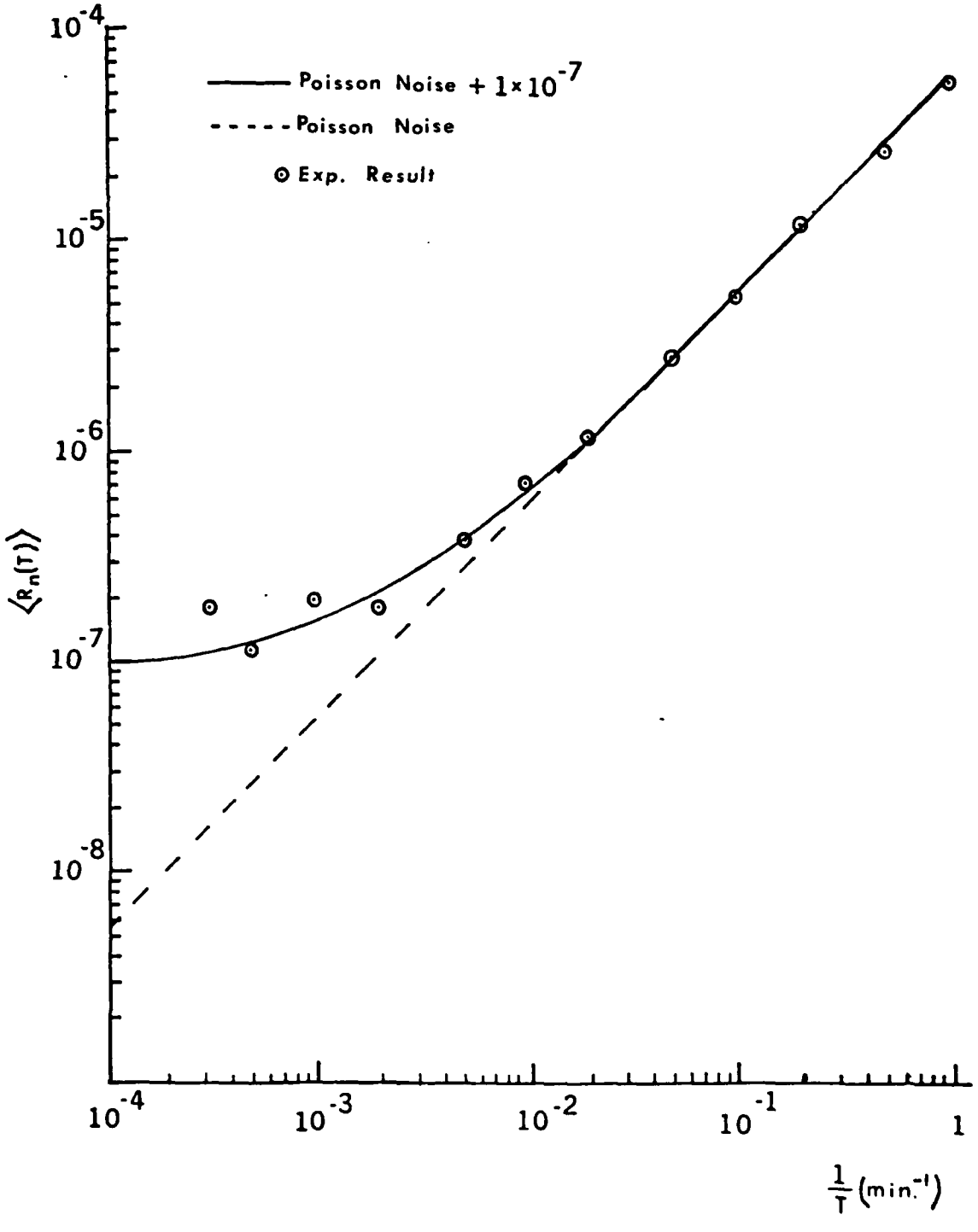

Figure 29. $\langle R_n(T) \rangle$ vs. 1/T for m_o = 18,000/min.

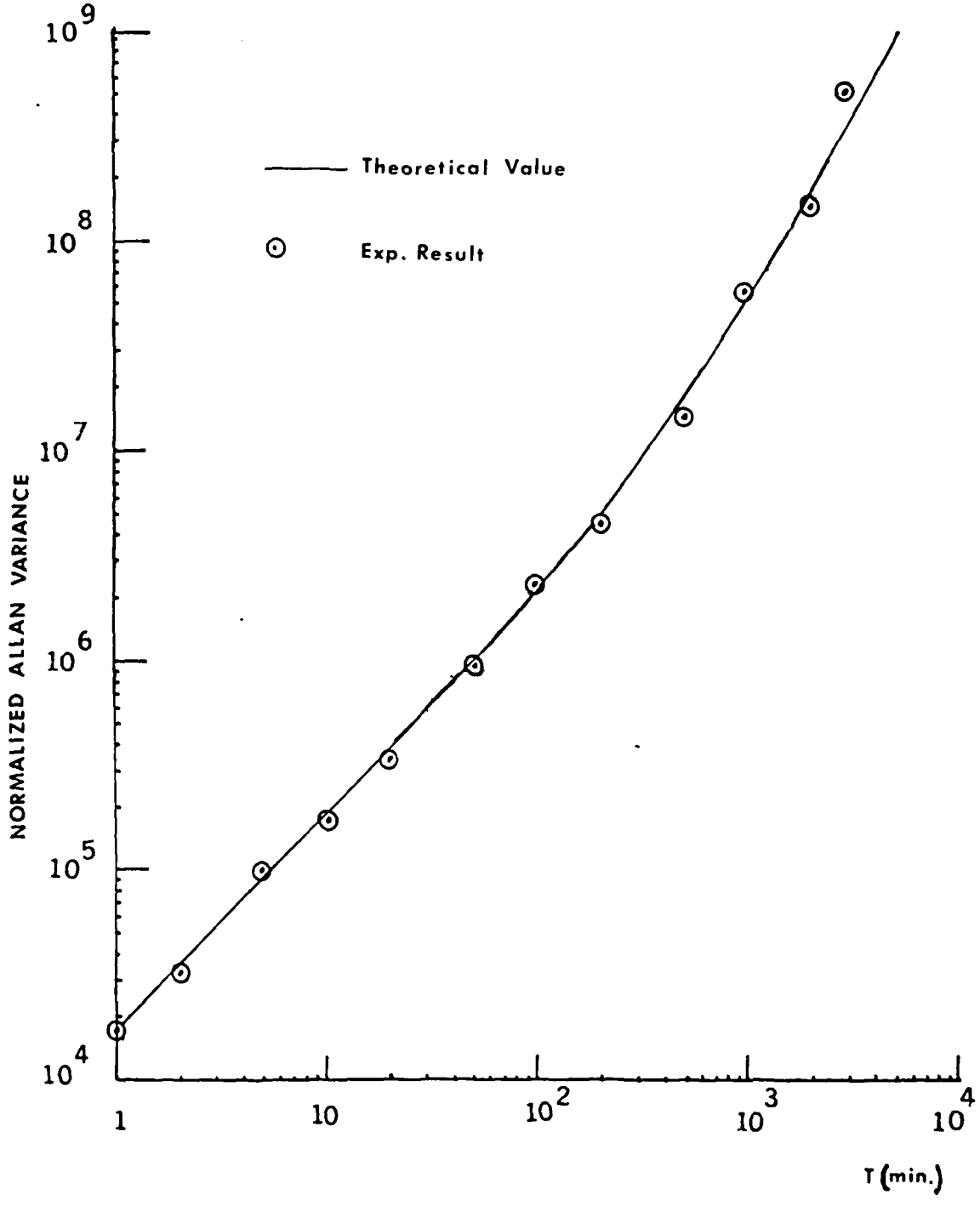

Figure 30. $\langle \sigma^{A2}_{M_T}(T) \rangle$ vs. T for m_o = 18,000/min.

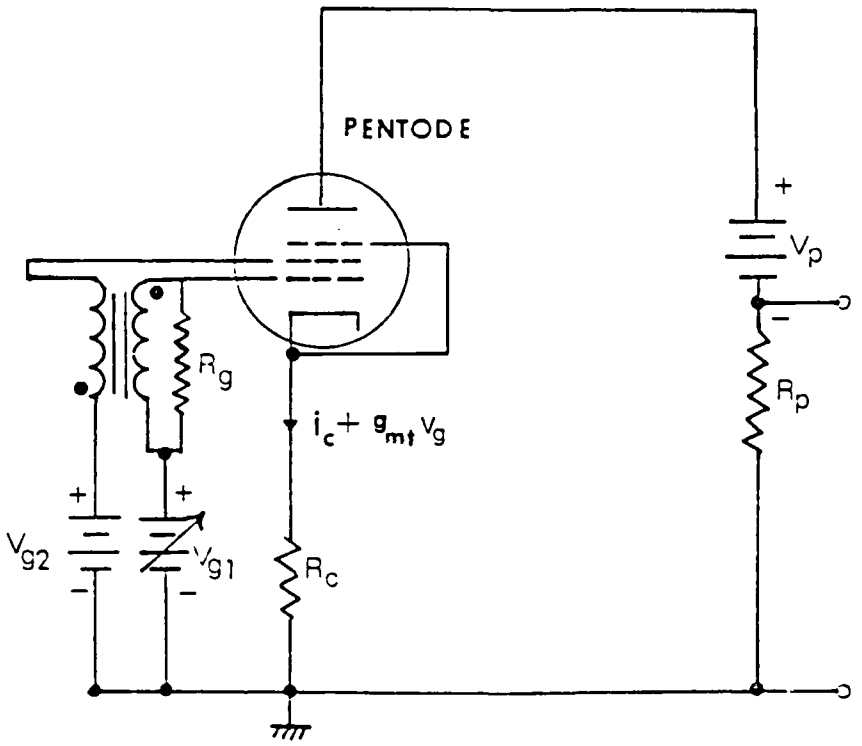

Figure 31. Feedback circuit in the cathode lead

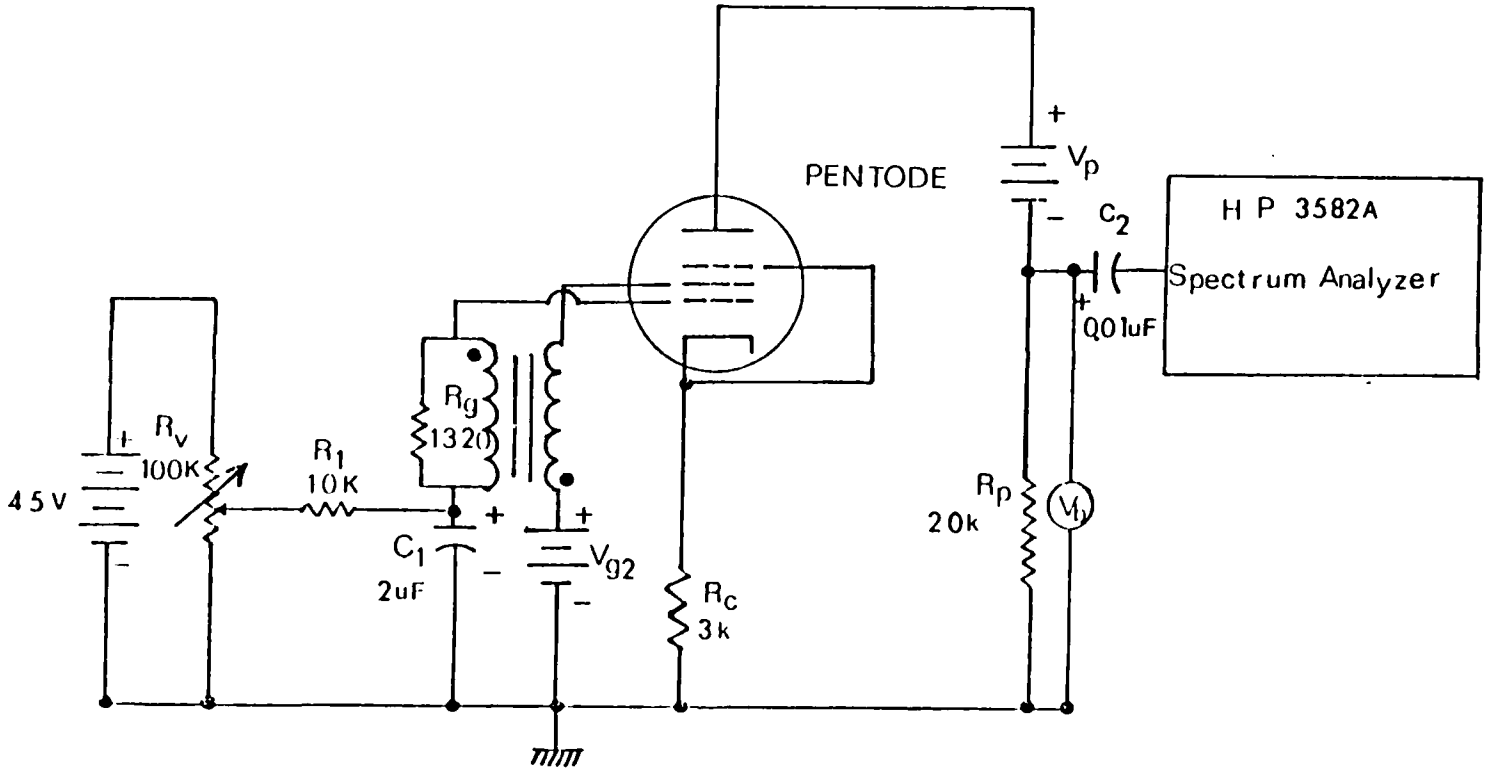

Figure 32. The circuit of the noise measurement system

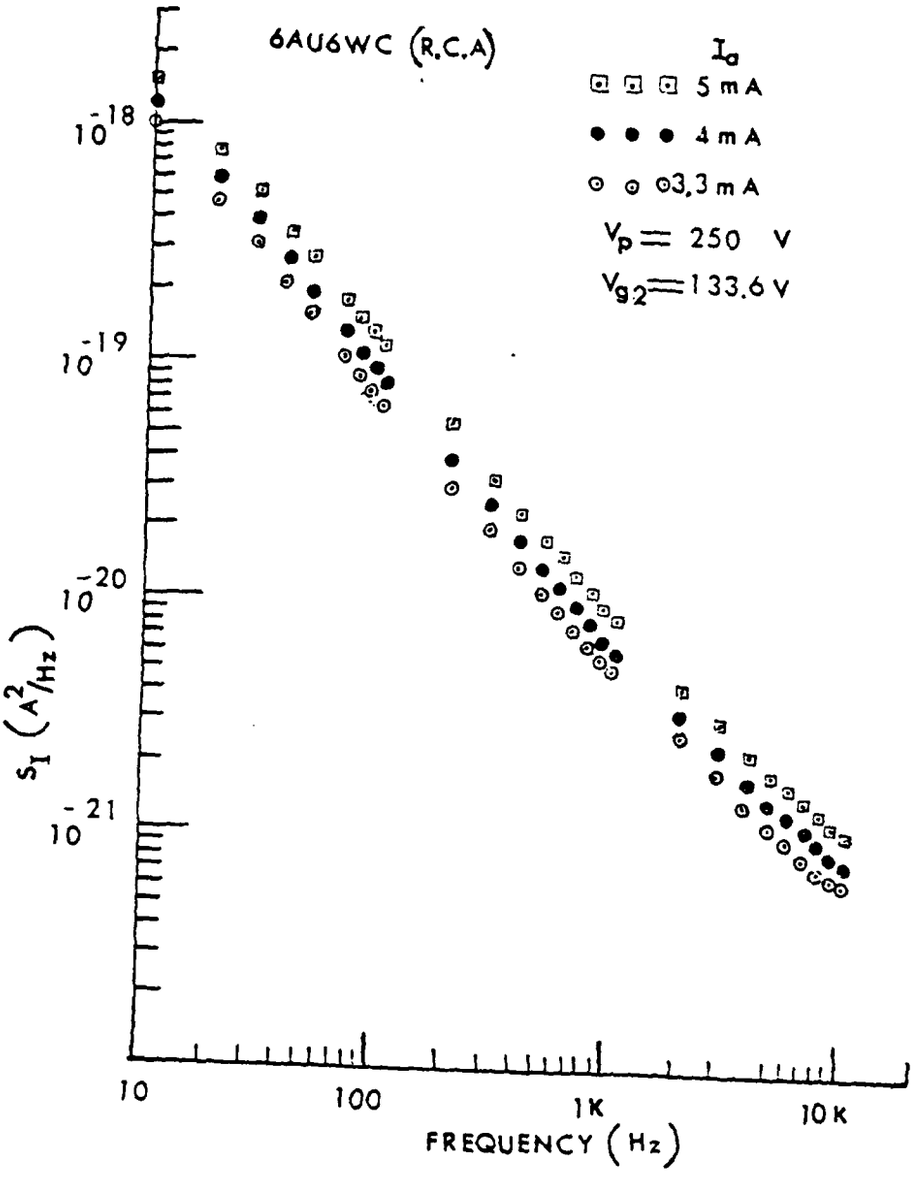

Figure 33. Current noise of 6AU6WC (RCA) device at three anode currents

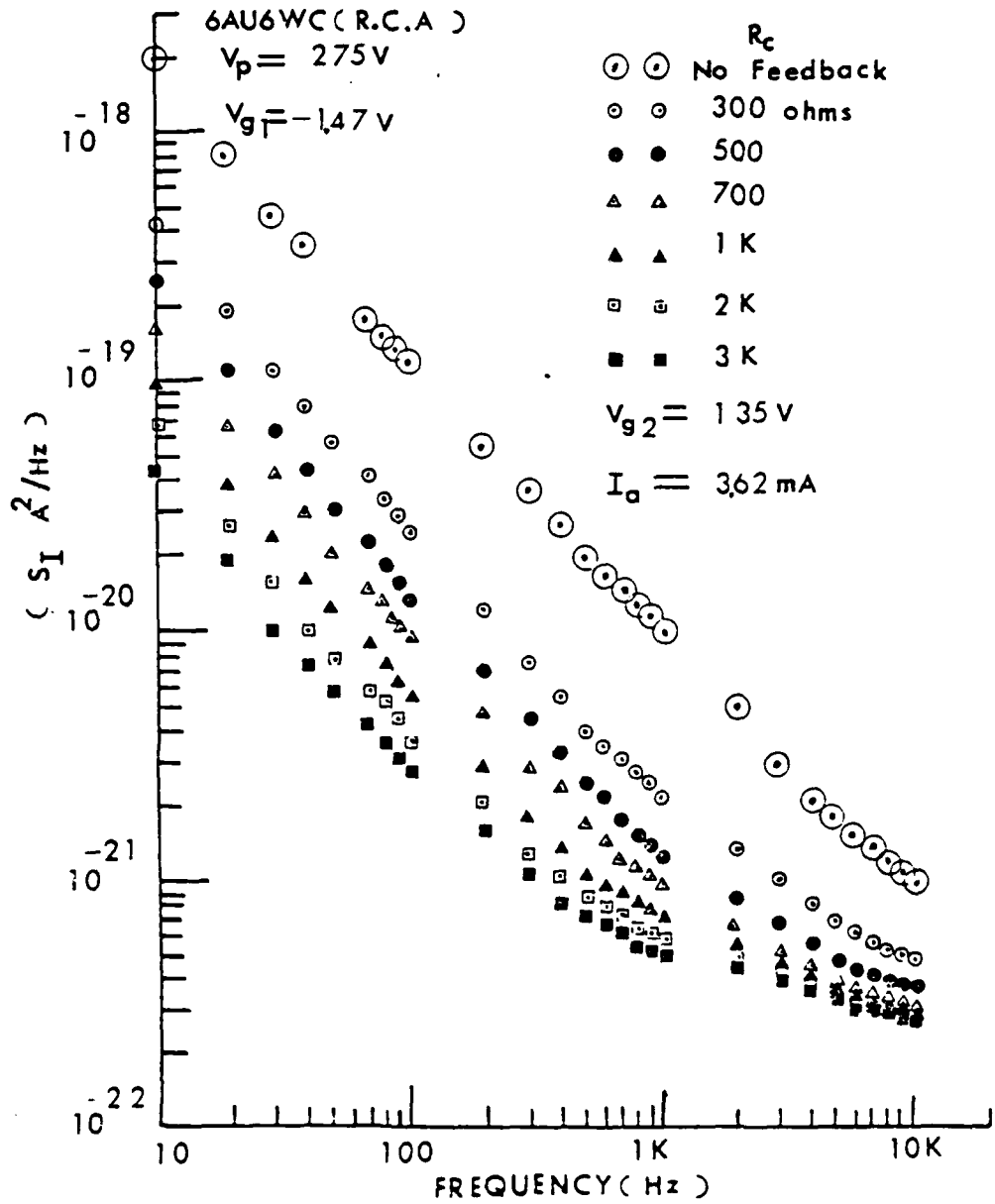

Figure 34. Current noise spectra of 6AU6WC (RCA) device for various values of R_c

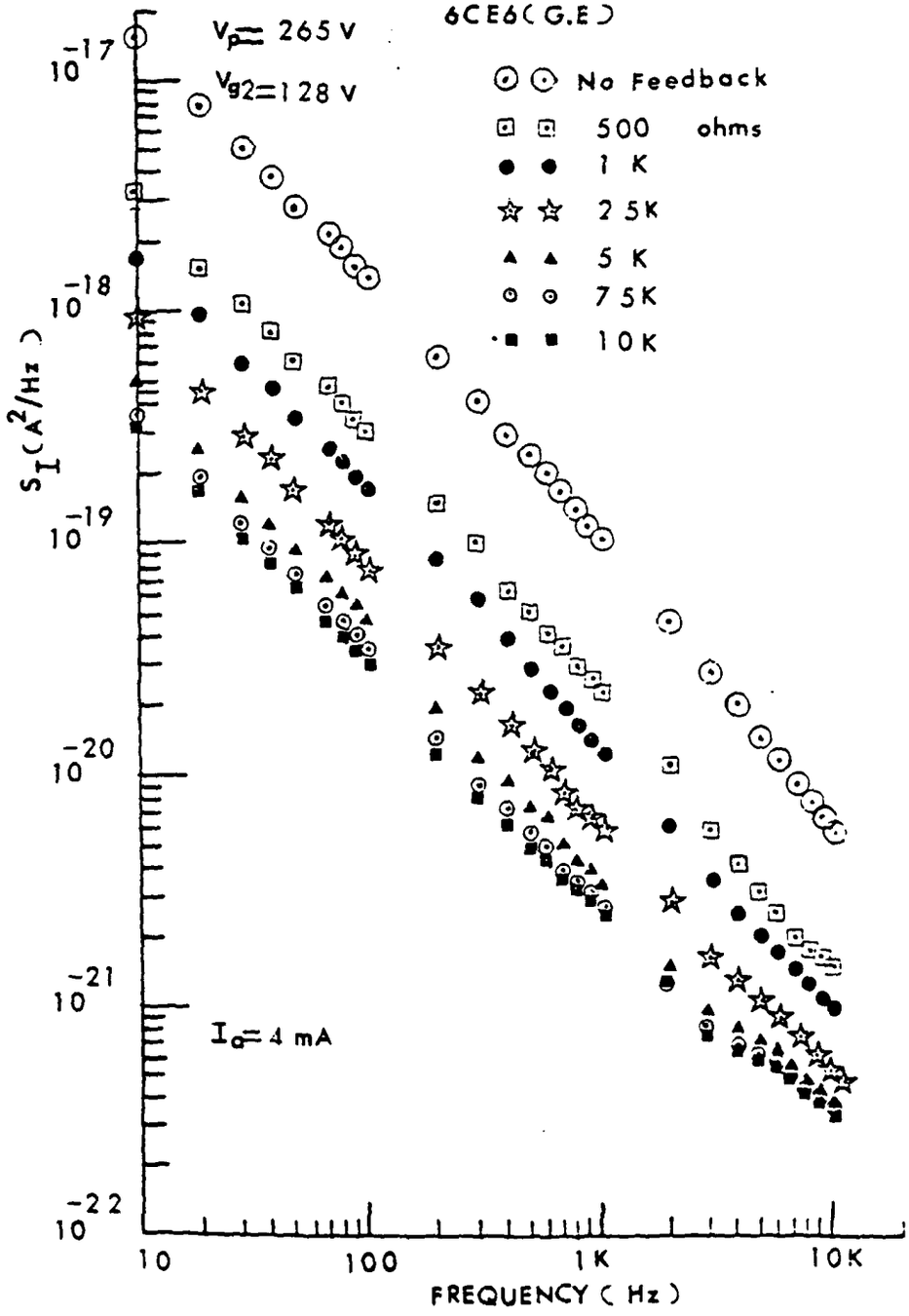

Figure 35. Current noise spectra of 6CE6 (GE) for various values of R_c

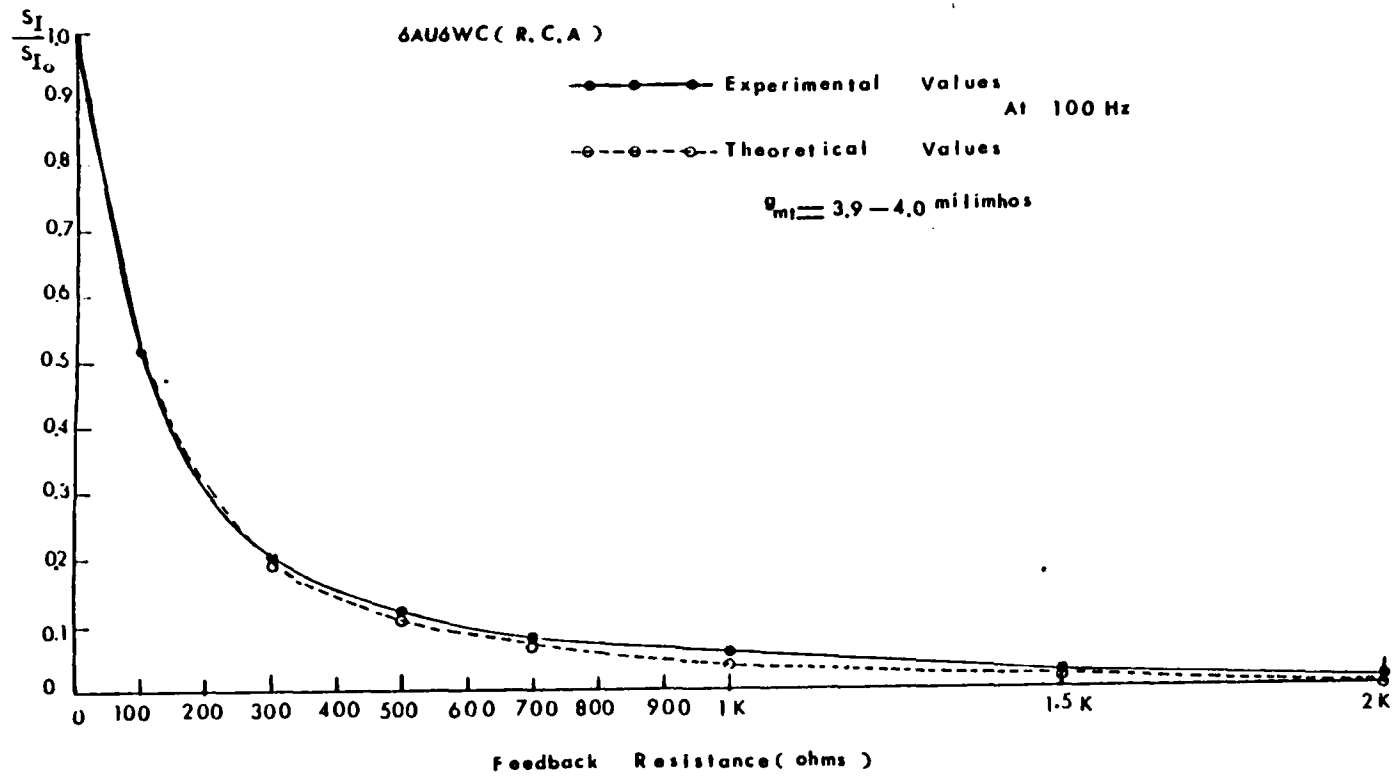

Figure 36. S_I/S_{I_o} vs. R_c for 6AU6WC (RCA) at 100 Hz

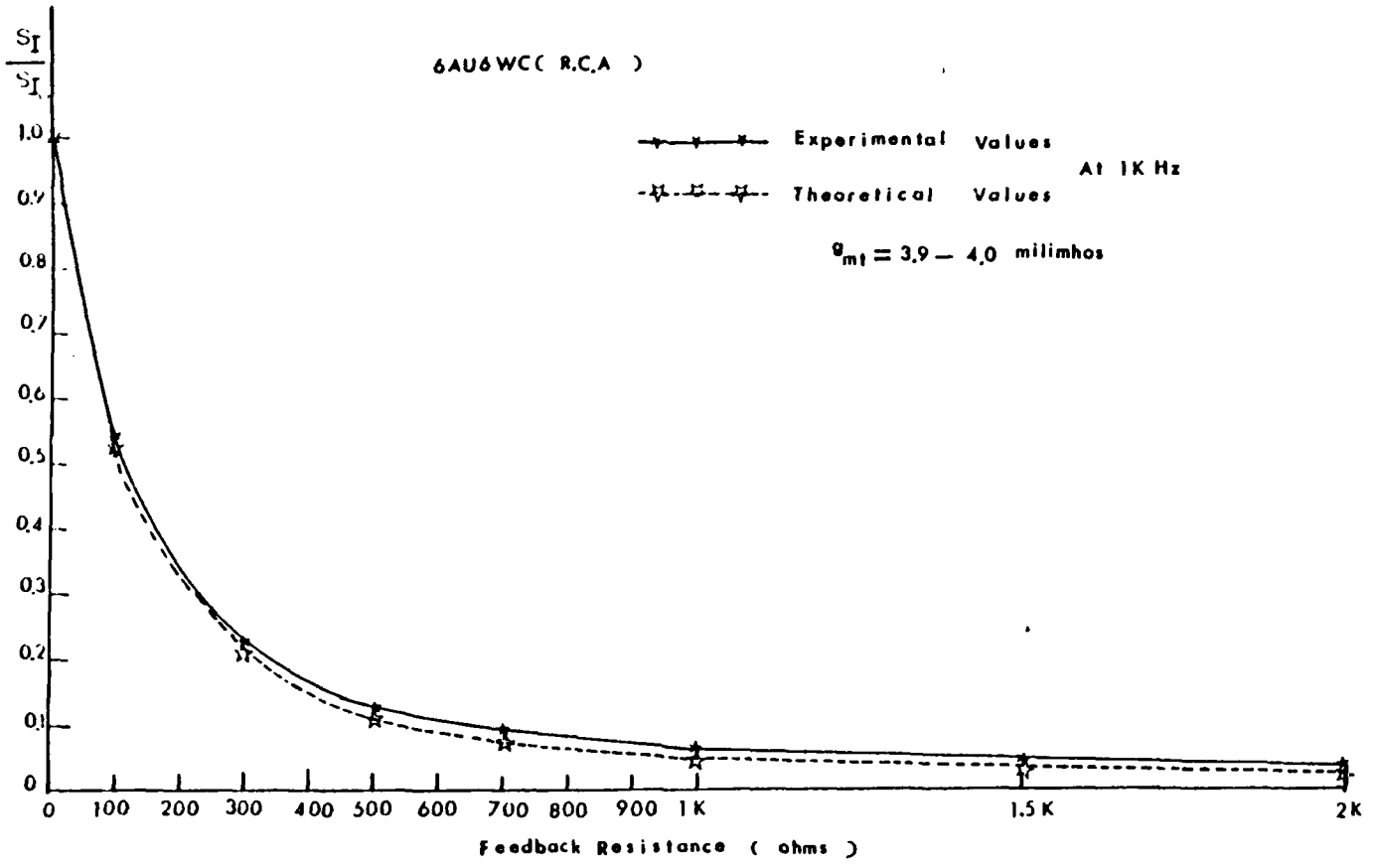

Figure 37. S_I/S_{I_0} vs. R_c for 6AU6WC (RCA) at 1 KHz

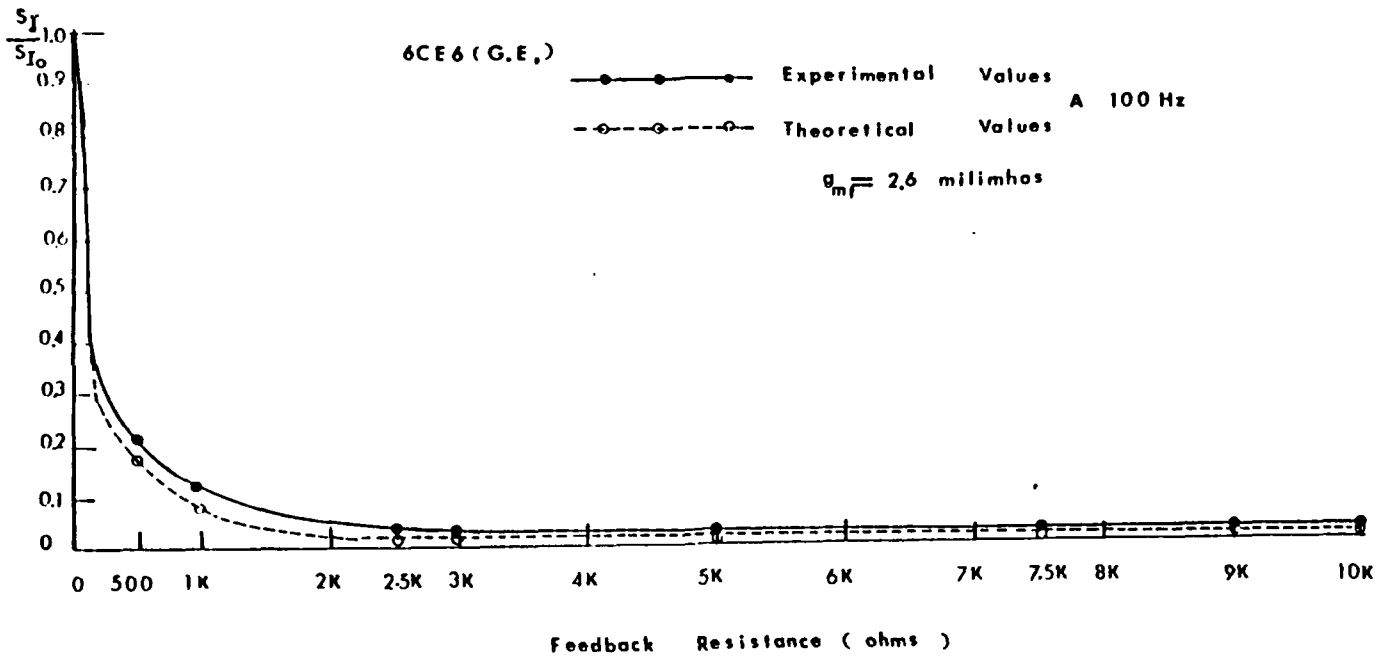

Figure 38. S_I/S_{I_o} vs. R_c for 6CE6 (GE) at 100 Hz

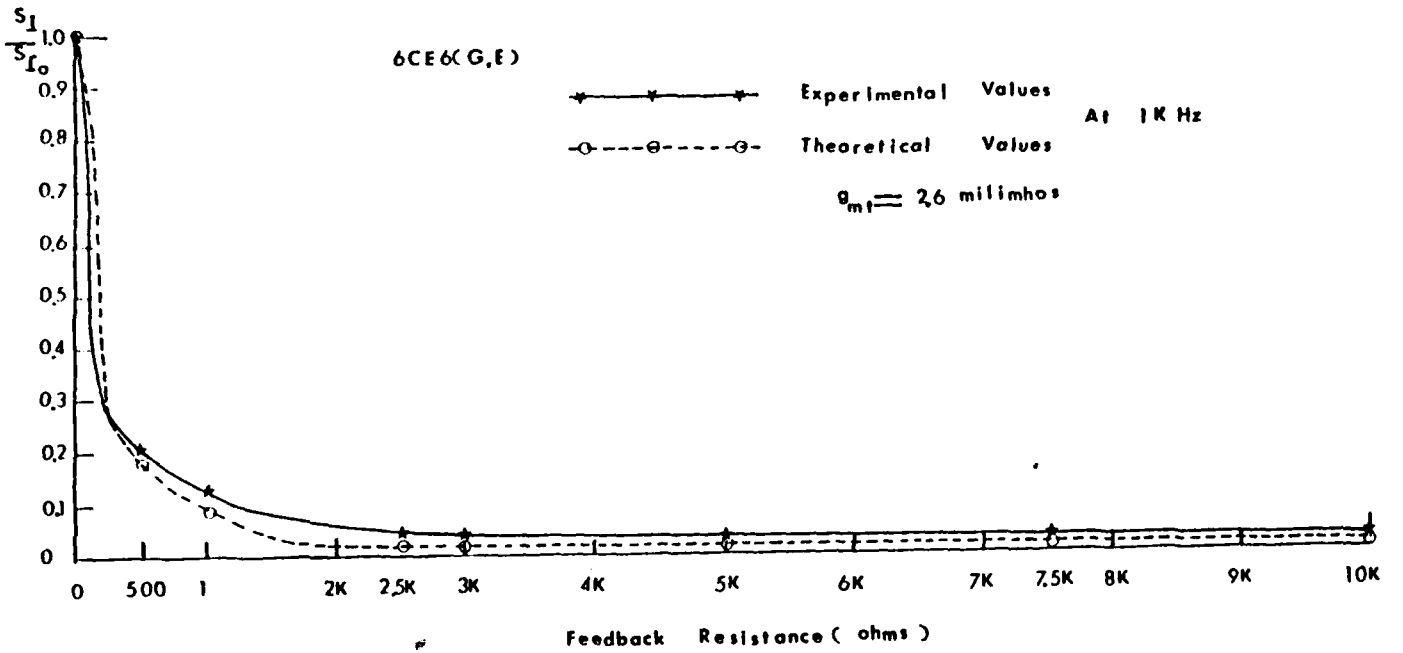

Figure 39. S_I/S_{I_o} vs R_c for 6CE6 (GE) at 1 KHz

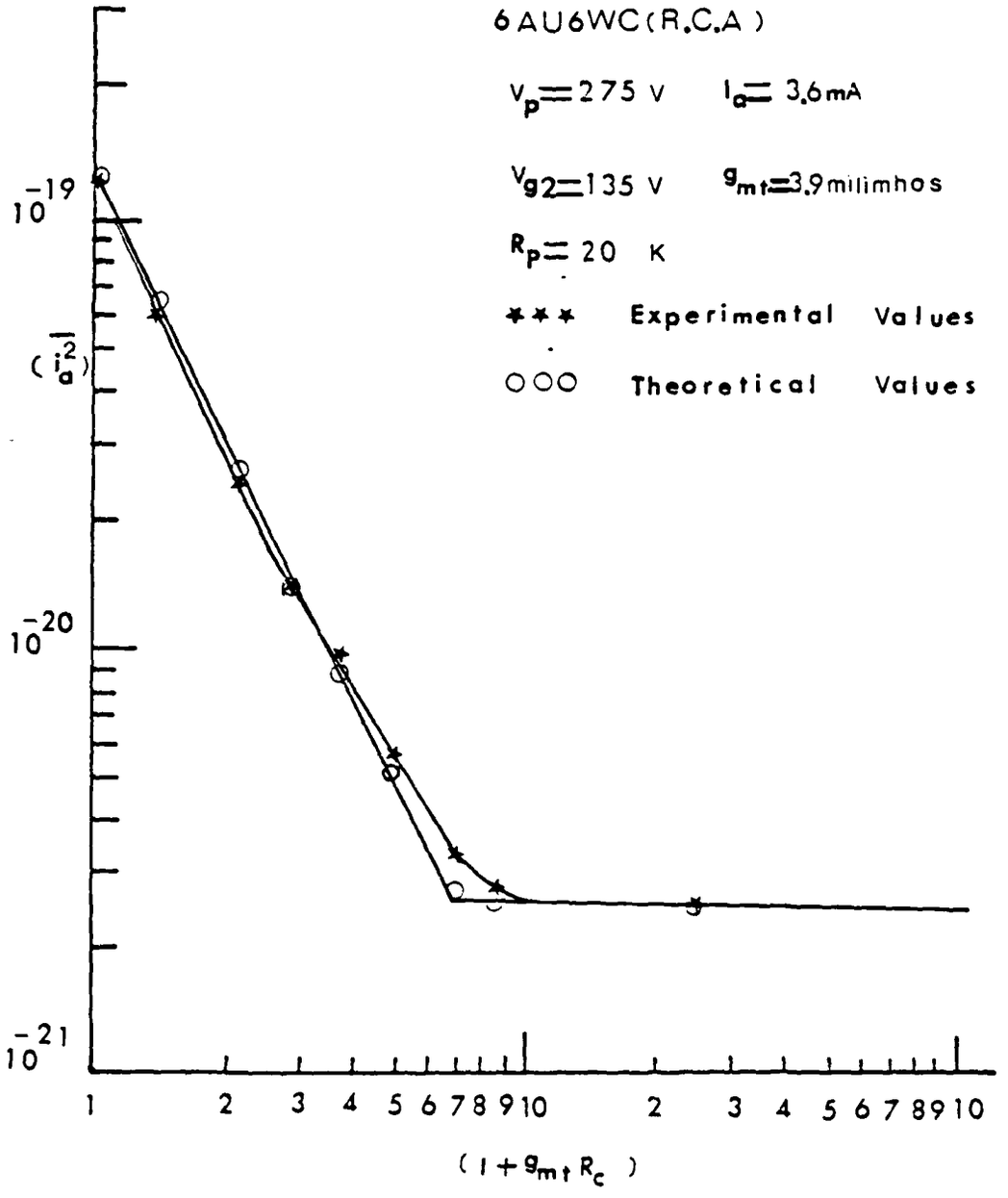

Figure 40. Log $(\overline{i_a^2})$ vs. log $(1 + g_{mt}R_c)$ for 6AU6WC (RCA) at 100 Hz

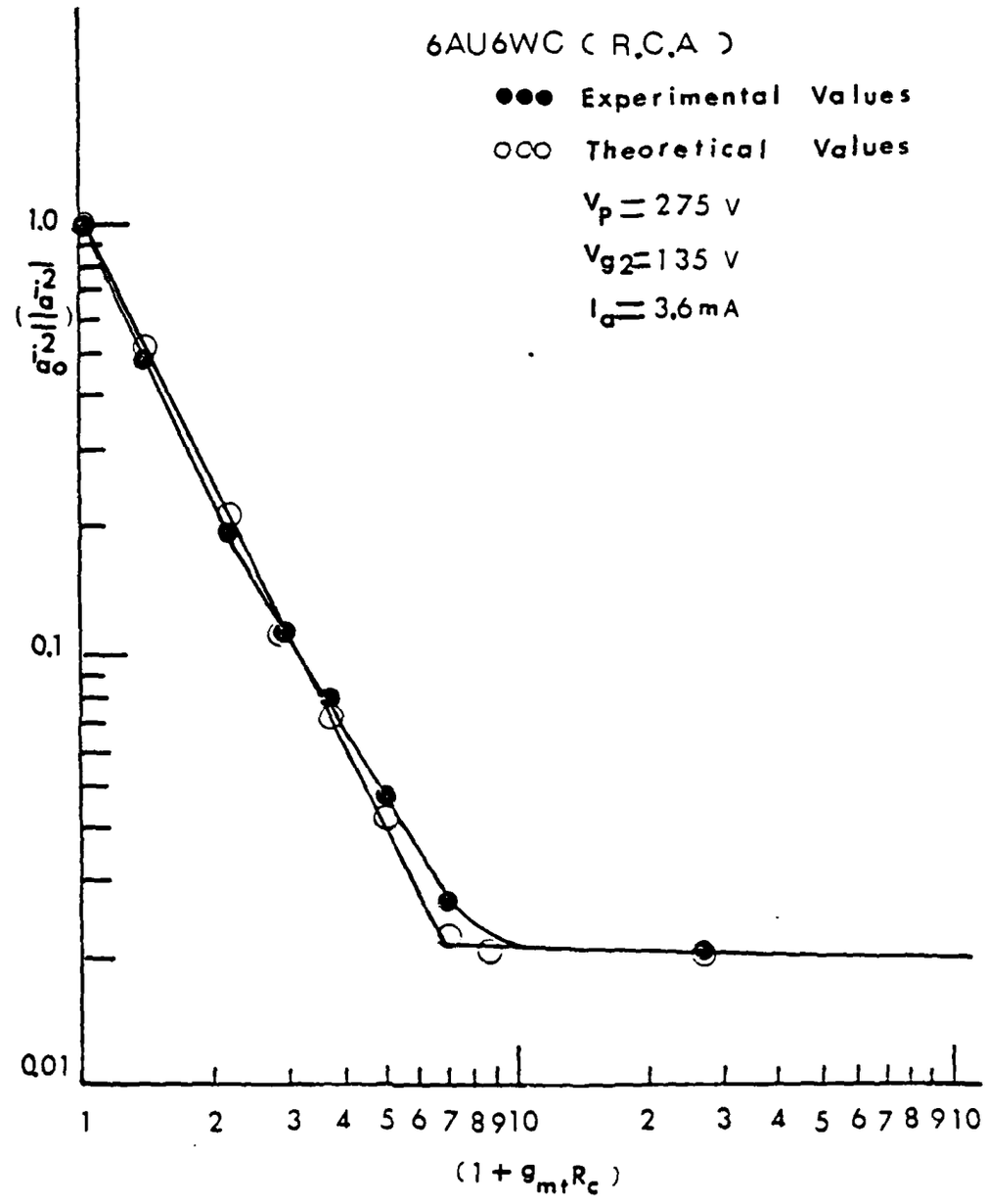

Figure 41. Log $\left(\frac{\overline{i_a^2}}{\overline{i_{ao}^2}}\right)$ vs. log $(1 + g_{mt}R_c)$ for 6AU6WC (RCA) at 100 Hz

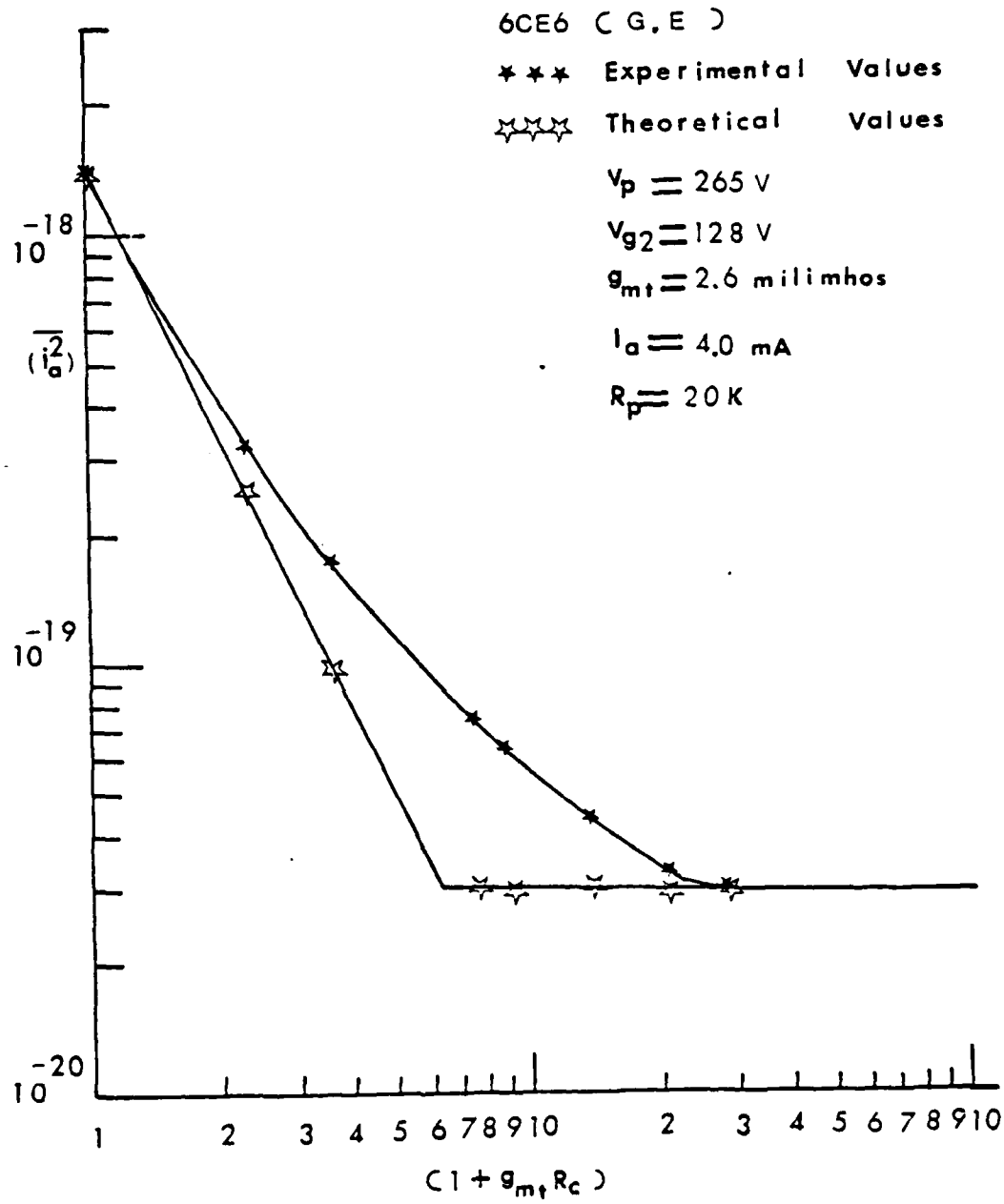

Figure 42. Log $(\overline{i_a^2})$ vs. log $(1 + g_{mt}R_c)$ for 6CE6 (GE) at 100 Hz

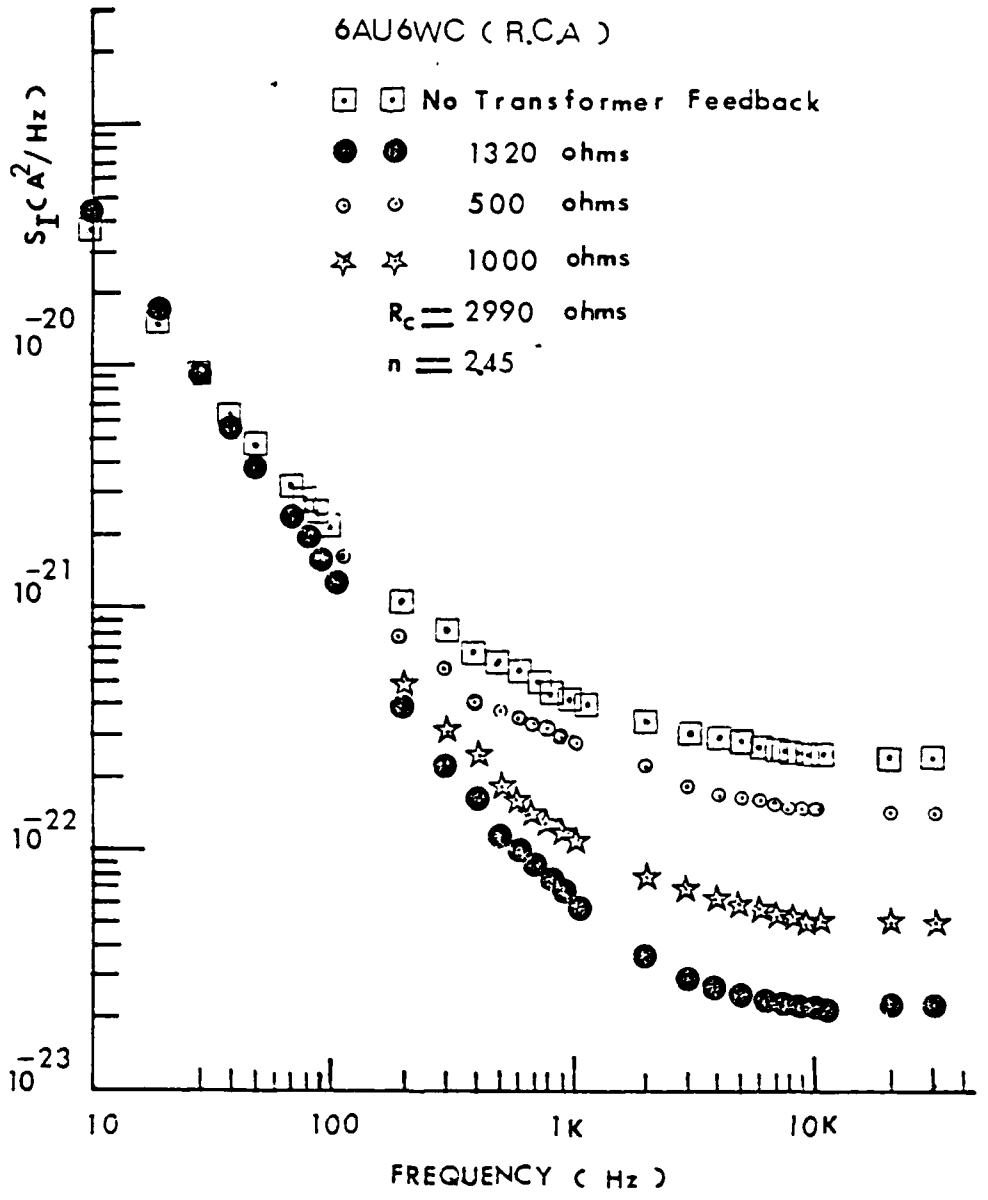

Figure 43. Current noise spectra of 6AU6WC (RCA) for various values of R_g

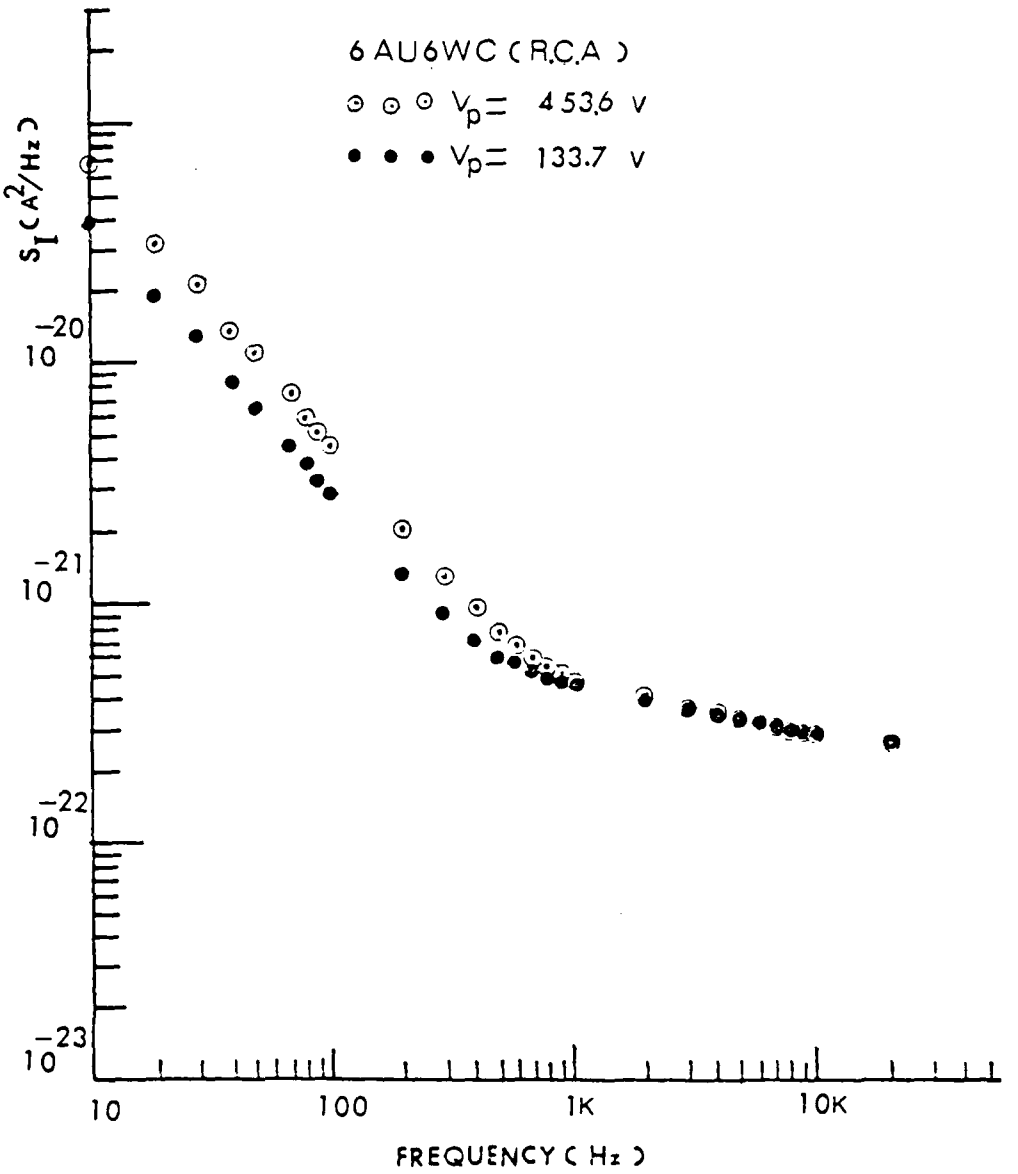

Figure 44. Current noise spectra of 6AU6WC (RCA) for two different anode voltages

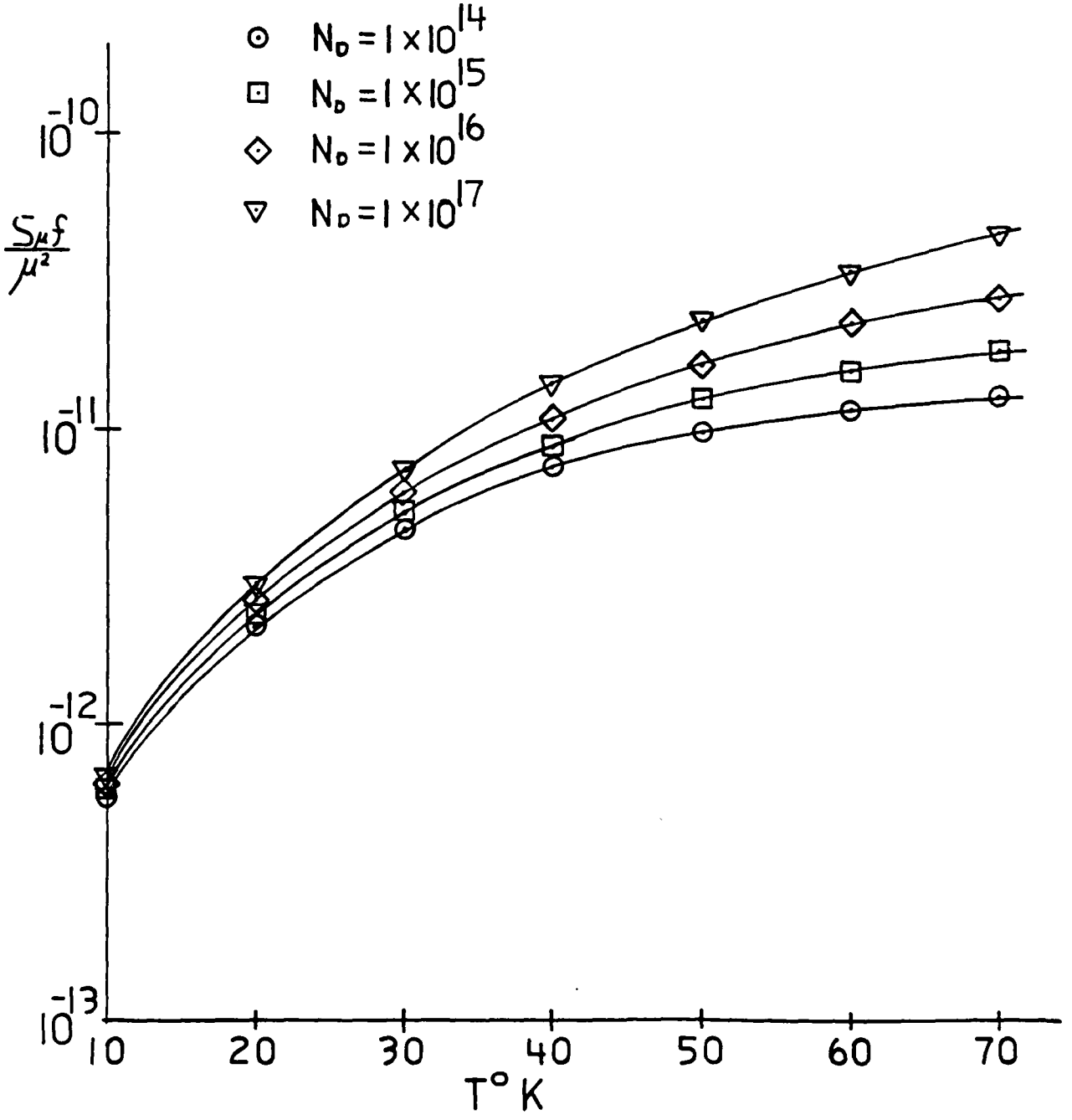
$N_D = 1 \times 10^{14}$
$N_D = 1 \times 10^{15}$
$N_D = 1 \times 10^{16}$
$N_D = 1 \times 10^{17}$
$\frac{S_\mu f}{\mu^2}$
10^{-10}
10^{-11}
10^{-12}
10^{-13}
10
20
30
40
50
60
70
T° K

Figure 45

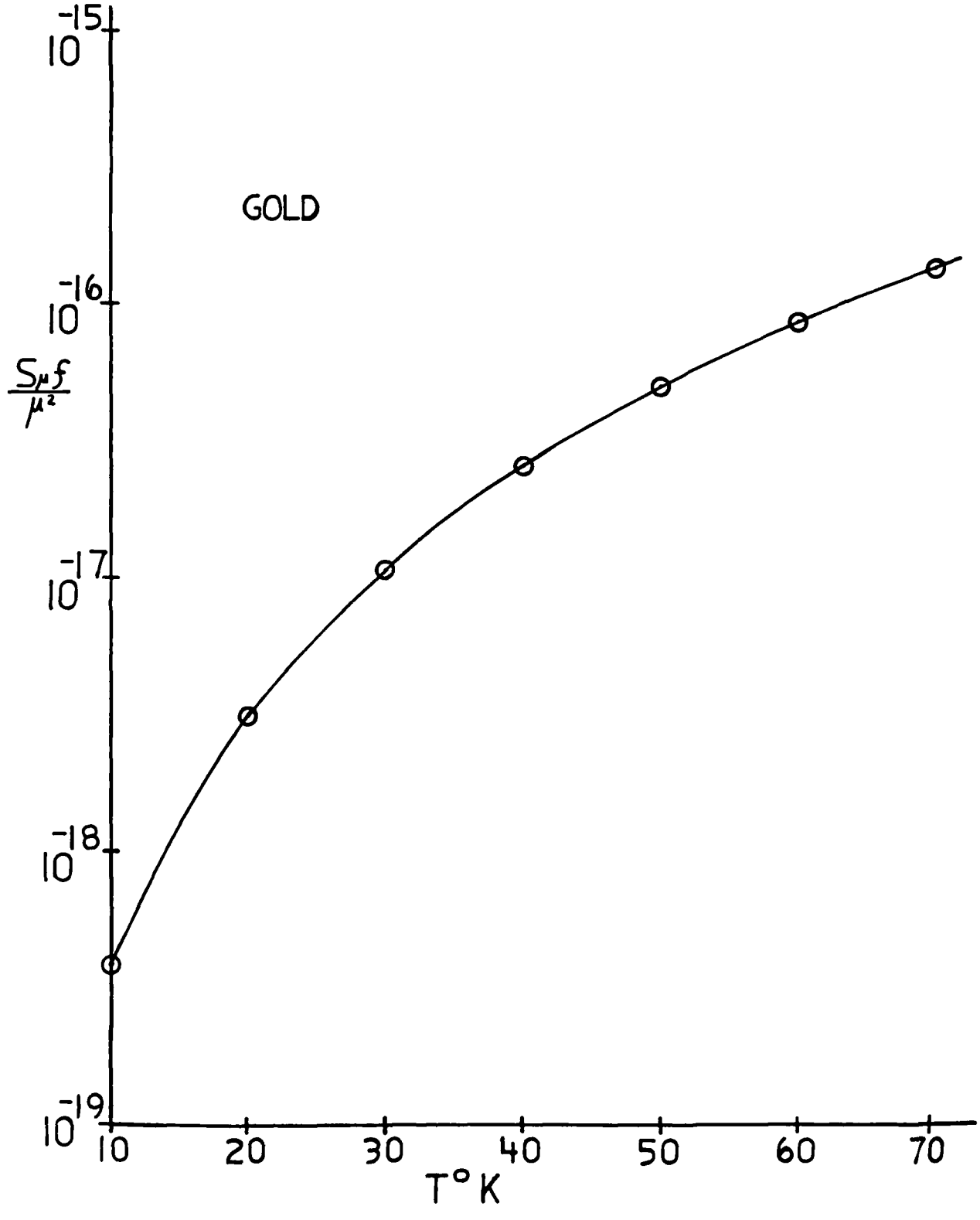
GOLD
10^{-15}
10^{-16}
10^{-17}
10^{-18}
10^{-19}
$\frac{S_{\mu f}}{\mu^2}$
10
20
30
40
50
60
70
T° K

Figure 46


DAT
ILM